THE "BROWN OCEAN" CONCEPT: A SPATIO-TEMPORAL AND THEORETICAL ANALYSIS OF INTENSIFYING TROPICAL CYCLONES OVER LAND

by

THERESA KATE ANDERSEN

(Under the Direction of J. MARSHALL SHEPHERD)

ABSTRACT

The Intergovernmental Panel on Climate Change (IPCC) has indicated the global water cycle is accelerating and may have an impact on the frequency and intensity of tropical cyclones (TCs). To protect life and property, it is important to identify how TC structure and intensity may respond to post-landfall conditions. Anomalously high soil moisture enhances surface latent heat flux (LHF) and has been theorized to provide energy to landfalling TCs. TCs can maintain or increase strength over inland regions (TCMIs) where they would otherwise be expected to dissipate or transition to extratropical cyclones (ETs). This framework has been termed the *brown ocean effect* because moisture from the ocean is normally the primary source for the energetics driving tropical systems.

The first objective of this research is to create a global climatology of post-landfall TC intensifications. Landfalling tropical systems 1979-2008 are identified and filtered by those that intensify inland (i.e., pressure drop or wind speed increase). Low-level thermal wind measurements, satellite images, and hurricane databases are used to interpret the post-landfall structure of each TC that intensifies inland: warm-core (TCMI), cold-core (ET), or hybrid. The second objective is to use HYDRUS-1D to model typical surface fluxes of an intensification

region. A comparison of land flux versus ocean flux provides an assessment of the feasibility that soil moisture can act as a substitute for the ocean. The third objective is to use a numerical weather model to simulate a historical TCMI case under various soil moisture regimes. This test of the *brown ocean* determines the relative role of soil moisture in TC evolution.

Results reveal 16 TCMI cases globally over the study period. The LHF over land leading up to intensification has a comparable magnitude to that over the ocean. Findings from objectives 1 and 2 suggest that antecedent precipitation, soil moisture, evaporation, and LHF could be important to the maintenance of warm-core TCs when baroclinicity is weak (i.e., lack of temperature gradients). WRF simulations from objective 3 indicate that TC structure is influenced by soil moisture conditions. A dry soil regime reduces LHF, low-level moisture, and total precipitation, and weakens cyclone rotation.

INDEX WORDS: brown ocean effect, extratropical transition, feedback, HYDRUS, landfall, latent heat flux, numerical model, soil moisture, tropical cyclones

THE "BROWN OCEAN" CONCEPT: A SPATIO-TEMPORAL AND THEORETICAL ANALYSIS OF INTENSIFYING TROPICAL CYCLONES OVER LAND

by

THERESA KATE ANDERSEN

BS, Iowa State University, 2008

MS, University of Georgia, 2010

A Dissertation Submitted to the Graduate Faculty of The University of Georgia in Partial Fulfillment of the Requirements for the Degree

DOCTOR OF PHILOSOPHY

ATHENS, GEORGIA

2013

THE "BROWN OCEAN" CONCEPT: A SPATIO-TEMPORAL AND THEORETICAL ANALYSIS OF INTENSIFYING TROPICAL CYCLONES OVER LAND

by

THERESA KATE ANDERSEN

Major Professor:	J. Marshall Shepherd
Committee:	David E. Radcliffe
	Thomas Mote
	Thomas Jordan

Electronic Version Approved:

Maureen Grasso
Dean of the Graduate School
The University of Georgia
August 2013

ACKNOWLEDGEMENTS

I would like to acknowledge the NASA Earth and Space Science Fellowship for supporting my dissertation research. I would also like to acknowledge my committee members for their insight, guidance, and support.

TABLE OF CONTENTS

Page

LIST OF TABLES

Page

LIST OF FIGURES

Page

CHAPTER 1

INTRODUCTION AND BACKGROUND

1.1 Introduction

A tropical cyclone (TC) is a center of low pressure that forms over the ocean between 7° and 15° latitude. These latitudes are characterized by relatively warm sea surface temperatures (SST) and a coriolis force strong enough to maintain a large vortex. Here, the warm tropical air produces low pressure and convective activity. The pressure drop initiates circulation (clockwise in the southern hemisphere and counterclockwise in the northern hemisphere) within the convective storms. Abundant evaporation, or latent heat flux (LHF), from the ocean surface fuels the TC and in turn, the TC redistributes energy by releasing heat through condensation. Regional Specialized Meteorological Centers (RSMC) and Tropical Cyclone Warning Centers (TCWC) provide data and forecasts for TCs. Although naming conventions vary, wind speed scales are similar across regions. For example, in the Atlantic and eastern Pacific (RSMC Miami), once a system is organized it is classified as a tropical disturbance. When closed circulation is observed, it is classified as a tropical depression and numbered. If the winds reach 34 knots, it becomes a tropical storm and receives a name. Upon reaching 64 knots, the system is classified as a hurricane on the Saffir-Simpson scale (categories 1-5) (Table 1.1). At the India Meteorological Department (RSMC New Delhi), classification is as follows: low pressure (winds < 17 kts), depression (winds 17-33 kts), cyclonic storm (winds 34-47 kts), severe cyclonic storm (winds 48-63 kts), very cyclonic storm (winds 64-119 kts), and supercyclone (winds > 119 kts) (Roy Bhowmik *et al.* 2005). All of the RSMC locations are shown in Figure 1.1. A hurricane is

characterized by spiraling thunderstorm clusters and a central eye of sinking air surrounded by intense updrafts in the eyewall (Figure 1.2). On average, 128.5 TCs are generated globally with the majority in the northern hemisphere. By basin, 12% develop in the Atlantic, 62% in the Pacific, and 26% in the Indian oceans (Rakhecha and Singh 2009). The cumulative tracks of all TCs 1985-2005 are shown in Figure 1.3.

Hazards associated with landfalling TCs include storm surge flooding along the coast, inland flooding from precipitation, damaging winds, and tornadoes. Slower moving TCs increase the potential for flooding. Globally, TCs are estimated to cause $1.5 billion in damage and 15,000-20,000 deaths annually (Rakhecha and Singh 2009). Climate change may impact the frequency, intensity, and distribution of TCs as the water cycle accelerates (Shepherd and Knutson 2007). It is predicted that intense and long-lived TCs will increase in frequency as the sea surface temperature warms, despite a decrease in the overall number of TCs globally (Bender *et al*. 2010, Hill and Lackmann 2011, Murakami *et al*. 2012).

Forecasting TC intensity changes is challenging, particularly over land where a TC may encounter synoptic, mesoscale, convective, and topographic features. While most tropical systems weaken over land in response to moisture loss, increased friction, and unfavorable atmospheric conditions (i.e., baroclinicity), there have been cases of TCs maintaining strength post-landfall. Such events have occurred in the United States (Arndt *et al.* 2009), India (Chang *et al*. 2009), China (Chen 2012), and Australia (Emanuel *et al.* 2008). These cases retain warm-core structures similar to their ocean-based counterparts and are referred to as tropical cyclone maintenance or intensification events (TCMIs). Alternatively, a TC may become embedded in the prevailing flow of higher latitudes and transition into an extratropical cyclone, switching out a warm-core for a cold-core structure. These cases are referred to as extratropical transition (ET).

For the purposes of this research, ET and TCMI events are considered the two primary post-landfall cyclone types.

1.2 Tropical cyclone climatology

TC landfalls are observed to occur in the North Atlantic, eastern North Pacific, western North Pacific, North Indian, and South Pacific/South Indian oceans (Figure 1.4). The western North Pacific is climatologically the most active TC basin and has the highest frequency of landfalls. Landfalls are least common in the Bay of Bengal (North Indian Ocean), however, the socio-economic impacts are significant. Collectively, global TC landfalls show high interannual variability (Weinkle *et al.* 2012). By basin, TC activity shows decadal-scale trends due to teleconnections (e.g., Atlantic Multidecadal Oscillation, AMO).

The Atlantic hurricane season is 1 June-30 November. Interannual variability is strongly linked to El Niño Southern Oscillation (ENSO) and stratospheric quasibiennial oscillation (QBO). In the United States, TCs contribute significantly to summer precipitation totals along the coasts and inland areas (Larson *et al.* 2005). The total number of TC strike days peaks in September in a typical year (Figure 1.5). Technological advances are improving TC observations and have impacted data used for determining long-term variability (Levinson *et al*. 2010) (Figure 1.6).

The North Indian hurricane season is 1 April-31 December. TC genesis is highly seasonal with a maximum during the post-monsoon season (September-December) and a secondary peak during the pre-monsoon season (April-May) (Mohanty *et al.* 2012). Cyclonic disturbances are most likely to form between 5-20 ºN and 87-91 ºE (Mohanty 1994). The Bay of Bengal (BB) accounts for 5-6% of the total annual number of cyclones globally. Due to the dense population along the coast, shallow bathymetry, shape of the coastline, and extent of low-lying delta, BB

TCs are considered among the deadliest in the world (Mandal and Mohanty 2010). The region holds the record for highest storm surge (45 ft) in 1876 (Mohanty *et al.* 2012).

The South Indian/South Pacific hurricane season is approximately 15 October-31 May. The Australian region experiences about 12.5 TCs per year and 5 landfalls (Ramsay and Leslie 2008). TC development in this region is influenced partly by the phase of ENSO. SST anomalies tend to displace TC origins eastward during El Niño and westward during La Niña (Flay and Nott 2007). Westward displacement results in more TCs forming near Australia. Complex terrain in the far northeastern region magnifies the hazards of landfalling TCs (Ramsay and Leslie 2008).

The West Pacific hurricane season is 1 May-30 November. In China, Tropical Depressions and Tropical Storms mainly develop over the South China Sea while typhoons are generated to the southeast of the Bashi Channel and east of the Philippines (Xu *et al.* 2011). Using clustering algorithms, Zhang *et al.* (2013) found that post-landfall TC movements can be classified into three groups (Figure 1.7). Cluster 1 makes landfall in Hainan province and moves across the western coast. These TCs may make secondary landfalls over Yunnan province after moving over the ocean for a period then dissipate inland while moving westward. Cluster 2 makes landfall at Guangdong and Fujian province, tracks inland, and dissipates. Cluster 3 makes landfall along the Fujian and Zhejiang coasts, maintains intensity, and recurves towards the midlatitudes.

1.3 Extratropical Transition

Transitioning cyclones bring damaging winds, flooding, and coastal erosion hundreds of kilometers beyond the storm center. Damaging winds associated with a transitioning cyclone may extend 2-3 times further than a TC of equal intensity (Hart and Evans 2001). An

extratropical transitioning storm develops an increasingly asymmetric temperature field and cold-core structure (e.g., geostrophic wind speed increasing with height) in response to the baroclinic atmosphere. Atlantic transitioning storms mainly occur August to October (Evans and Hart 2003). In the North Atlantic, ETs are suggested to be more common than in the Pacific, particularly near the United States east coast and Canadian maritime areas. Hart and Evans (2001) cite that 46% of Atlantic tropical cyclones undergo transformation. An indication of ET is a meridional trough-ridge pattern to the northwest of the storm (Hart and Evans 2001). Figure 1.8 shows infrared satellite views and 500-hPa analyses of Hurricane Michael (2000) as it was undergoing ET (Abraham *et al.* 2004). The synoptic evolution of Hurricane Floyd (1999) is shown in Figure 1.9. The increasing asymmetry associated with ET is apparent in 1.9c (Evans and Hart 2003).

In the western North Pacific, three types of ET have been identified based on surface pressure: complex (preexisting midlatitude front interacts with a tropical cyclone to produce a new ET cyclone), compound (midlatitude cyclone merges with tropical cyclone and transformed into an ET cyclone), and a dissipating tropical cyclone after recurvature (Klein *et al.* 2000). The transformation stage begins when visible, infrared, and water vapor imagery indicate an asymmetric appearance of clouds and decrease of convection in the western quadrant. The edge of the circulation will encounter a preexisiting baroclinic zone to the north. Transformation is successful when the storm contains the characteristic baroclinic cyclone traits (i.e., the center has cold descending air). If the storm subsequently deepens, it is considered in the reintensification stage (beginning when the storm has reached peak sea level pressure and ending with the lowest pressure). Reintensification is dependent on the midlatitude circulation structure. Failure to complete both stages renders the cyclone a “decayer” (Klein *et al*. 2000).

In the southwest Pacific, tropical cyclones have an easterly component, unlike those in other ocean basins, due to early encounters with baroclinic westerlies. Thus, they tend to transition to ET quickly. Between 20 °S and 25 °S, the storm weakens due to upper-level shear, and poleward from 25 °S it exhibits midlatitude cyclone characteristics. ET in the Northern Hemisphere may not occur until poleward of 40 °N (Sinclair 2002).

1.4 Tropical Cyclone Maintenance or Intensification

The situations in which TCs are reinforced instead of transformed post-landfall may occur when the environment mimics barotropic conditions (i.e., low wind shear and uniform temperature), or when peripheral weather systems contribute moisture and energy to the system. Low-level jets transport moisture and momentum, upper-level jets enhance outflow, and mesoscale vortices can merge with and strengthen TCs in some situations (Chen 2012). Four well-studied North American examples are tropical cyclones David in 1979 (Bosart and Lackmann 1995), Fran in 1996 (Pasch and Avila 1999), Danny in 1997 (Blackwell 2000), and Erin in 2007 (Arndt *et al.* 2009). Tropical Storm Erin is particularly interesting as it reintensified more than 500 km inland and actually surpassed its peak maritime strength (Arndt *et al.* 2009).

Upper air forcing and changes in the shear environment are critical features feeding landfalling TC intensity, but an additional process that has not been thoroughly explored as an energy source is land surface moisture flux. Shepherd and Niyogi (personal communication, 2009) have termed this framework the *brown ocean* because moisture from the ocean is typically the primary source for the energetics driving tropical systems. Under certain soil moisture and atmospheric conditions, landfalling TCs may intensify in a similar manner to oceanic tropical cyclones. Such intensification over the *brown ocean* is the focus of this research.

Soil moisture has a direct effect on the atmosphere through moisture and energy exchanges (Mahmood *et al.* 2006). Soil moisture conditions can also create "soil moisture memory" that affect future convective activity (Pal and Eltahir 2001, Wu and Dickinson 2004). Numerical experiments show soil moisture-rainfall feedback plays an important role in sustaining drought conditions or flood conditions (Pal and Eltahir 2001). It has also been found that soil moisture memory in tropical climates lasts longer in dry conditions and deeper soils. Under wet conditions, soil moisture memory is likely controlled by the climate while under dry conditions soil moisture relies on evapotranspiration and runoff (Wu and Dickinson 2004).

1.5 Research objectives

After landfall, the escalating number of factors that could influence TC intensity/track and associated hazards complicate forecasts. For example, Tropical Storm Erin unexpectedly re-intensified over Oklahoma in August 2007 which led to 7 floodwater-related deaths and extensive damage (Arndt *et al.* 2009). TCs that intensify post-landfall have not been as extensively studied as ET and merit further research to aid forecasting and disaster management (Bozeman *et al.* 2012). The goals of this dissertation are to determine the climatology of TCMIs and to better understand the physical mechanisms that lead to intensification. The specific objectives are as follows:

Objective 1

(1) Differentiate extratropical transition (ET) from tropical cyclone maintenance or intensification (TCMI) inland, (2) address the global spatio-temporal characteristics of TCMIs to produce the first global climatology of inland intensifications, and (3) quantify the possible physical mechanistic, geographical, and/or topographical factors associated with TCMIs.

It is hypothesized that excess soil moisture enhances sensible and latent heat fluxes, thermal conductivity, and thermal diffusivity to energize TCs inland. The primary geographical factors are proximity to a moisture source, soil moisture conditions leading up to the hurricane season (e.g. soil moisture memory), and amount of precipitation preceding the storm landfall. The dominant topographical features are soils with high heat capacities and ability to store and release moisture. Irrigated and vegetated areas may be more likely to increase the moisture supply near the surface. Landfalling TCs are more likely to intensify over regions with above average rainfall antecedent to the warmest months of the hurricane season (soil moisture memory) and/or plentiful rainfall within 2-3 weeks preceding storm landfall. This allows the soils to be sufficiently warm and moist to transfer energy back to the storm. This information could be used to predict locations and environmental conditions that are more likely to host inland intensifications.

Objective 2

Employ the HYDRUS-1D model to simulate the typical surface fluxes over TCMI regions in the weeks leading up to intensification in order to compare the energy potential to ocean energy fluxes.

It is hypothesized that the land surface releases a comparable amount of latent heat energy to the ocean when the soil is anomalously wet from previous rainfall, however, the results will vary with soil texture. Using meteorological input data, HYDRUS-1D simulations of latent heat flux preceding a TCMI should be higher than the hurricane-season average.

Objective 3

Analyze a historical TCMI event with emphasis on soil moisture interactions, flux magnitudes, and storm evolution using the Weather Research Forecast (WRF-ARW) model.

It is hypothesized that perturbing the soil moisture regime will affect the intensification of the TC over land. Increasing (decreasing) the soil moisture will result in a strengthening (weakening) of the cyclone owing to increased (reduced) upward energy fluxes. The LHF magnitude will be a function of soil texture with the largest fluxes over wet sand.

Study area

The study area is global with emphasis on four major landfall regions. Tropical cyclones are most often observed to move inland from the North Atlantic (NA), West Pacific (WP), North Indian (NI), and South Indian/South Pacific oceans (SI/SP). These landfalls affect eastern North America, eastern Asia, India, and Australia, respectively (Figure 1.10). The background, data, methodologies, results, and discussions for each of the three objectives are provided in Chapters 2-4. The major findings and concluding remarks are provided in Chapter 5.

1.6 References

Abraham, J., J.W. Strapp, C. Fogarty, and M. Wolde (2004). Extratropical transition of Hurricane Michael: An aircraft investigation. *Bulletin of the American Meteorological Society* **85**, 1323-1339. doi: 10.1175/BAMS-85-9-1323

Alonge, C.J., K.I. Mohr, and W.-K. Tao (2007). Numerical studies of wet versus dry soil regimes in the West African Sahel. *Journal of Hydrometeorology* **8**, 102–116. doi: 10.1175/JHM559.1

Arndt, D.S., J.B. Basara, R.A. McPherson, B.G. Illston, G.D. McManus, and D.B. Demko (2009). Observations of the overland reintensification of Tropical Storm Erin (2007). *Bulletin of the American Meteorological Society* **90**, 1079–1093. doi: 10.1175/2009BAMS2644.1

Bender, M.A., T.R. Knutson, R.E. Tuleya, J.J. Sirutis, G.A. Vecchi, S.T. Barner, and I.M. Held (2010). Modeled impact of anthropogenic warning on the frequency of intense Atlantic hurricanes. *Science* **327**, 454–458.

Blackwell, K.G. (2000). The evolution of Hurricane Danny (1997) at landfall: Doppler-observed eyewall replacement, vortex contraction/intensification, and low-level wind maxima. *Monthly Weather Review* **128**, 4002-4016.

Bosart, L.F., and G.M. Lackmann (1995). Postlandfall tropical cyclone reintensification in a weakly baroclinic environment: A case study of Hurricane David (September 1979). *Monthly Weather Review* **123**, 3268-3291.

Bosilovich, M.G., and W.-Y. Sun (1999). Numerical simulation of the 1993 midwestern flood: Land atmosphere interactions. *Journal of Climate* **12**, 1490–1505.

Bozeman, M.L., D. Niyogi, S. Gopalakrishnan, F. Marks, X. Zhang, and V. Tallapragada. (2012). An HWRF-based ensemble assessment of the land surface feedback on the post-landfall intensification of Tropical Storm Fay (2008). *Natural Hazards* **63**, 1543-1571. doi: 10.1007/s11069-011-9841-5

Chang, H.-I., D. Niyogi, A. Kumar, C.M. Kishtawal, J. Dudhia, F. Chen, U.C. Mohanty, and M. Shepherd (2009). Possible relation between land surface feedback and the post-landfall structure of monsoon depressions. *Geophysical Research Letters* **36**, 1-6.

Chen, L.-S. (2012). Research progress on the structure and intensity change for the landfalling tropical cyclones. *Journal of Tropical Meteorology* **18**, 113–118. doi: 10.3969/j.issn.1006-8775.2012.02.001

Emanuel, K., J. Callaghan, and P. Otto (2008). A hypothesis for the redevelopment of warm-core cyclones over northern Australia. *Monthly Weather Review* **136,** 3863–3872. doi: 10.1175/2008MWR2409.1

Evans, J.L., and R.E. Hart (2003). Objective indicators of the life cycle evolution of extratropical transition for Atlantic tropical cyclones. *Monthly Weather Review* **131**, 909–925.

Evans, C., R.S. Schumacher, and T.J. Galarneau (2011). Sensitivity in the overland reintensification of Tropical Cyclone Erin (2007) to near-surface soil moisture characteristics. *Monthly Weather Review* **139**, 3848–3870. doi: 10.1175/2011MWR3593.1

Flay, S., and J. Nott (2007). Effect of ENSO on Queensland seasonal landfalling tropical cyclone activity. *International Journal of Climatology* **27**, 1327-1334. doi: 10.1002/joc.1447

Hart, R.E., and J.L. Evans (2001). A climatology of the extratropical transition of Atlantic tropical cyclones. *Journal of Climate* **14**, 546–564.

Hill, K.A., and G.M. Lackmann (2011). The impact of future climate change on TC intensity and structure: A downscaling approach. *Journal of Climate* **24**, 4644-4661. doi: 10.1175/2011JCLI3761.1

Klein P., P. Harr, and R. Elsberry (2000). Extratropical transition of western North Pacific tropical cyclones: An overview and conceptual model of the transformation stage. *Weather Forecasting* **15**, 373-395.

Larson, J., Y. Zhou, and R.W. Higgins (2005). Characteristics of landfalling tropical cyclones in the United States and Mexico: Climatology and interannual variability. *Journal of Climate* **18**, 1247-1262.

Levinson, D.H., P.J. Vickery, and D.T. Resio (2010). A review of the climatological characteristics of landfalling Gulf hurricanes for wind, wave, and surge hazard estimation. *Ocean Engineering* **37**, 13-25. doi: 10.1016/j.oceaneng.2009.07.014

Mahmood, R., S.A. Foster, T. Keeling, K.G. Hubbard, C. Carlson, and R. Leeper (2006). Impacts of irrigation on 20th century temperature in the northern Great Plains. *Global and Planetary Change* **54**, 1–18. doi: 10.1016/j.gloplacha.2005.10.004

Mandal, M., and U.C. Mohanty (2010). Simulation of severe land-falling Bay of Bengal cyclones during 1995-1999 using mesoscale model MM5. *Marine Geodesy* **33**, 315-337. doi: 10.1080/01490419.2010.518070

Mohanty, U.C. (1994). Tropical cyclones in Bay of Bengal and deterministic methods for prediction of their trajectories. *Sadhana* **19**, 567–582.

Mohanty, U.C., K.K. Osuri, S. Pattanayak, and P. Sinha (2012). An observational perspective on tropical cyclone activity over Indian seas in a warming environment. *Natural Hazards* **63**, 1319-1335.

Murakami, H. and coauthors (2012). Future changes in tropical cyclone activity projected by the new high-resolution MRI-AGCM. *Journal of Climate* **25**, 3237-3260. doi: 10.1175/JCLI-D-11-00415.1

Pal, J.S., and E.A.B. Eltahir (2001). Pathways relating soil moisture conditions to future summer rainfall within a model of the land-atmosphere system. *Journal of Climate* **14**, 1227-1242.

Pasch, R.J., and L.A. Avila (1999). Atlantic hurricane season of 1996. *Monthly Weather Review* **127**, 581-610.

Rakhecha, P. and V.P. Singh (2009). *Applied Hydrometeorology* (1st edition). Springer-Verlag New York, LLC. pp. 364.

Ramsay, H.A., and L.M. Leslie (2008). The effects of complex terrain on severe landfalling tropical cyclone Larry (2006). *Monthly Weather Review* **136**, 4334-4354. doi: 10.1175/2008MWR2429.1

Roy Bhowmik, S.K., S.D. Kotal, and S.R. Kalsi (2005). An empirical model for predicting the decay of tropical cyclone wind speed after landfall over the Indian region. *Journal of Applied Meteorology* **44**, 179-185.

Shepherd, J.M. (2012). What we can learn from the satellite-based rainfall footprint of Superstorm Sandy: A preliminary synopsis. *Earthzine*. Published online 16 Dec (<http://www.earthzine.org/2012/12/16/what-we-can-learn-from-the-satellitebased-rainfall-footprint-of-superstorm-sandy-a-preliminarysynopsis/>)

Shepherd, J.M., and T. Knutson (2007). The current debate on the linkage between global warming and hurricanes. *Geography Compass* **1**, 1–24. doi: 10.1111/j.1749-8198.2006.00002.x

Sinclair, M.R. (2002). Extratropical transition of Southwest Pacific tropical cyclones. Part I: Climatology and mean structure changes. *Monthly Weather Review* **130**, 590-609.

Weinkle, J., R. Maue, and R. Pielke, Jr. (2012). Historical global tropical cyclone landfalls. *Journal of Climate* **25**, 4729-4735. doi: 10.1175/JCLI-D-11-00719.1
Wu, W., and R.E. Dickinson (2004). Time scales of layered soil moisture memory in the context of land atmosphere interactions. *Journal of Climate* **17**, 2752-2764.

Zhang, W, Y. Leung, and Y. Wang (2013). Cluster analysis of post-landfall tracks of landfalling tropical cyclones over China. *Climate Dynamics* **40**, 1237-1255. doi: 10.1007/s00382-012-1519-5

Table 1.1: Saffir-Simpson hurricane wind scale ratings (NOAA).

Category	Sustained Winds	Types of Damage
1	64-82 kt	Very dangerous winds will produce some damage
2	83-95 kt	Extremely dangerous winds will cause extensive damage
3 (major)	96-112 kt	Devasting damage will occur
4 (major)	113-136 kt	Catastrophic damage will occur
5 (major)	137 kt +	Catastrophic damage will occur

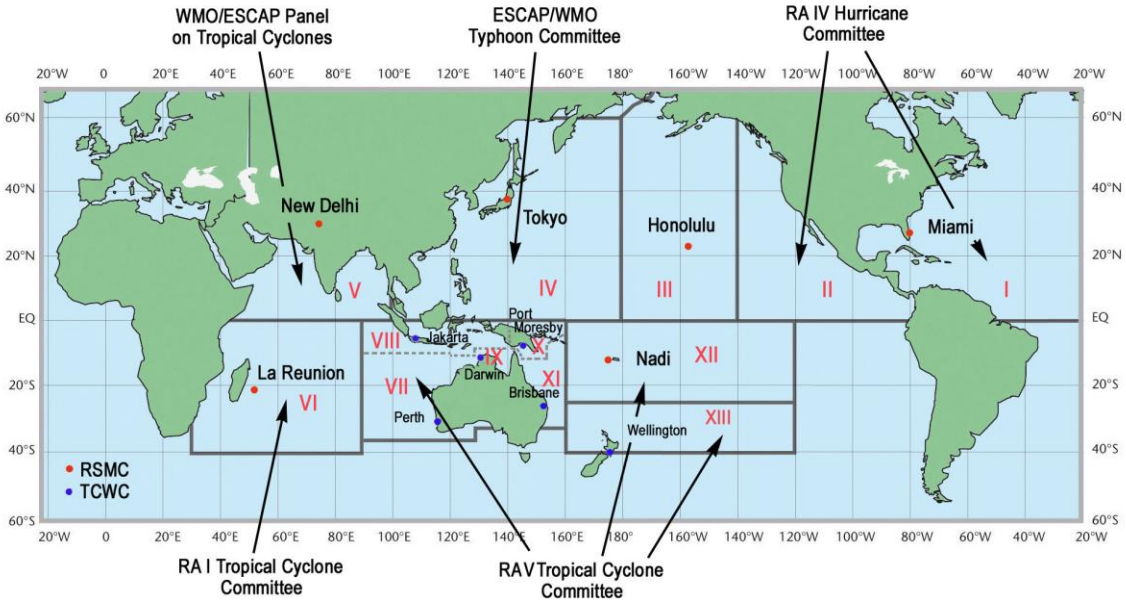

Figure 1.1: Tropical cyclone centers and designated regions (WMO).

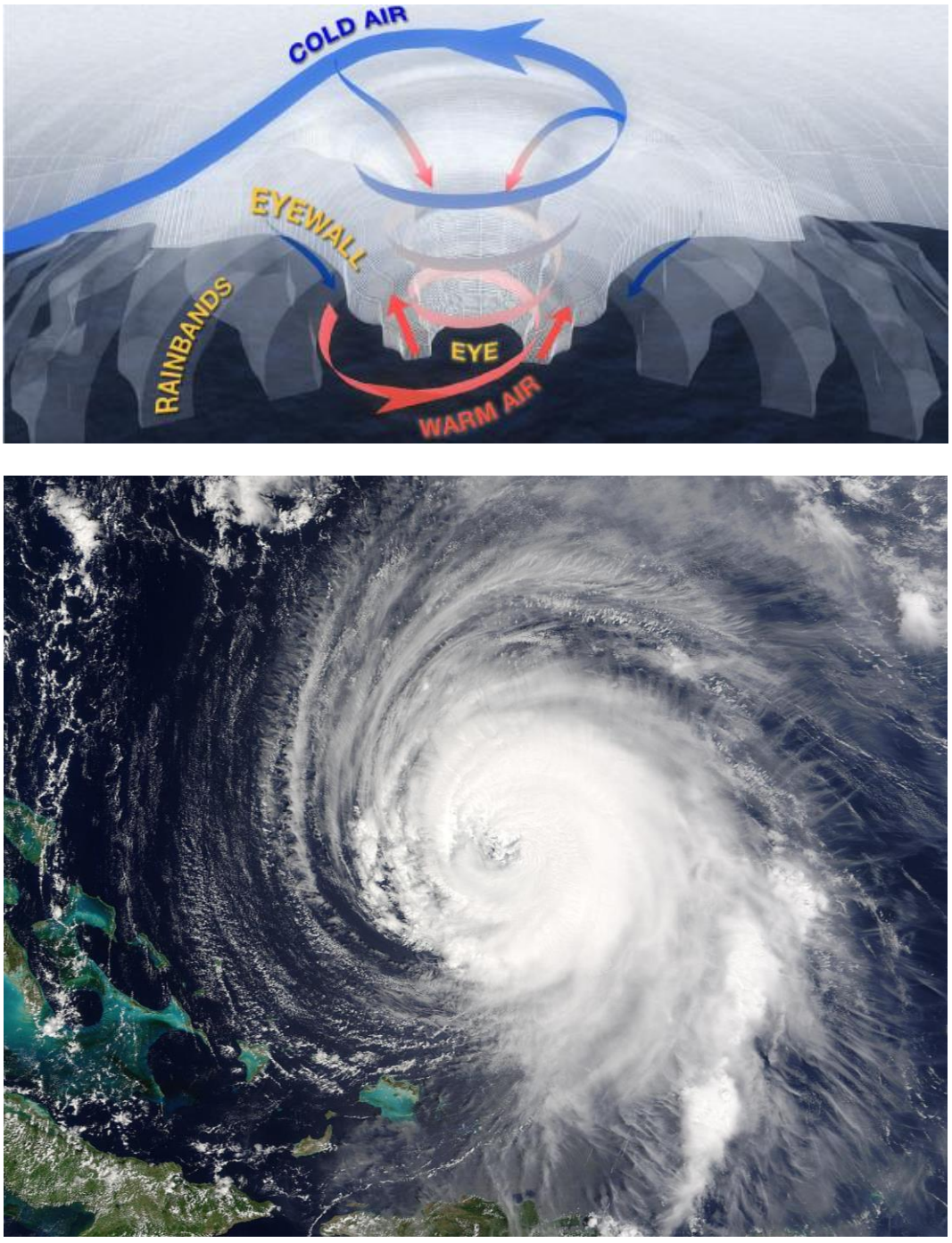

Figure 1.2: Top: Hurricane structure features spiraling rainbands, warm air inflow into the eyewall, cold air outflow aloft, and sinking air in the central eye (Credit: The COMET Program Steven Deyo/USGS Betsy Boynton). Bottom: Hurricane captured by satellite (Credit: NASA).

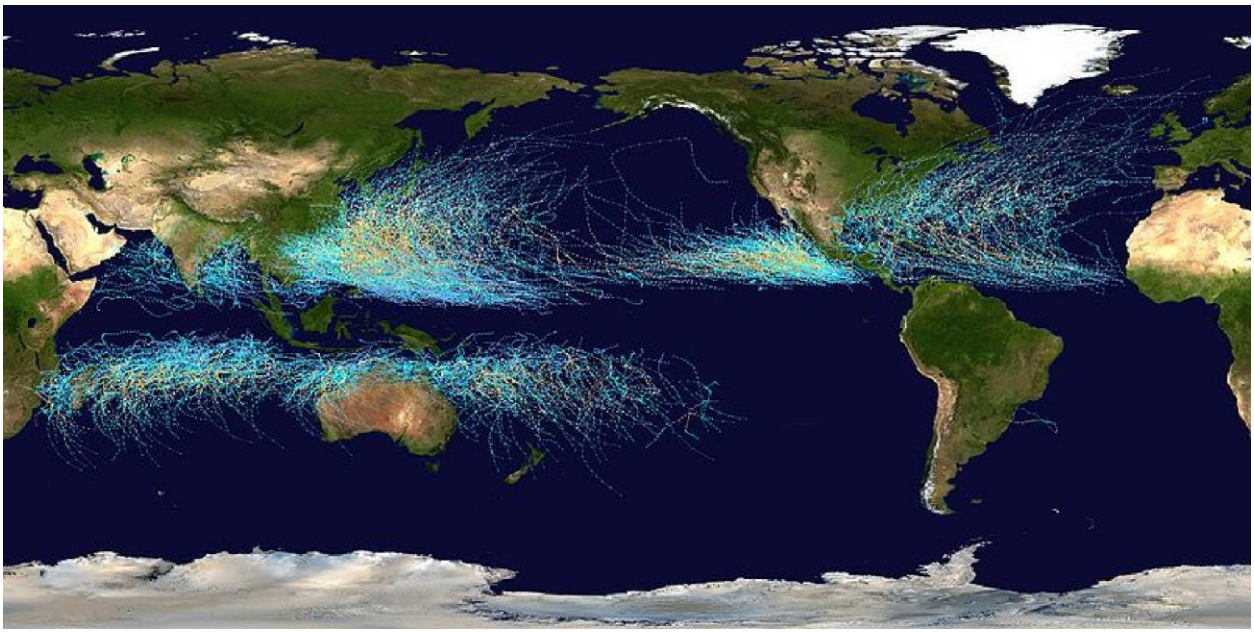

Figure 1.3: Cumulative tropical cyclone tracks 1985-2005 (Credit: NASA).

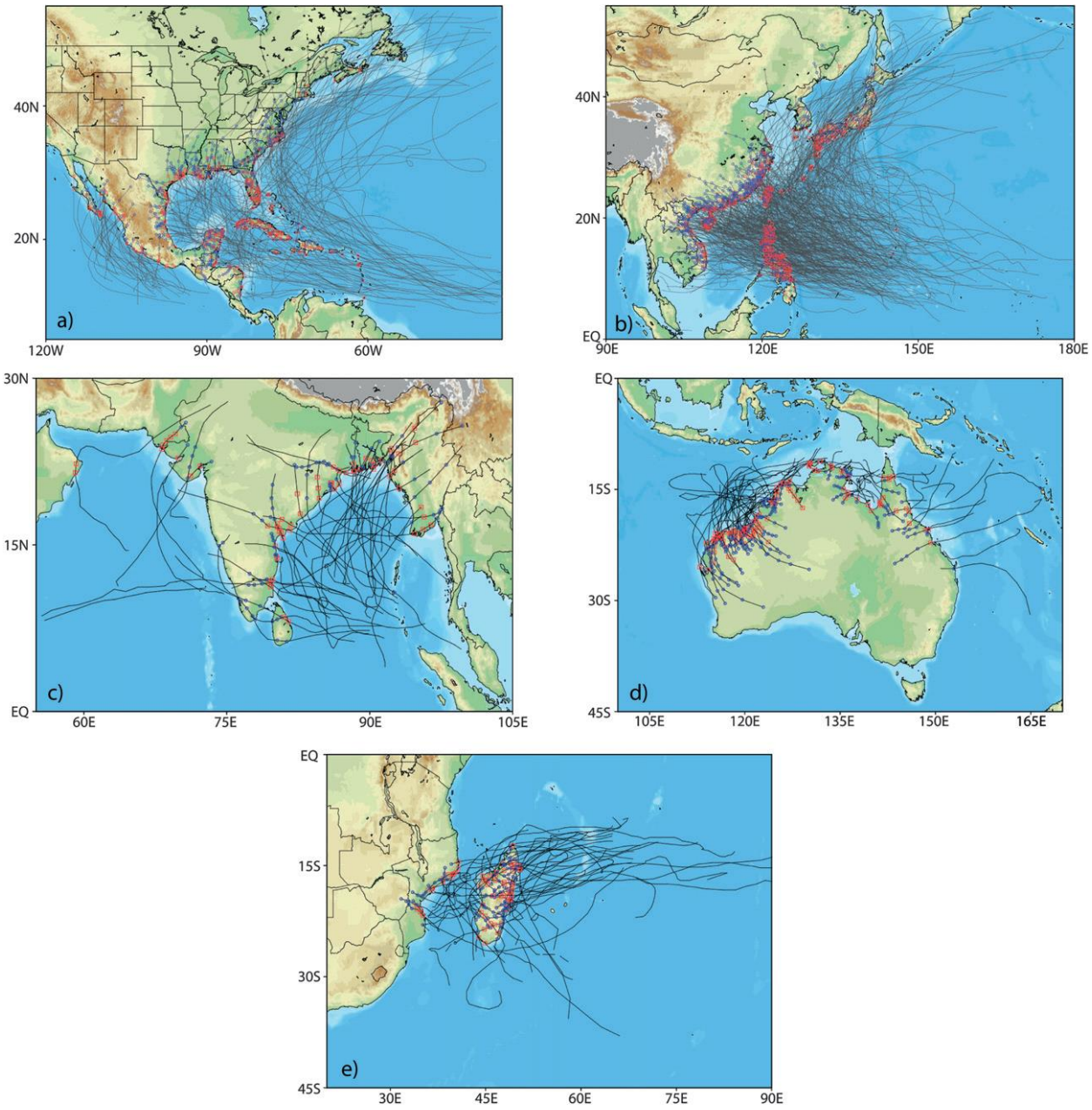

Figure 1.4: Hurricane landfalls globally for the North Atlantic (1944-2010) and northeastern Pacific (1970-2010), western North Pacific (1950-2010), North Indian (1970-2010), southern hemisphere (1970-2010) (Weinkle *et al*. 2012).

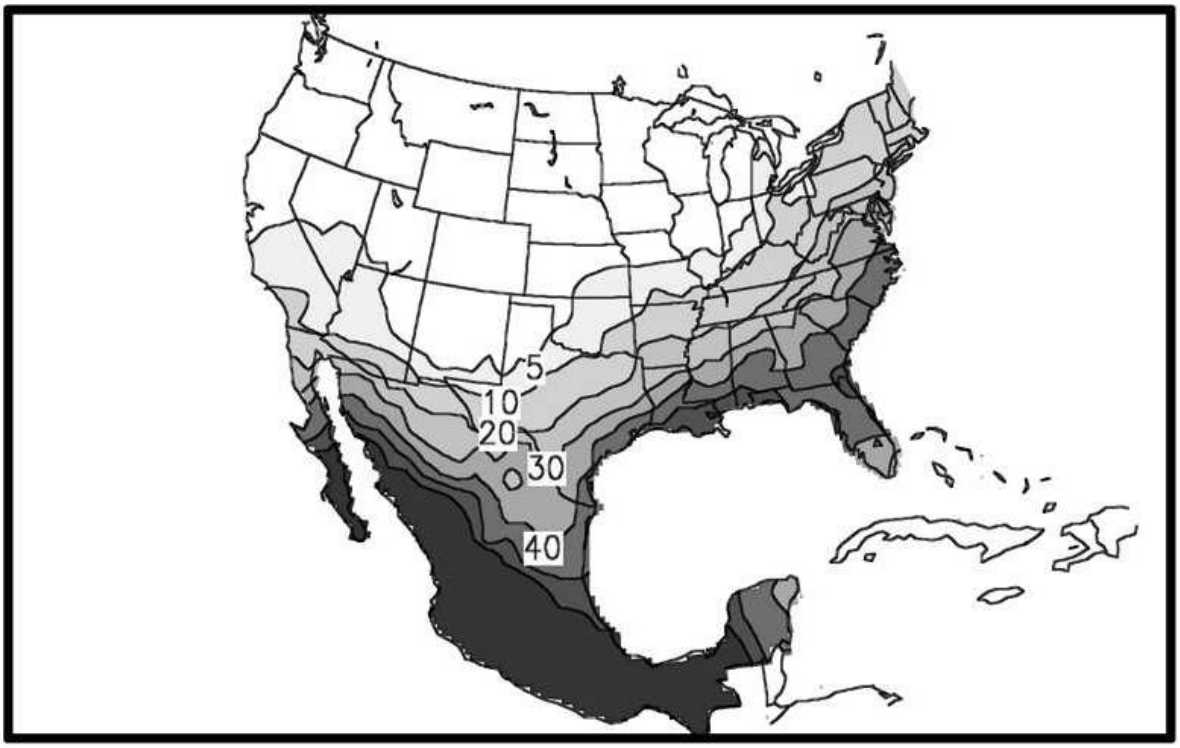

Figure 1.5: Total number of TC strike days (1950-1998) during the month of September (Larson *et al.* 2005).

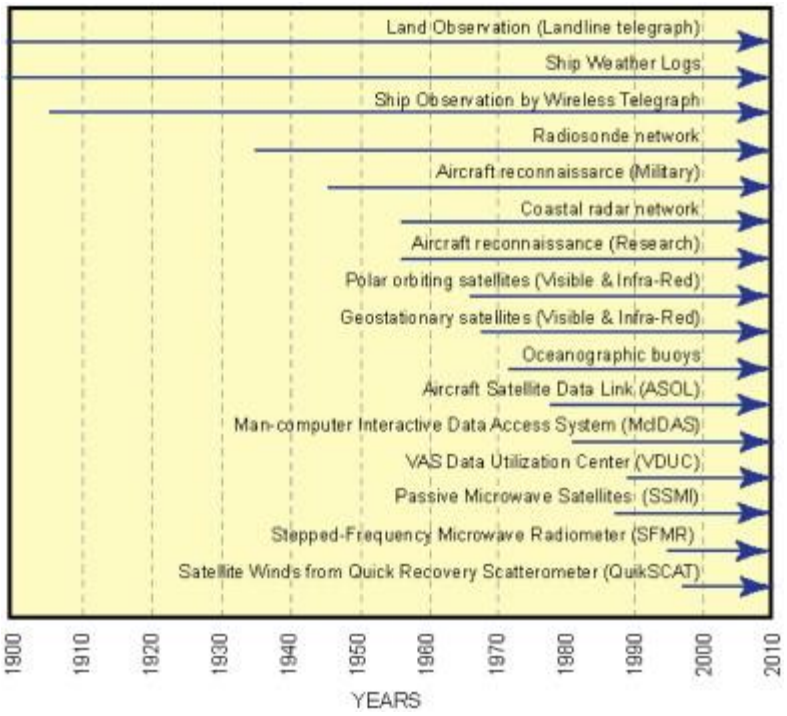

Figure 1.6: Technological advances in Atlantic Ocean TC observations (1900-2010) (Levinson *et al.* 2010).

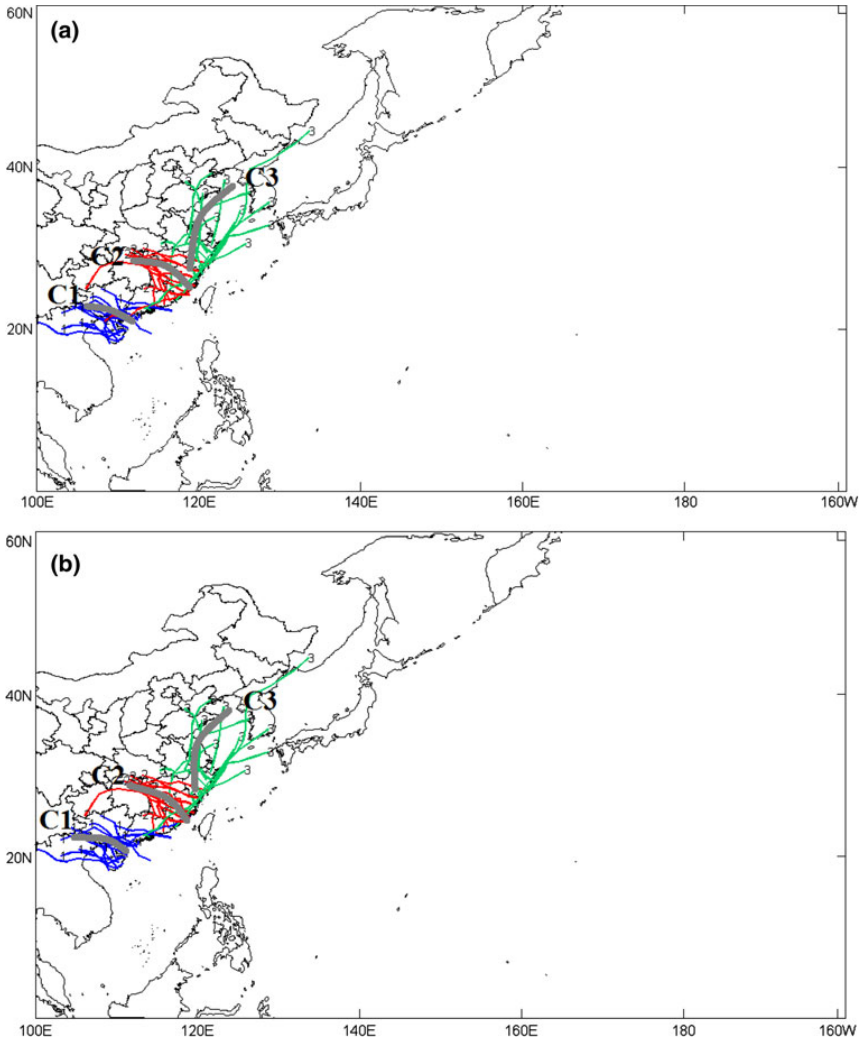

Figure 1.7: Three primary clusters of post-landfall TCs over China based on (a) time orders and elevation and (b) only time orders (Zhang *et al*. 2013).

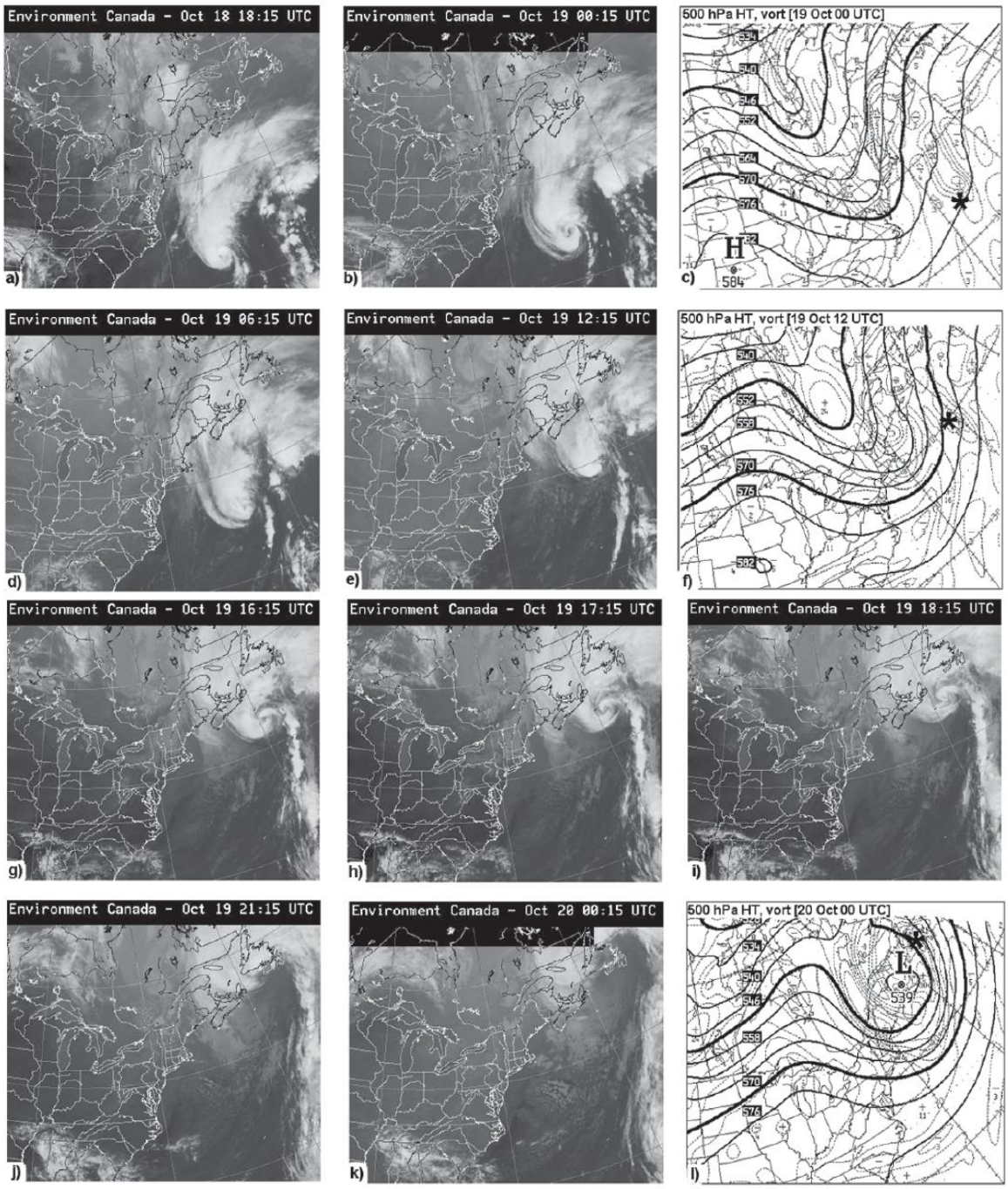

Figure 1.8: GOES infrared satellite images and 500 hPa geopotential heights showing the ET evolution of Hurricane Michael (2000) (Abraham *et al*. 2004).

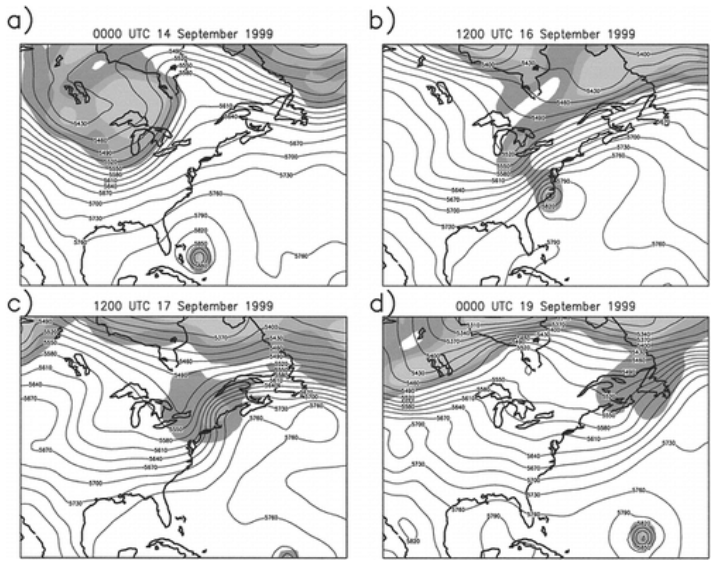

Figure 1.9: Synoptic evolution of Hurricane Floyd 14 September – 19 September 1999 during extratropical transition (Evans and Hart 2003).

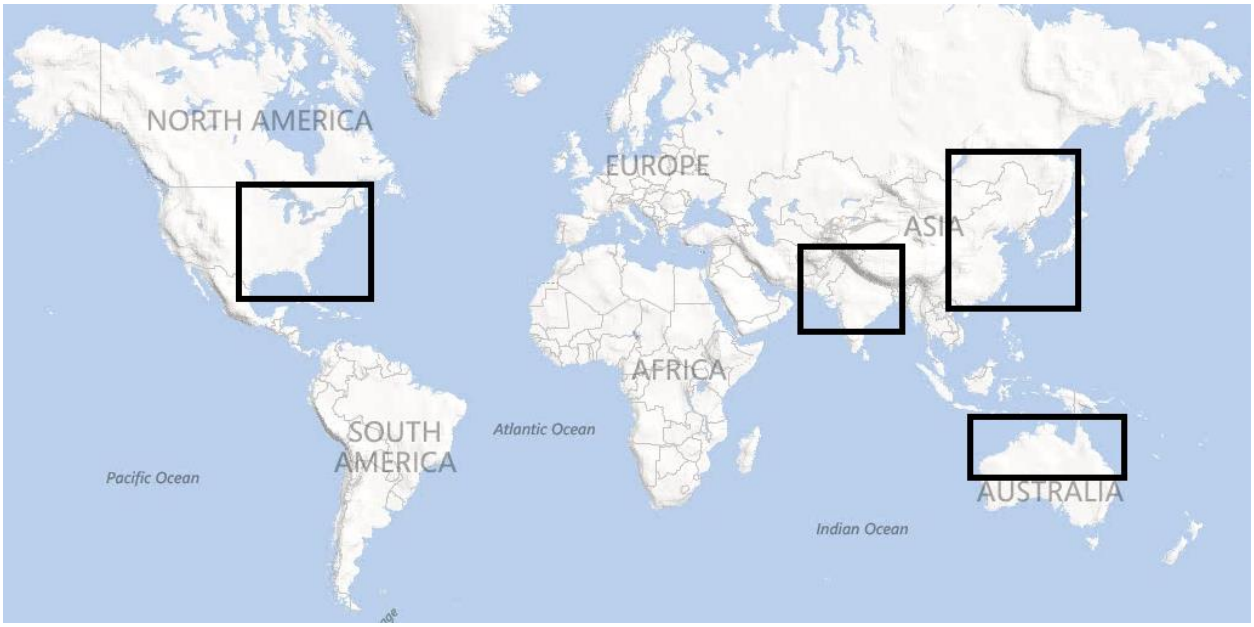

Figure 1.10: Major tropical cyclone landfall regions worldwide.

CHAPTER 2

A GLOBAL SPATIO-TEMPORAL ANALYSIS OF INLAND TROPICAL CYCLONE MAINTENANCE OR INTENSIFICATION[1]

[1] Andersen, T.K., and J.M. Shepherd (2013). A global spatiotemporal analysis of inland tropical cyclone maintenance or intensification. *International Journal of Climatology*, 1-12. DOI: 10.1002/joc.3693. Reprinted here with permission of the publisher.

Abstract

Forecasting tropical cyclone (TC) intensity changes over land is complicated by interactions of various surface and atmospheric features. Due to generally unfavorable conditions, many TCs weaken and decay soon after landfall. In some cases, TCs may also transition to extratropical cyclones (ETs). Despite the absence of oceanic forcing, a number of TCs have been observed to maintain or increase strength inland, termed "tropical cyclone maintenance or intensification' (TCMIs). This study identifies the environments and characteristic features of TCMIs and explores physical processes that may help to produce an atmosphere conducive for tropical systems. The objectives are to compile an inland TC dataset over a 30-year period, quantify TC traits that may relate to maximum strength over land, and analyse surface and atmospheric conditions leading up to intensification. Of 227 inland TCs globally, 45 maintained or increased strength inland: 17 cold-core (ET), 16 warm-core (TCMI), and 12 hybrid cases. Analysis of synoptic conditions indicates that TCs persist when low-level temperature gradients are weak. Soil moisture gradients were in the vicinity of the cyclones at the time of intensification and may be forcing the TCMIs via increased surface latent heat flux (LHF). The area-averaged LHF threshold is found to be around 70 W m^{-2} for TCMI occurrence. In the 2 weeks leading up to each TCMI, the LHF tends to be higher than average over the intensification regions and provides further evidence of land surface forcing.

2.1 Introduction

Current climate change may impact the frequency, intensity, and distribution of tropical cyclones (TCs) as the water cycle accelerates and weather patterns shift (Shepherd and Knutson, 2007). Forecasting TC intensity changes has proved difficult, especially over land where tropical systems may interact with a variety of synoptic, mesoscale, convective, and topographic features. Most tropical systems weaken over land owing to increased friction, moisture loss, and general baroclinicity. However, there have been cases of TCs actually maintaining or increasing strength inland far from the preferred oceanic energy source. Such events have occurred in the United States (Arndt *et al*. 2009), India (Chang *et al.* 2009), China (Chen 2012), and Australia (Emanuel *et al.* 2008). It is hypothesized that these TCs are forced from below by soil moisture and energy fluxes, termed the *brown ocean* effect.

This study identifies the environments and characteristic features of TCs maintaining warm cores inland and explores physical processes that may help to produce a moisture-rich boundary layer. Specifically, the objectives are to (1) compile an inland TC dataset over a 30-year period and further classify events based on intensity and thermal structure, (2) quantify path length, over-ocean intensity, and other cyclone traits that may relate to maximum strength over land, and (3) analyze surface and atmospheric conditions to understand physical mechanisms associated with maintaining a warm-core tropical low pressure system. The remainder of the paper is organized into four sections. Section 2.2 provides background information on TC classification and soil moisture–atmospheric feedbacks. Section 2.3 lists the datasets used and methodology for assessing inland TCs. The results of the three objectives are presented in Section 2.4, followed by a discussion and concluding remarks in Section 2.5.

2.2 Background

Over land, the defined spectrum of TC types is limited as there is no comprehensive post-landfall scale in place. The traditional Saffir-Simpson scale, based on wind speed, does not sufficiently account for total damage following landfall (Senkbeil and Sheridan 2006, Kantha 2010). A supplemental classification system for postlandfall hurricanes in the United States has been proposed owing to the increasing urbanization and population along the Atlantic coast (Senkbeil and Sheridan 2006). An updated hurricane classification system would use air pressure, maximum sustained winds, gust score, storm surge, duration, and precipitation for post-landfall identification of hurricane types. Other studies have focused on standardizing wind speed scales for global applicability (Dotzek 2009). Additionally, research contributed to the World Meteorological Organization (WMO) Seventh International Workshop on Tropical Cyclones (Gyakum 2010) describes several types of tropical systems that deviate from the Saffir-Simpson scale (i.e. hybrid, subtropical, and frontal). Research from the present study may add another type, termed tropical cyclone maintenance or intensification (TCMI). TCMIs describe tropical systems that maintain tropical characteristics over land where forcing is not from the ocean.

Soil moisture, an important component of the water cycle, has a direct effect on the atmosphere through moisture and energy exchanges (Mahmood *et al*. 2006). The moisture supply and instability of the planetary boundary layer (PBL) are key elements for convective storm development. Studies have shown that differential heating caused by wet–dry soil boundaries can initiate a thermal circulation in a conditionally unstable atmosphere (Rabin *et al*. 1990, Hong *et al.* 1995). These wet–dry boundaries can form from previous rainfall,

deforestation boundaries, or alternating bare soil-vegetation areas. Land cover boundaries, such as urban to agricultural, have been linked to convective cloud mass clustering (Brown and Arnold 1998). Other studies have shown that wet soil alone, because of sensible and latent heat fluxes (LHFs), can transport energy and moisture into the atmosphere to enhance convective available potential energy (CAPE) (Clark and Arritt 1995, Lynn *et al*. 1998, Bosilovich and Sun 1999). These fluxes create 'land–land breezes' that help lift parcels to initiate convection (Hanesiak *et al.* 2004). Moisture transfer through plant evapotranspiration can also cause differential heating in the atmosphere, leading to local thermal circulations and convective instability (Chang and Wetzel 1991, Pan *et al*. 1996, Hanesiak *et al.* 2004, Alonge *et al.* 2007, Iwasaki *et al*. 2008, Frye and Mote 2010).

The energy contributed by the land surface may help sustain tropical systems through similar processes. Arndt *et al.* (2009), Evans *et al.* (2011) and Kellner *et al.* (2012) suggest that anomalously wet soils in Oklahoma aided in the reintensification of Tropical Storm Erin (2007) by creating a favourable thermodynamic environment with enhanced moist static energy and latent heat. Chang *et al.* (2009) found, using the weather research and forecast (WRF) model, that monsoon depressions (MDs) are sensitive to soil moisture (i.e. heavy rainfall events 1 week prior to landfall are associated with longer sustained MD intensity over land). Emanuel *et al.* (2008) cite that large vertical heat fluxes from moistened, hot sands in northern Australia can help intensify landfalling TCs. Sandy soil must be wetted from the cyclone itself, very recently wetted from prior rain events, or exhibit moisture persistence in order to impact TC intensity. Kishtawal *et al*. (2012) state that soil heat flux is an important consideration in assessing inland decay of TCs due to heat and moisture transfer. Chen (2012) found that frictional effects over land can increase radial wind convergence and convection helping to sustain typhoons that

would otherwise decay over China. Alternatively, large reservoirs, lakes, and wetlands can supply energy to typhoons post-landfall.

Over land, synoptic-scale features interact with tropical systems often resulting in weakening of the cyclone or a transition to an extratropical system. The National Hurricane Center (NHC) defines extratropical transition (ET) by subjective satellite interpretation of storm structure within 1–2 d of transition (Hart and Evans 2001). Transitioning cyclones cause damaging winds, floods, and coastal erosion hundreds of kilometers beyond the storm center. An extratropical transitioning storm will develop an increasingly asymmetric temperature field and cold-core structure (geostrophic wind speed increasing with height) in response to the baroclinic atmosphere. In the North Atlantic, ETs are suggested to be more common than in the Pacific, particularly near the United States east coast and Canadian maritime areas. Superstorm Sandy is a recent example of tropical to extratropical transition as documented in the study by Shepherd (2012). The situations in which inland TCs are reinforced instead of transformed may occur when the environment mimics barotropic conditions (i.e. low shear and uniform temperature), or when peripheral weather systems contribute moisture and energy to the system. Low-level jets transport moisture and momentum, upper-level jets enhance outflow, and mesoscale vortices can merge with and strengthen TCs in some cases (Chen 2012).

2.3 Data and methodology

Data

Geographic Information Systems (GIS) software, along with satellite-based datasets, provide the tools essential to spatially and temporally analyze TCs globally. The tracks and attributes (i.e. location, wind speed, and pressure) of TCs are obtained from International

Best Track Archive for Climate Stewardship (IBTrACS, http://www.ncdc.noaa.gov/oa/ibtracs/) during the satellite era (1979–2008). IBTrACS merges multiple datasets from international meteorological centers into one cohesive archive for public use. The originating data centers applicable to this study are the US National Hurricane Center, Australian Bureau of Meteorology, Hong Kong Observatory, China Meteorological Administration, and India Meteorological Department.

Atmospheric and environmental data prior to and during TC events are obtained from NASA Modern Era Retrospective-Analysis for Research and Applications (MERRA, http://gmao.gsfc.nasa.gov/research/merra/intro.php). MERRA integrates multiple observing systems with numerical models to produce gridded variables. The atmospheric assimilation emphasizes the hydrological cycle, which helps minimize uncertainty in precipitation and inter-annual variability. The data include 3-hourly 600 and 900 hPa geopotential heights (m), 300 hPa maximum eastward wind component, monthly surface LHF (W m^{-2}), monthly fractional topsoil layer wetness, and 3-hourly surface LHF (W m^{-2}).

Methodology

The NHC defines landfalling as 'the intersection of the surface center of a TC with a coastline'. The central points along the paths of TCs can be found in data records making it straightforward to determine the time of landfall. The time of reaching 'inland' is less well-defined because of the varying sizes of hurricanes and disorganized nature of weaker TCs. In determining TC size, Frank (1977) found the cyclonic, convergent inflow to be within a 4º–6º radius of the center and Evans and Hart (2003) found the potential vorticity signature to be well within a 500 km radius. To ensure the energetics are not being driven by the ocean but still capture all potential TCMI cases, inland tropical cyclones (ITCs) are defined as those landfalling

storms that subsequently have a central pressure measurement at least 350 km away from the nearest coast. This radius corresponds to the typical edge of outer rainbands based on research by Frank (1977).

ITC types are determined by the cyclone phase spacing technique of Evans and Hart (2003). Cyclone phase space is a useful tool for retroanalysis of ET (Kofron *et al*. 2010) and can help differentiate cold-core versus warm-core systems. This method computes the thermal wind for assessing the thermal nature of the storm at any given time. Here it is computed during maintenance (steady pressure and/or wind speed since landfall) or intensification (lowering pressure or increasing wind speed inland) (termed 'MIs'). The warm-core and cold-core structures are distinguished with the 600–900 hPa thermal wind measurement:

$$- v_T^L = \frac{\P(z_{\max} - z_{\min})}{\P \ln p}\Bigg|_{900hPa}^{600hPa} \qquad \text{(Eq. 2.1)}$$

where z_{max} is the maximum height value and z_{min} is the minimum height value at a pressure level between 600 and 900 hPa within the storm's radius. The radius is measured from center of the surface cyclone at a given time. The method for sub-categorizing TCs is summarized in Figure 2.1.

After TCMI events are identified, the spatiotemporal distribution, maximum sustained wind speed, minimum central pressure, over-ocean intensity, and path length are assessed for common features using analysis of variance (ANOVA). Atmospheric pre-existing conditions for ET and TCMI are examined with the 850 hPa temperature range and 300 hPa maximum u-component wind speed using two-sample t -tests. Surface conditions are assessed with fractional soil wetness and surface LHF to better understand the physical mechanisms associated with maintaining TCs over land.

2.4 Results

Climatology

Of 227 ITC cases, 45 maintained or increased strength inland (MIs) (Table 2.1). Figure 2.2 shows the spatial distribution of the neutral, cold-core (ET), and warm-core (TCMI) cyclones based on thermal wind calculations. There were 17 ET events, which occurred mainly over North America, 16 TCMI cases occurring primarily over Australia, and 12 neutral/hybrid cases occurring over the United States, India, and China. India has the fewest events overall.

The years with the most ITCs do not necessarily produce the most TCMI cases. The 4 years with the highest counts of inland TCs (i.e. 1996, 1999, 2005, and 2008) actually have relatively low TCMI counts (Figure 2.3). Pearson's correlation coefficient is r = 0.22 for global ITCs versus all MIs and r = 0.12 for global ITCs versus TCMIs. A linear fit suggests that ITC frequency is increasing by 1 every 11 years possibly from better reporting or the positive phase of the Atlantic multidecadel oscillation (AMO).

China and the United States have the most TCs trekking over land, but Australia exhibits the most TCMI cases over the study period (Figure 2.4). Therefore, TCMIs are not a function of the total number of storms in the region. The TCMIs at time of intensification inland over the four study regions, represented by hurricane symbols, are shown in Figure 2.5. The hurricane symbol size represents pressure fall (0 to 9+ hPa) and tone represents sustained wind speed increase (0 to 15+ knots) during the intensification process. Each cyclone is numbered and can be referenced to Table 2.2.

Previous studies have defined rapid intensification as +30 knots per day based on 95th percentile of wind speed change (Kaplan and DeMaria 2003) or −42 hPa d^{-1} based on 75th percentile pressure change (Holliday and Thompson 1979). These rates are ocean-based

calculations that may not necessarily apply to inland intensification; however, they help to gauge the magnitudes of values given in Table 2.2. For example, a 30 knot per day increase equals a 7.5 knot per 6-h increase, indicating at least one of the TCMIs rapidly intensified (i.e., TS Erin).

TCMI characteristics

The characteristics of TCMIs and paths are examined for any possible trends that could relate to strength over land. The over-ocean maximum wind speed for the dataset ranged from Tropical Depression to Category 3 hurricane. The pre- and post-landfall pairs of values for minimum pressure and maximum sustained wind speed indicate maximum strength over ocean does not control the strength over land (Figure 2.6). The mean path length for all TCMIs is 3820 km. Broken down by regions, mean path length is 5396 km (China), 3413 km (Australia), 2180 (India), and 5536 km (United States). The regional path lengths correspond to the vastness of the originating ocean basin, and do not correspond to intensification strength. Generally, ET cases have the longest treks, TCMI cases have a wide range of track lengths, and neutral cases have the shortest treks. However, ANOVA reveals the path length differences between regions (F-ratio = 2.23 and Fcrit = 4.81) and path length differences among the three cyclone types (F-ratio = 2.40 and Fcrit = 4.30) are best explained by chance.

It has been suggested that landfalling TCs intensify over areas with large upward heat fluxes and enhanced thermal conductivity such as warm, swampy terrain, hot sands, and recently moistened soils (Emanuel *et al.* 2008). The soil types (NRCS, http://soils.usda.gov/use/worldsoils/mapindex/order.html), major biomes (NRCS, http://soils.usda.gov/use/worldsoils/mapindex/biomes.html), and land cover (NASA, http://earthobservatory.nasa.gov/Newsroom/view.php?id=22585) of the primary TCMI regions are as follows:

- Eastern China: ultisols (red clay), temperate humid biome, and croplands and mixed forest.
- South-central United States: mollisols, temperate semiarid and temperate humid biomes, and grasslands.
- Northern Australia: entisols (sandy), tropical semi-arid and desert temperate biomes, and open shrublands and savannas.
- India: alfisols, tropical semi-arid and temperate semiarid, and croplands.

Although China experiences the most hurricane landfalls, Australia has the most TCMIs. Northern Australian soil is sandy and may have relatively high sensible and LHFs during the hurricane season. Soils, climates, and vegetation vary regionally, and more in-depth modelling studies are needed to determine if surface–atmospheric feedbacks are similar across these regions.

TCMI environments

To maintain warm-core structures, it is hypothesized that TCMIs do not encounter strong wind shear and temperature gradients post-landfall (i.e. the atmosphere is baroclinically weak). To test this hypothesis, ET and TCMI atmospheric conditions (within a 750 km radius) at the time of intensification are analyzed using two-sample t-tests. Analysis of the low-level temperature gradients indicates that ET environments exhibit significantly greater 850 hPa temperature ranges than TCMI environments ($p = 0.01$). It is proposed that ITCs persist when temperature gradients are weak, while ET is encouraged by local frontal boundaries. Analysis of the upper level winds indicates that the 300 hPa maximum u-wind component is on average 12 knots higher for ET environments, but not significantly different from TCMI environments ($p = 0.16$) (Table 2.3).

TCs derive their energy from ocean surface evaporation. Latent heat release within the storm sustains the 'heat engine', allowing it to last up to several weeks (Kelley and Halverson 2011, Shepherd 2012). To remain warm-core structures over land, a similar moisture-rich environment may need to exist. Surface water content and associated LHF help to quantify the near-surface moisture and energy availability. The 1-month antecedent surface LHF (W m^{-2}), 1-month antecedent fractional top soil layer wetness, and LHF at time of TCMI exhibit similar spatial patterns, an indication that LHF is a good approximation of surface moisture and that these trends are persistent on a weekly to monthly scale. Soil moisture gradients are evident in the vicinity of intensification regions, which is consistent with the *brown ocean* concept (Figure 2.7). Over north-central Australia, three strong intensification events occurred consecutively: Sam in December 2000 (#9), Wylva in February of 2001 (#10), and Abigail in March 2001 (#11). Here, TCs are a primary source of precipitation and may provide the surface wetting to force subsequent TCMI events.

Minimum, maximum, and area-averaged LHF for each TCMI at the time of maintenance/intensification are presented in Figure 2.8. The difference between the maximum and minimum values over the intensification region is over 400 W m^{-2} in some cases and can be used to quantify the LHF gradient. Although some cases appear to have low LHF, the magnitude should only be considered relative to the particular area. To put the magnitudes in context, time series of daily LHF over the intensification region ($6^{o} \times 6^{o}$) in the 3 weeks leading up to the TCMI are examined. The mean value over the associated hurricane season is plotted for comparison. It can be seen from Figures 2.9 and 2.10 that these TCs are sustained following high LHF days to weeks prior. The high flux values are consistent with the peak of the hurricane

season (when most TCMIs occur) as summer rainfall and abundant surface heating promote evaporation. The total surface precipitation flux (kg m^{-2} s^{-1}) confirms that significant rainfall events precede TCMIs.

For each TCMI, the area-mean LHF over the 3-week antecedent period is compared to that of all weakening TCs that passed within a 3º radius of the TCMI latitude, longitude over the study period. Only TCs that occurred in a similar time of year (within 2 weeks) as the TCMIs are considered to facilitate a better comparison. Some regions experience more tropical activity overall; therefore, the number of TCs to compare vary among the TCMIs. The results indicate that North Atlantic (NA) and South Pacific/South Indian (SP/SI) regions at the time of TCMI have the highest or above average flux values as compared with instances of a weakening TC (Figure 2.11). West Pacific (WP) and North Indian (NI) TCMIs tend to exhibit average or below average LHF compared to weakening cyclones. On the basis of the results, it is suggested that there is an area-averaged LHF threshold near 70 W m^{-2} for TCMI occurrence.

2.5 Discussion and conclusion

As TCs make landfall, they often weaken owing to increased friction, wind shear, loss of moisture source, and temperature gradients. Those that remain strong tropical systems inland (i.e., TCMIs) are not well understood and are the focus of this study. An inland TC (ITC) database was derived from IBTrACS and further analysed on the basis of the observation that a system maintained or increased strength at least 350 km inland from the coast. Of 227 ITC cases, 45 maintained or increased strength inland: 17 cold-core (ET), 16 warm-core (TCMI), and 12 neutral/hybrid cases. Analysis of synoptic conditions at the time of intensification indicates that

ITCs persist when temperature gradients are weak, while ET is associated with frontal boundaries. The upper-level winds are not significantly different between ET and TCMI events. Despite the wind shear, the jet stream may aid inland TC outflow in some cases (Chen 2012).

The primary energy source for hurricanes is latent heat provided by the ample moisture originating from the ocean. Post-landfall, it is suggested that land surface feedbacks may provide the energy to continue sustaining the tropical system under certain scenarios. In previous studies, soil moisture gradients have been shown to increase the potential energy of the boundary layer, consequently enhancing instability and convection. In this study, spatial analyses of surface conditions revealed that soil moisture gradients, and associated LHF, were in the vicinity of the cyclones at the time of intensification. Analysis of LHF leading up to each TCMI reveals an overall tendency of higher than average values over the intensification regions. A TC may be more likely to intensify inland during the peak of the hurricane season when other TCs or rainfall events directly precede it.

Comparisons of each TCMI to weakening TCs found over the same region between 1979 and 2008 reveal that the intensification region consistently has higher surface LHF during an intensifying cyclone than during a weakening cyclone in the United States and Australia. These regions may exhibit stronger land surface–atmospheric feedbacks that relate to TC maintenance inland; however, comprehensive analysis of atmospheric conditions would be required to isolate the role of surface LHF. The WP and NI weakening cyclone events used here may have experienced strong synoptic forcing that encouraged TC decay despite high LHF. For all regions, an important finding is the area-averaged LHF threshold near 70 W m^{-2} for TCMI occurrence. The criteria for ‘warm-core’ and ‘inland’ used here limit the sample size of TCs for statistical analysis and may exclude events that were influenced by land surface forcing. However, the 16

TCMI cases identified showed some clear trends and commonalities that merit additional research. Future objectives using a finite element soil heat flow model and mesoscale numerical weather prediction model will help to differentiate land surface effects from larger atmospheric effects on inland TCs.

2.6 References

Alonge, C.J., K.I. Mohr, and W.-K. Tao (2007). Numerical studies of wet versus dry soil regimes in the West African Sahel. *Journal of Hydrometeorology* **8**, 102–116. doi: 10.1175/JHM559.1

Arndt, D.S., J.B. Basara, R.A. McPherson, B.G. Illston, G.D. McManus, and D.B. Demko (2009). Observations of the overland reintensification of Tropical Storm Erin (2007). *Bulletin of the American Meteorological Society* **90**, 1079–1093. doi: 10.1175/2009BAMS2644.1

Bosilovich, M.G., and W.-Y. Sun (1999). Numerical simulation of the 1993 midwestern flood: Land atmosphere interactions. *Journal of Climate* **12**, 1490–1505.

Brown, M.E., and D.L. Arnold (1998). Land-surface-atmosphere interactions associated with deep convection in Illinois. *International Journal of Climatology* **18**, 1637–1653.

Chang, J.-T., and P. Wetzel (1991). Effects of spatial variations of soil moisture and vegetation on the evolution of a prestorm environment: A numerical case study. *Monthly Weather Review* **119**, 1368–1390.

Chang, H.-I., D. Niyogi, A. Kumar, C.M. Kishtawal, J. Dudhia, F. Chen, U.C. Mohanty, and M. Shepherd (2009). Possible relation between land surface feedback and the post-landfall structure of monsoon depressions. *Geophysical Research Letters* **36**, 1-6.

Chen, L.-S. (2012). Research progress on the structure and intensity change for the landfalling tropical cyclones. *Journal of Tropical Meteorology* **18**, 113–118. doi: 10.3969/j.issn.1006-8775.2012.02.001

Clark, G.A., R.W. Arritt (1995). Numerical simulations of the effect of soil moisture and vegetation cover on the development of deep convection. *Journal of Applied Meteorology* **34**, 2029–2045.

Dotzek, N. (2009). Derivation of physically motivated wind speed scales. *Atmospheric Research* **93**, 564–574. doi: 10.1016/j.atmosres.2008.10.015

Emanuel, K., J. Callaghan, and P. Otto (2008). A hypothesis for the redevelopment of warm-core cyclones over northern Australia. *Monthly Weather Review* **136,** 3863–3872. doi: 10.1175/2008MWR2409.1

Evans, J.L., and R.E. Hart (2003). Objective indicators of the life cycle evolution of extratropical transition for Atlantic tropical cyclones. *Monthly Weather Review* **131**, 909–925.

Evans, C., R.S. Schumacher, and T.J. Galarneau (2011). Sensitivity in the overland reintensification of Tropical Cyclone Erin (2007) to near-surface soil moisture characteristics. *Monthly Weather Review* **139**, 3848–3870. doi: 10.1175/2011MWR3593.1

Frank, W.M. (1977). The structure and energetics of the tropical cyclone I. Storm structure. *Monthly Weather Review* **105**, 1119–1135.

Frye, J.D., and T.L. Mote (2010). The synergistic relationship between soil moisture and the low-level jet and its role on the pre-storm environment in the southern Great Plains. *Journal of Applied Meteorology and Climatology* **49**, 775–791. doi: 10.1175/2009JAMC2146.1

Gyakum, J.R. (2010). Subtropical and hybrid systems. WMO 7th International Workshop on Tropical Cyclones, La R´eunion France, 15–20 November 2010.

Hanesiak, J.M., R.L. Raddatz, and S. Lobban (2004). Local initiation of deep convection on the Canadian prairie provinces. *Boundary Layer Meteorology* **110**, 455–470. doi: 10.1023/B:BOUN.0000007242.89023.e5

Hart, R.E., and J.L. Evans (2001). A climatology of the extratropical transition of Atlantic tropical cyclones. *Journal of Climate* **14**, 546–564.

Hong, X., M.J. Leach, and S. Raman (1995). A sensitivity study of convective cloud formation by vegetative forcing with different atmospheric conditions. *Journal of Applied Meteorology* **34**, 2008–2028.

Iwasaki, H., T. Sato, T. Nii, F. Kimura, K. Nakagawa, I. Kaihotsu, and T. Koike (2008). Diurnal variation of convective activity and precipitable water around Ulaanbaator, Mongolia, and the impact of soil moisture on convective activity at nighttime. *Monthly Weather Review* **136**, 1401–1415. doi: 10.1175/2007MWR2062.1

Kantha, L. (2010). Discussion of "A hydrodynamics-based surge scale for hurricanes". *Ocean Engineering* **37**, 1081–1084. doi: 10.1016/j.oceaneng.2010.04.003

Kaplan, J., and M. DeMaria (2003). Large-scale characteristics of rapidly intensifying tropical cyclones in the North Atlantic basin. *Weather and Forecasting* **18**, 1093–1108.

Kelley, O.A., and J.B. Halverson (2011). How much tropical cyclone intensification can result from the energy released inside of a convective burst? *Journal of Geophysical Research* **116**, 1-14.

Kellner, O., D. Niyogi, M. Lei, and A. Kumar (2012). The role of anomalous soil moisture on the inland reintensification of Tropical Storm Erin (2007). *Natural Hazards* **63**, 1-27. doi: 10.1007/s11069-011-9966-6

Kishtawal, C.M., D. Niyogi, A. Kumar, M.L. Bozeman, and O. Kellner (2012). Sensitivity of inland decay of North Atlantic tropical cyclones to soil parameters. *Natural Hazards* **63**, 1527-1542.

Kofron, D.E., E.A. Ritchie, and J.S. Tyo (2010). Determination of a consistent time for extratropical transition of tropical cyclones. Part I: examination of existing methods for finding "ET time". *Monthly Weather Review* **138**, 4328–4343. doi: 10.1175/2010MWR3180.1

Lynn, B. H., W.-K. Tao, and P. J. Wetzel (1998). A study of landscape–generated deep moist convection. *Monthly Weather Review* **126**, 928-942.

Mahmood, R., S.A. Foster, T. Keeling, K.G. Hubbard, C. Carlson, and R. Leeper (2006). Impacts of irrigation on 20th century temperature in the northern Great Plains. *Global and Planetary Change* **54**, 1–18. doi: 10.1016/j.gloplacha.2005.10.004

Pan, Z., E. Takle, M. Segal, and R. Turner (1996). Influences of model parameterization schemes on the response of rainfall to soil moisture in the central US. *Monthly Weather Review* **124**, 1786–1802.

Rabin, R.M., D.J. Stensrud, S. Stadler, P.J. Wetzel, and M. Gregory (1990). Observed effects of landscape variability on convective clouds. *Bulletin of the American Meteorological Society* **71**, 272–280.

Senkbeil, J.C., and S.C. Sheridan (2006). A postlandfall hurricane classification system for the United States. *Journal of Coastal Research* **22**, 1025–1034. doi: 10.2112/05-0532.1

Shepherd, J.M. (2012). What we can learn from the satellite-based rainfall footprint of Superstorm Sandy: A preliminary synopsis. *Earthzine*. Published online 16 Dec (<http://www.earthzine.org/2012/12/16/what-we-can-learn-from-the-satellitebased-rainfall-footprint-of-superstorm-sandy-a-preliminarysynopsis/>)

Table 2.1: The maximum sustained wind speed (kts), minimum central pressure (hPa), and 600-900 hPa thermal wind measurements for cyclones during maintenance or intensification inland. *Cold-core* indicates the storm transitioned from tropical to extratropical cyclone (ET). *Warm-core* indicates the storm maintained tropical characteristics (TCMI). *Neutral* indicates the storm is a hybrid of both types.

Cyclone	**UTC/Date**	**Wind Speed** [kts]	**Pressure** [hPa]	**Δ900-Δ600** [hPa]	**Core type**
Hope	0600 8-9-1979	25	--	< 10	neutral
Freda	0000 8-9-1984	17	996	-13	cold
Nelson	1800 8-25-1985	19	997	< 10	neutral
Winifred	0600 2-3-1986	21	999	+14	warm
Bonnie	0000 6-28-1986	15	1014	< 10	neutral
Connie	0600 1-22-1987	39	992	-26	cold
Irma	0000 1-22-1987	30	--	+20	warm
Gilbert	1200 9-19-1988	25	999	-19	cold
Hugo	0600 9-23-1989	40	990	-71	cold
1990226N19088	0000 8-16-1990	27	995	< 10	neutral
1990232N22089	1200 8-24-1990	27	994	-12	cold
Daphne	0000 2-20-1991	20	--	+10	warm
1991208N21090	0000 7-30-1991	30	988	+25	warm
1991234N20089	1200 8-23-1991	25	992	< 10	neutral
Nat	0600 10-3-1991	--	1008	+10	warm
Tim	0600 7-12-1994	29	992	+10	warm
Annette	0600 12-19-1994	35	995	-16	cold
Opal	1800 10-5-1995	40	986	-15	cold
Fran	0000 9-8-1996	30	999	+10	warm
Amber	0600 8-31-1997	--	1002	< 10	neutral
Olga	0600 8-5-1999	--	996	+14	warm
1999219N21089	0600 8-8-1999	20	992	< 10	neutral
Dennis	1800 9-8-1999	20	1005	-10	cold
Sam	1200 12-12-2000	44	--	+17	warm
Terri	0000 2-1-2001	41	990	-30	cold
Winsome	0000 2-13-2001	25	988	< 10	neutral
Wylva	1200 2-18-2001	--	988	+21	warm
Abigail	0000 3-3-2001	25	992	+10	warm
Barry	0000 8-8-2001	10	1016	< 10	neutral
2003206N21089	1200 7-26-2003	30	988	-10	cold
2003279N17084	0600 10-9-2003	25	1000	+23	warm
Fritz	0600 2-14-2004	25	992	-19	cold
2004163N16090	1200 6-14-2004	25	990	< 10	neutral
Frances	1200 9-9-2004	30	1001	< 10	neutral
Haima	0600 9-16-2004	29	993	-25	cold
Arlene	0600 6-14-2005	20	1003	-26	cold
Dennis	0000 7-18-2005	10	1010	-18	cold
Emma	1200 2-28-2006	29	988	+10	warm
Sepat	0600 8-23-2007	19	1002	-10	cold
George	0600 3-10-2007	30	986	+24	warm
2007172N15088	0000 6-23-2007	20	1007	+10	warm
Erin	0600 8-19-2007	50	995	+19	warm
Gustav	1800 9-4-2008	20	1000	-15	cold
Ike	1200 9-14-2008	40	987	-19	cold
Two	1800 9-18-2008	25	996	< 10	neutral

Table 2.2: Global tropical cyclone maintenance/intensification events (TCMIs) 1979-2008. The pressure drop and wind speed increase during the inland intensification process (ranging 6 h to 42 h) are listed. The number in the first column corresponds to the cyclone in Figure 2.5.

	Cyclone	**TCMI Location** [Lat, Lon]	**Span of Intensification** [hours]	**Pressure Change** [hPa]	**Wind Speed Change** [kts]
1	Winifred	-20.9, 141.4	6	0	+5
2	Irma	-17.3, 132.4	6	--	0
3	Daphne	-18.5, 131.8	6	--	+5
4	1991208N21090	22.5, 80.0	6	-2	0
5	Nat	27.9, 116.8	6	-4	--
6	Tim	29.5, 115.1	6	0	0
7	Fran	42.9, -80.1	6	-1	0
8	Olga	50.9, 131.1	6	-4	--
9	Sam	-20.5, 130.0	18	--	+11
10	Wylva	-18.6, 130.5	18	-7	--
11	Abigail	-19.7, 124.7	42	-6	0
12	2003279N17084	24.0, 86.3	6	0	0
13	Emma	-24.2, 117.1	6	-2	0
14	George	-24.0, 122.0	12	-2	0
15	2007172N15088	18.0, 77.5	6	-3	+5
16	Erin	35.6, -98.8	12	-12	+30

Table 2.3: To quantify baroclinicity, the 300 hPa eastward wind component and 850 hPa temperature range (over 1500 km diameter) between ET and TCMI cyclones are statistically analyzed. The two-sample t-test for equal variances indicates that at the 95% confidence level, the 300 hPa maximum wind is not significantly different between ETs and TCMIs, however, the 850 hpa temperature range is significantly greater for ET cases than for TCMIs. These results support the hypothesis that TCMI events are more likely to occur in environments with relatively weak temperature gradients (i.e., lack of frontal boundaries).

	300 hPa u-wind$_{max}$		850 hPa temp$_{range}$	
	TCMI	ET	TCMI	ET
mean	56.6	68.7	8.6	13.1
standard deviation	19.7	27.5	2.9	6.1
observations	16	17	16	17
p-value	0.16 (> 0.05)		**0.01** (< 0.05)	

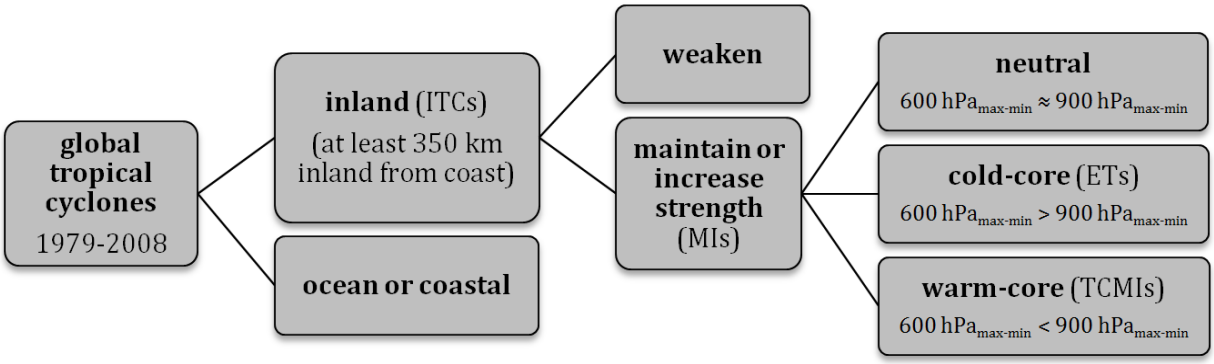

Figure 2.1: Schematic showing tropical cyclone sub-categorization.

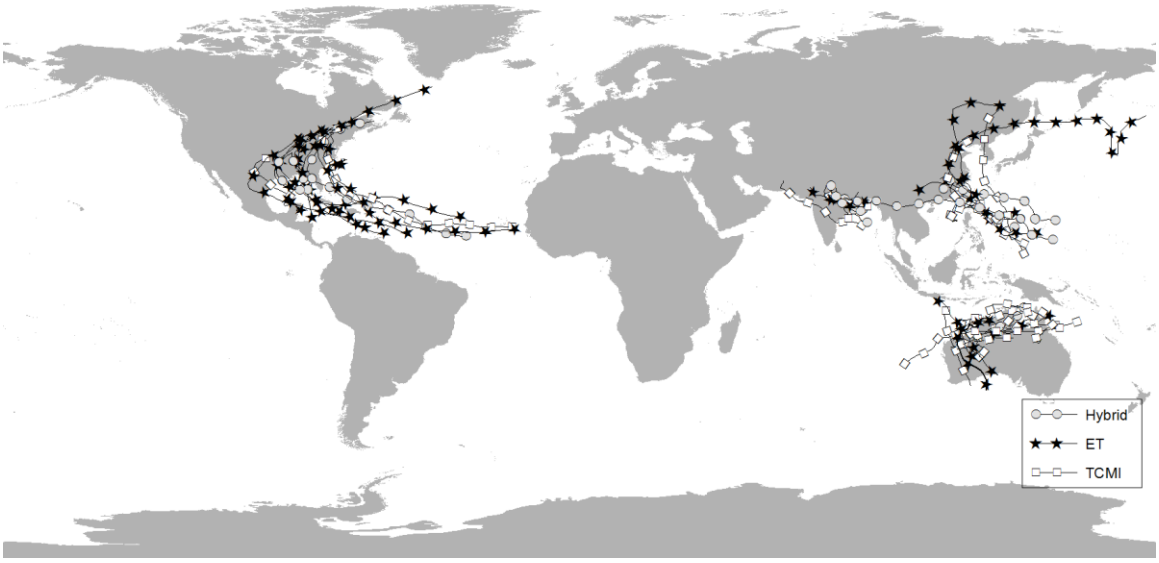

Figure 2.2: Tropical cyclones maintaining or increasing strength inland (1979-2008). Thermal wind analysis finds 17 ET (stars), 16 TCMI (squares), and 12 hybrid (circles) cases.

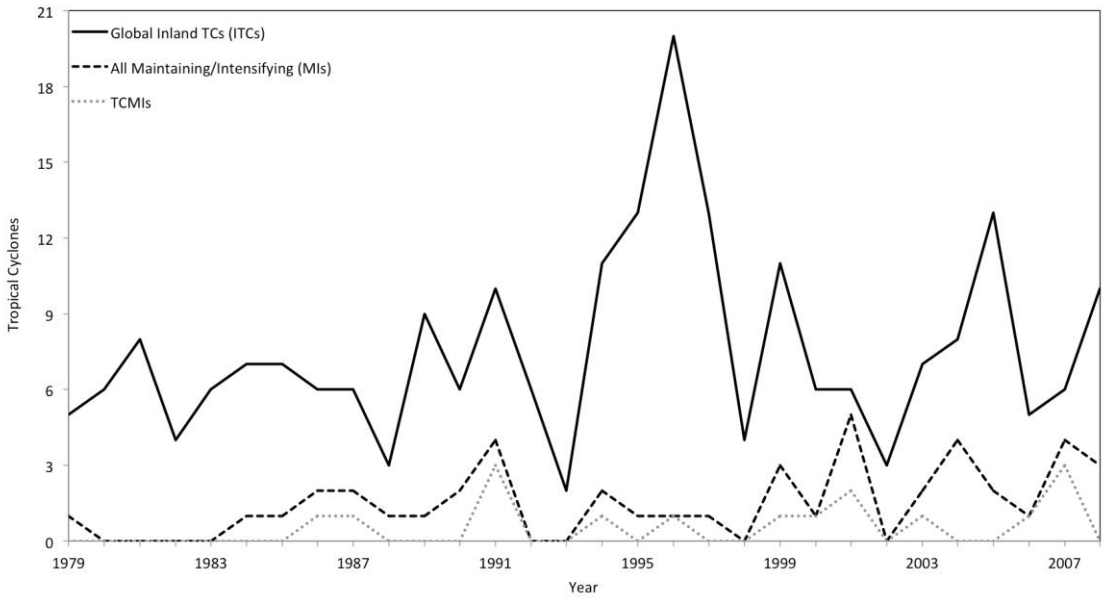

Figure 2.3: Time series of the total number of global inland TCs (solid), TCs maintaining strength or intensifying (dashed), and TCs maintaining/intensifying with warm-cores (TCMIs, dotted) between 1979-2008. Years with relatively high tropical cyclone frequency (peaks) do not necessarily produce more intensification events (r=0.22) nor TCMIs (r=0.12).

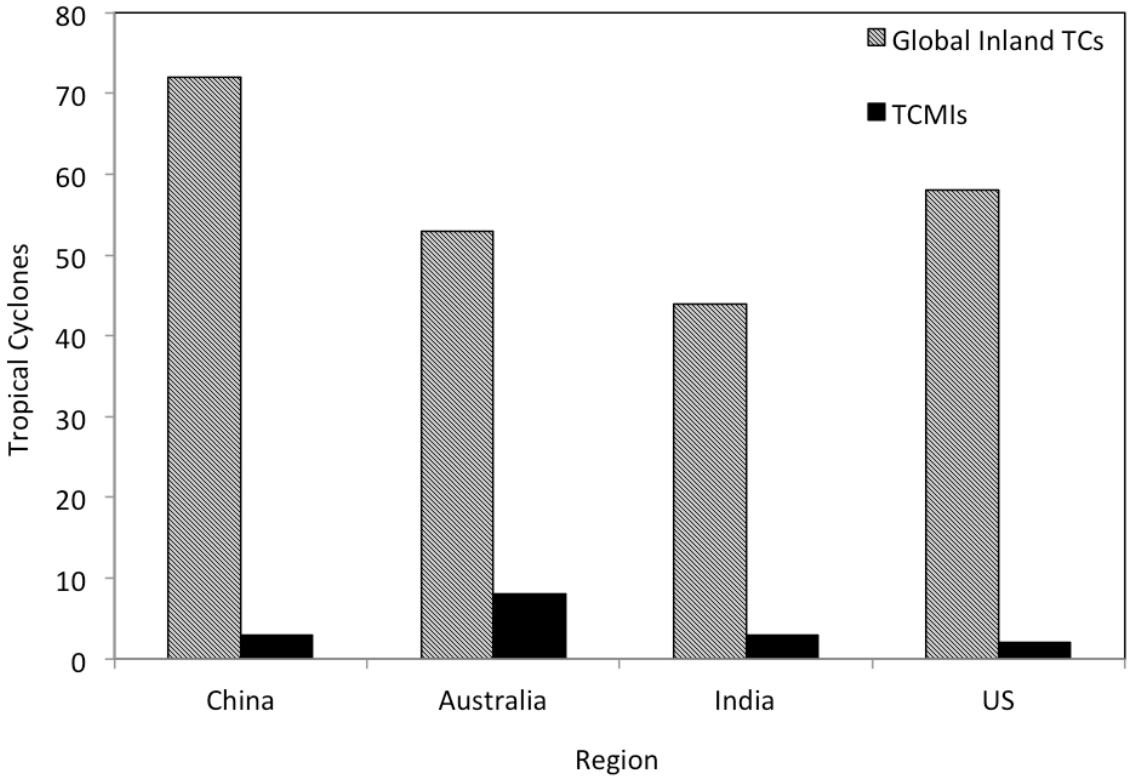

Figure 2.4: Graph of global inland TCs and TCMIs 1979-2008 by region. The US and China have high overall counts, but low TCMI counts indicating the number of TCMIs is not a function of the total number of cyclones trekking over the region.

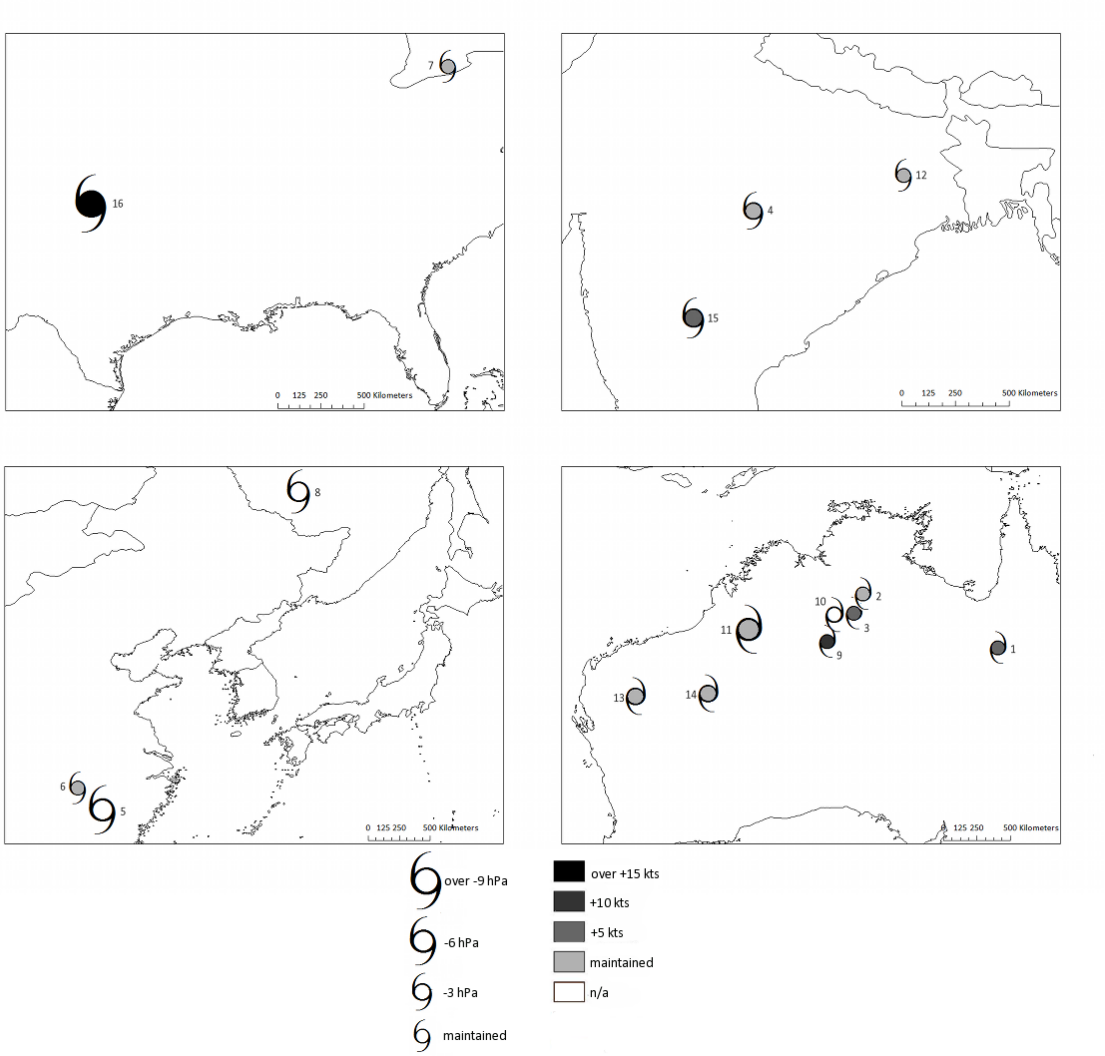

Figure 2.5: TCMIs over the US (top left), India (top right), China (bottom left), and Australia (bottom right). The hurricane symbol represents the location at time of inland maintenance or intensification. The symbol size represents pressure fall (0 to 9 hPa) and tone represents sustained wind speed increase (0 to 15+ knots) since landfall *or* previous maximum over land.

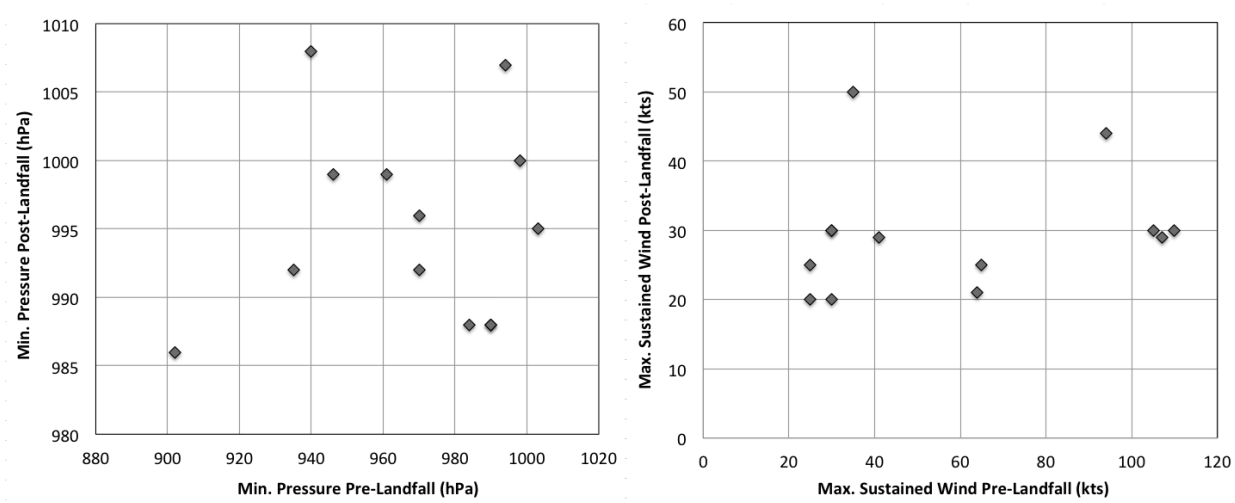

Figure 2.6: Pre- and post-landfall values for minimum pressure (left) and maximum sustained wind (right) for TCMIs. TCMIs do not appear to be a function of storm strength over the ocean.

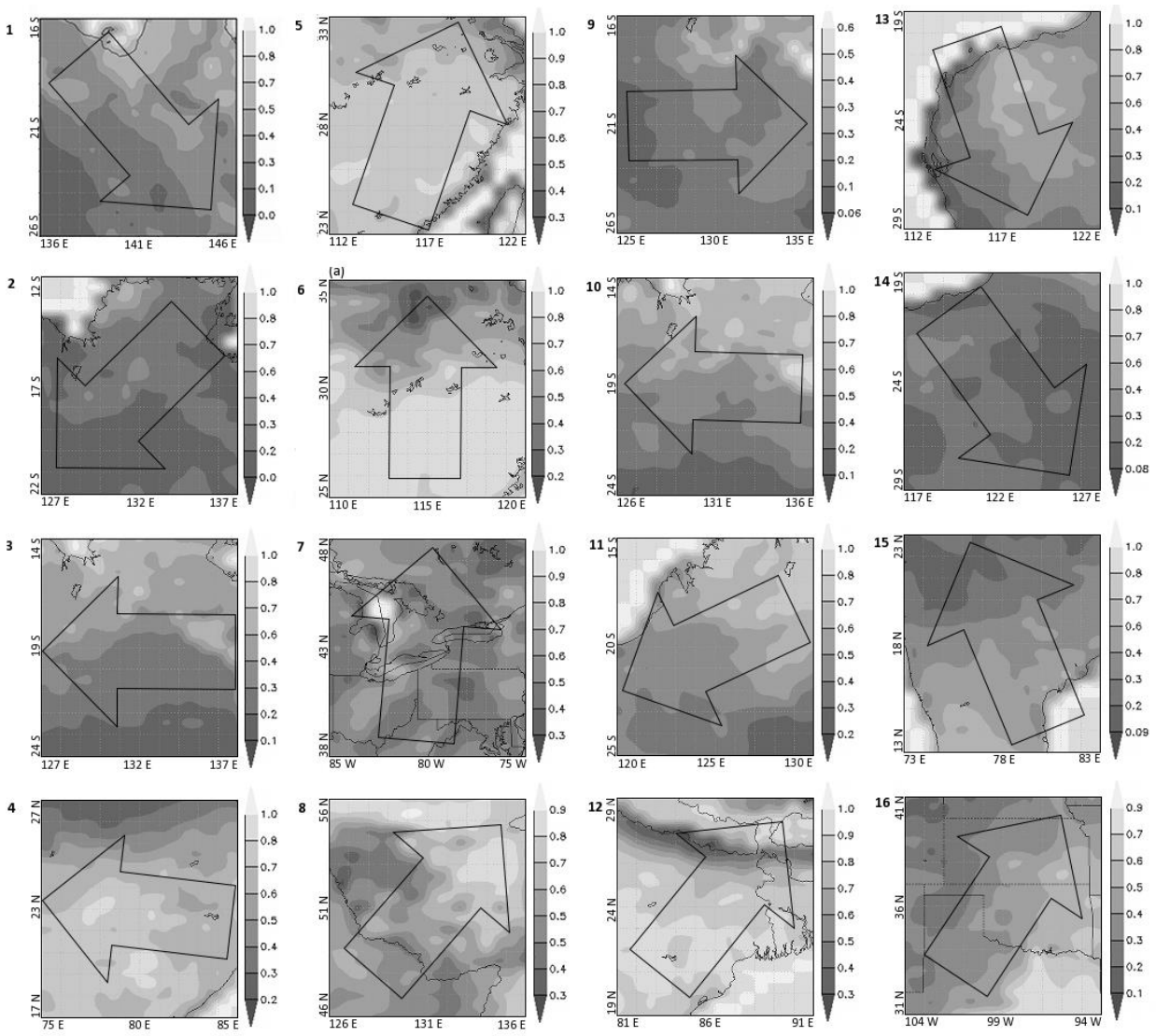

Figure 2.7: 1-month antecedent fractional top soil layer wetness for TCMI events. The arrow denotes the cyclone direction. Soil moisture gradients are evident in the vicinity of the intensification region.

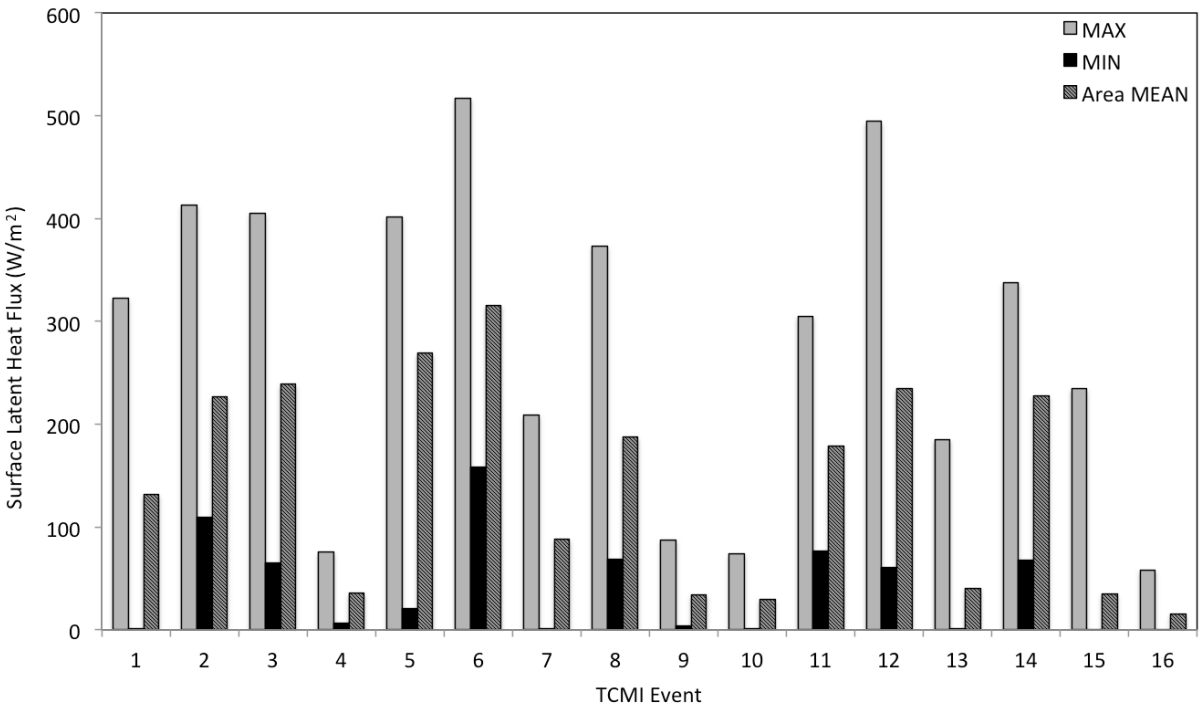

Figure 2.8: Maximum, minimum, and area-averaged surface latent heat flux (W m^{-2}) for TCMIs at time of maintenance/intensification.

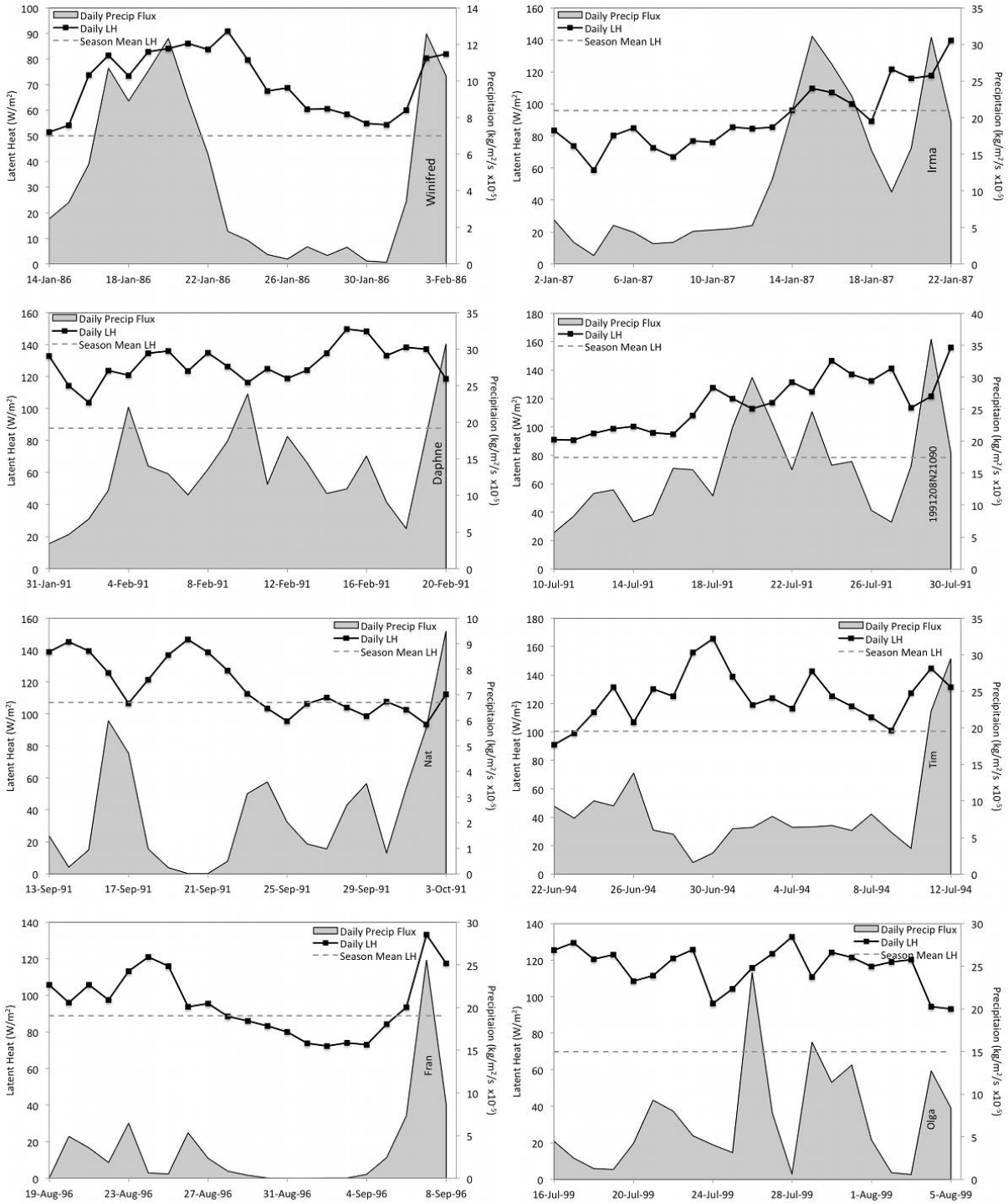

Figure 2.9: Daily area-averaged surface latent heat (squares) and precipitation flux (shading) leading up to TCMI (cyclones 1 through 8) and associated hurricane season-averaged latent heat flux (dashed line) for comparison. The final time is TCMI occurrence.

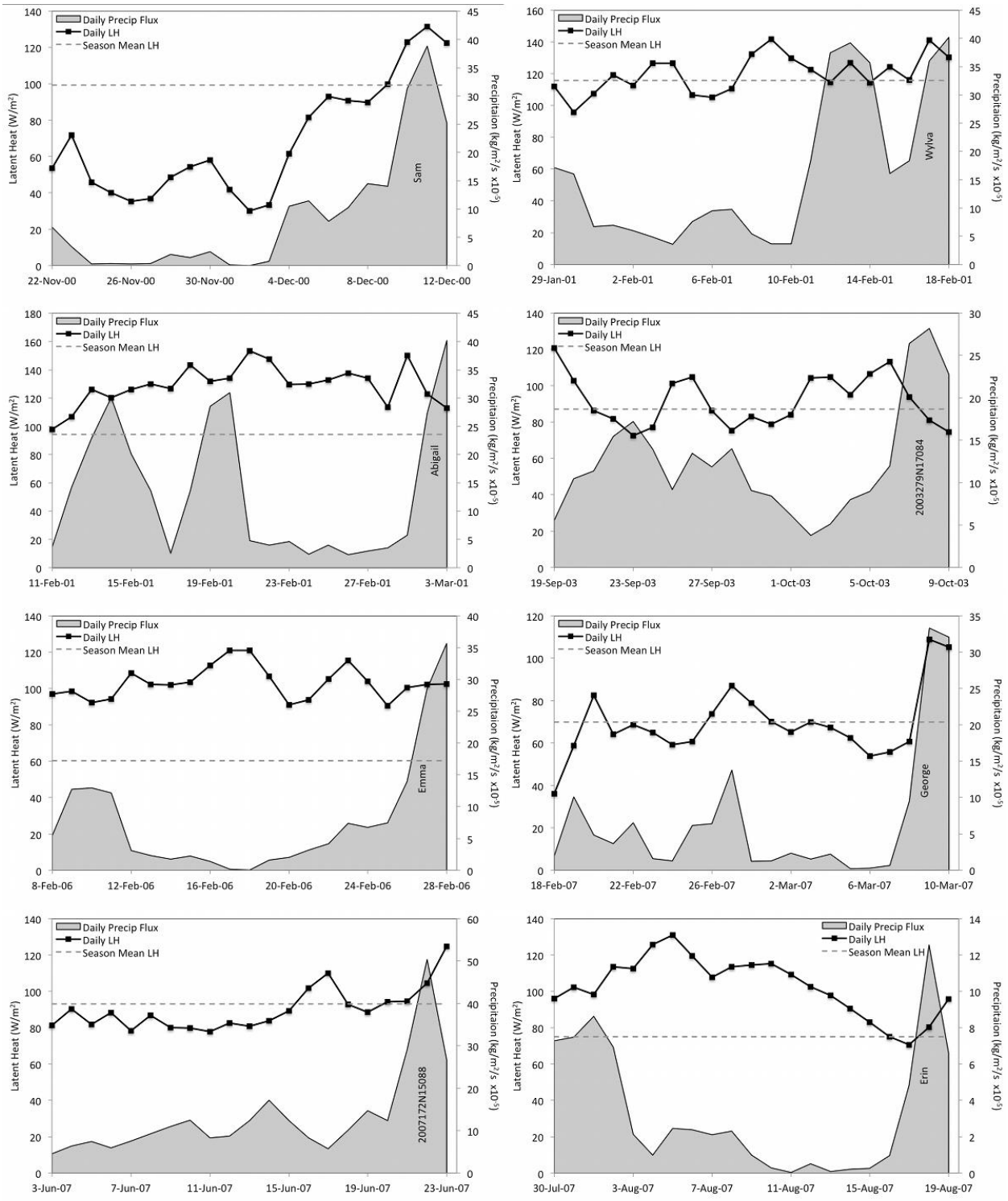

Figure 2.10: Same as in Figure 2.9, but for cyclones 9-16.

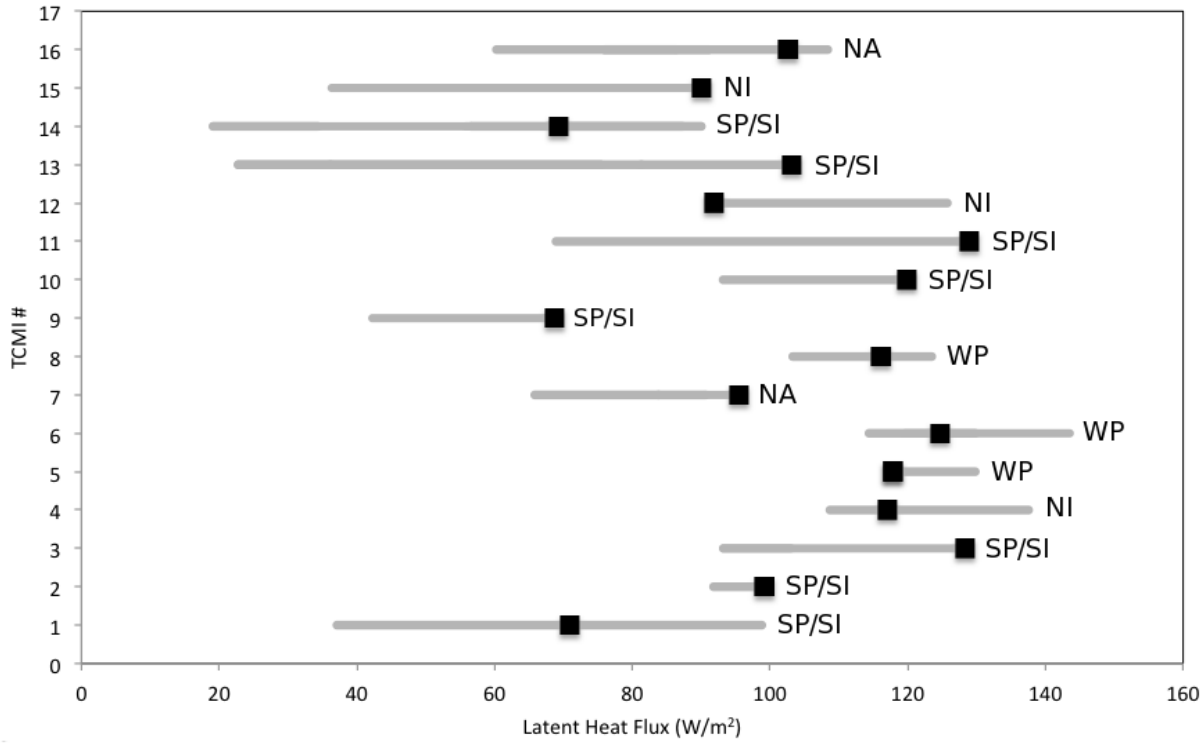

Figure 2.11: Area-averaged LHF (W m^{-2}) for the 16 TCMI regions at time of intensification (black square). The grey line indicates the range of LHF for *weakening* tropical cyclones recorded in a similar area and time of year to the TCMI between 1979-2008. The originating ocean basin is indicated to the right of each TCMI region.

CHAPTER 3

QUANTIFYING SURFACE ENERGY FLUXES IN THE VICINITY OF INLAND-TRACKING TROPICAL CYCLONES[2]

[2] Andersen, T.K., D.E. Radcliffe and J.M. Shepherd (2013). Quantifying surface energy fluxes in the vicinity of inland-tracking tropical cyclones. Submitted to *Journal of Applied Meteorology and Climatology*, 1/9/13.

Abstract

Tropical cyclones (TCs) typically weaken or transition to extratropical cyclones after making landfall. However, there are cases of TCs maintaining warm-core structures and intensifying inland unexpectedly, referred to as TC maintenance or intensification events (TCMIs). It has been proposed that wet soils create an atmosphere conducive to TC maintenance by enhancing surface latent heat flux (LHF). In this study, HYDRUS-1D is used to simulate the surface energy balance in intensification regions leading up to four different TCMIs. Specifically, the 2-week magnitudes and trends of soil temperature, sensible heat flux (SHF) and LHF are analyzed and compared across regions. While TCMIs are most common over northern Australia, theoretically linked to large fluxes from hot sands, the results revealed that SHF and LHF are equally large over the south-central US. Modern Era Retrospective-Analysis for Research and Applications (MERRA) 3-hourly LHF data were obtained for the same HYDRUS study regions as well as nearby ocean regions along the TC path 3 days prior ("pre-storm") to the TC appearance. Results indicate that the simulated pre-storm mean LHF is similar in magnitude to that obtained from MERRA, with slightly lower values overall. The modeled 3-day *mean* fluxes over land are less than those found over the ocean, however, the *maximum* LHF over the 3-day period is greater over land (HYDRUS) than over the ocean (MERRA) for 3 of 4 cases. It is concluded that LHF inland can achieve similar magnitudes to that over the ocean during the daytime and should be pursued as a potential energy source for inland TCs.

3.1 Introduction

Landfalling tropical cyclones (TCs) bring storm surge flooding, high winds, heavy precipitation, and tornadoes to coastal regions. After landfall, a TC may dissipate or transition to an extratropical cyclone (i.e., cold-core low pressure system) by merging with the midlatitude flow. Alternatively, TCs may maintain their tropical characteristics (i.e., warm-core low pressure system) and produce hazardous conditions for inland areas. Andersen and Shepherd (2013) have suggested that anomalously moist soils in the vicinity of the TC enhance the surface latent heat flux (LHF), providing energy to the cyclone that would otherwise be lacking over land. This process is characterized as the *brown ocean* effect. A global analysis of TCs maintaining or increasing in strength inland (TCMIs) over a 30-year period revealed that precipitation and soil moisture were unusually high preceding most TCMI cases while atmospheric features amenable to extratropical transition were absent (i.e., weak baroclinicity). Sixteen cases were observed in northern Australia, eastern China, India, and the US (Andersen and Shepherd 2013). Further understanding of the environment conducive to intensification events can improve forecasting and draw attention to this oft overlooked stage of tropical cyclones.

Tropical cyclones are warm-core low pressure systems that develop over the tropical oceans. The North Atlantic, North and South Indian, South Pacific and West Pacific oceans are ideal development regions when the sea surface temperature (SST) is >26.5 °C and the atmosphere is characterized by weak vertical wind shear, conditional instability, enhanced mid-troposphere relative humidity, and enhanced lower troposphere relative vorticity (Gray 1968). Latent heat flux from the warm oceans is a primary contributor to TC intensification (Kleinschmidt 1951, Miller 1958, Malkus and Riehl 1960, Liu *et al*. 2012). Latent and sensible heat transfer from the ocean surface, along with potential energy, increase the moist static energy

of the boundary layer. Convection converts moist static energy to kinetic energy thereby intensifying the primary circulation of the TC. Typically, tropical systems weaken or transition to extratropical cyclones after landfall due to the loss of the energy source from the ocean, increased wind shear, and increased friction from the land surface, among other factors (Tuleya 1994). However, in instances of weak baroclinicity, wetter than normal soil conditions may provide adequate energy to sustain TCs in a similar manner to the ocean environment (Figure 1).

Wetter soils tend to absorb more radiation compared to dry soils due to the high heat capacity of water. The net downward radiation at the soil surface can be described as:

$$R_n = SHF + L * ET + J_H \quad \text{(Eq. 3.1)}$$

where *SHF* is sensible heat flux (W m^{-2}), *L* is latent heat of vaporization (J kg^{-1}), *ET* is evapotranspiration (kg m^{-2} s^{-1}), and J_H is the soil heat flux between the surface and a deeper layer (W m^{-2}) (Radcliffe and Šimůnek 2010). Wet soils enhance evaporation and LHF which produce a moist, unstable boundary layer (Clark and Arritt 1995, Lynn *et al*. 1998, Bosilovich and Sun 1999). Although the boundary layer under these conditions is often shallow, evaporational cooling is minimal (Evans *et al*. 2011).

Strengthened moisture transport, rainfall reinforcement, and an associated latent heat trigger are identified as important factors for inland tracking storm intensity (Dong *et al*. 2010, Kishtawal *et al*. 2012). In model simulations, Chang *et al*. (2009) found that the intensity and longevity of monsoon depressions (MDs) are sensitive to soil moisture. Arndt *et al*. (2009), Kellner *et al*. (2012), and Evans *et al*. (2011) suggest that saturated soils and moisture transport in Oklahoma contributed to the reintensification of Tropical Storm Erin in 2007 by enhancing

moist static energy and latent heat release. Emanuel *et al*. (2008) performed simulations using a simple tropical cyclone model coupled to a one-dimensional soil model to determine the role of large vertical heat fluxes from recently moistened soil on northern Australia cyclone redevelopment. Results indicated that warm, wet soils may help to maintain or energize landfalling TCs through heat transfer. In Asia, freshwater bodies and wetlands are hypothesized to supply energy to typhoons removed from the ocean (Chen 2012). Shen *et al*. (2002) found that hurricane decay rate is a function of surface water depth. A 2 m layer of water can adequately maintain a hurricane's intensity over land (e.g., 950 hPa), a 0.5 m layer of water is sufficient to reduce landfall decay (e.g., 965 hPa) and no surface water leads to rapid decay (e.g., 980 hPa) 24 hours after landfall.

Herein, a numerical water and heat flow model is utilized to simulate soil characteristics and surface energy fluxes over observed regions of TC intensification. Four TCMI regions are simulated to output a time series of energy flux values two weeks leading up to the event. Fully coupled land surface-atmospheric models have been successfully employed in similar studies (Emanuel *et al*. 2008, Evans *et al*. 2011, Kellner *et al*. 2012). However, the accuracy of non-coupled versus coupled models for this particular application is beyond the scope of this research. It has been demonstrated that HYDRUS-1D effectively adapts meteorological data to simulate the surface energy balance and provides many options for soil parameters (e.g., soil type, soil texture, temperature and moisture profiles, plant rooting depth, water table, etc). HYDRUS-1D is valuable as a meteorological application because it solves coupled equations governing liquid water, water vapor, and heat transport within the soil. The model is tested public domain code that requires a minimal amount of computational resources, it has a straight-forward user interface, and it is well-documented (Saito *et al*. 2006). While recent re-analysis

datasets provide surface energy flux data globally, using a soil model such as HYDRUS-1D allows flexibility and control over the environmental conditions. Specifically, the model is used to simulate heat and moisture fluxes over bare soil conditions. Vegetation moderates the LHF of an area while energy fluxes over bare soil are more variable. Previous work has suggested that TCMIs are unique to Australia because of the ability of sandy soil to suddenly release huge amounts of energy when moistened (Emanuel *et al*. 2008). By simulating the energy balance of each intensification region without vegetation, the fluxes can be directly linked to soil texture.

The objectives of this research are to (1) simulate the soil profiles of TC intensification regions in the two weeks leading up to TCMI events, (2) determine the trends and magnitudes of surface energy fluxes prior to a TC tracking over and intensifying and (3) compare the simulated energy flux values to typical values over the tropical ocean. Although the purpose of this study coincides with Emanuel *et al.* (2008) (i.e., quantification of surface energy fluxes in relation to TCs), the focus is on the feasibility of moist soil acting as a substitute for the ocean environment, identifying a LHF threshold for inland intensification using multiple cases, and comparing flux trends across four major landfall regions. The remainder of the paper is divided into three sections. Section 3.2 describes the inland TC case studies, data and model setup. The results are presented in Section 3.3, followed by a discussion and conclusions in Section 3.4.

3.2 Cases and model setup

Case studies

Andersen and Shepherd (2013) identified sixteen inland tropical cyclone maintenance and intensification events globally between 1979-2008. These events displayed a drop in minimum central pressure and/or increase in maximum sustained wind speed at least 350 km inland from the coast while maintaining warm-core tropical structures (determined by thermal

wind calculations). From this dataset, the strongest intensification case (i.e., greatest pressure drop) from each major hurricane basin that is minimally influenced by strong baroclinicity is chosen for analysis (Figure 3.2). The TC best track, minimum central pressure, and maximum sustained wind speed are obtained from the International Best Track Archive for Climate Stewardship (IBTrACS, http://www.ncdc.noaa.gov/oa/ibtracs/index.php). IBTrACS merges TC information from Regional Specialized Meteorological Centers, international centers, and individuals to create the most complete global best track dataset available (Knapp *et al*. 2010).

Tropical Storm (TS) Erin developed 15 August 2007 in the Gulf of Mexico. It achieved tropical storm status with 35 kt winds and subsequently made landfall near Corpus Chrisi, Texas. Re-intensification occurred over Oklahoma with the strength surpassing that of its ocean counterpart. The wind was recorded as 50 kts and pressure at 995 hPa. Studies have highlighted the anomalously wet soil in Oklahoma at this time and possible influence on TS Erin (Arndt *et al*. 2009, Evans *et al*. 2011, Kellner *et al*. 2012, Andersen and Shepherd 2013).

Typhoon Nat developed 14 September 1991 in the Philippine Sea. It reached Category 3 strength on the Saffir-Simpson Wind Scale before tracking over Taiwan and making landfall near Chaozhou, Guangdong (China). Nat weakened over land, but maintained a relatively constant pressure near the end of its lifecycle with a slight pressure drop (minimum central pressure of 1008 hPa). TC best track datasets in the West Pacific suffer from discrepanies due to varying algorithms used by the Joint Typhoon Warning Center (JTWC), Japan Meteorological Agency (JMA), and the China Meteorological Administration (CMA) (Barcikowska *et al*. 2012). Therefore, the post-landfall records for Typhoon Nat are not as reliable as more recent cases due to uncertain or missing data near the end of its lifecycle, but it proved to be the only case from the West Pacific that maintained a warm-core over land without significant meridional flow to

complicate the analysis. Considering the overall lack of TCMI cases in eastern Asia (Andersen and Shepherd 2013), it is more than likely that extratropical transition or dissipation dominates in this region (perhaps due to the extreme terrain). Nevertheless, it is still useful to include a typhoon in this study in order to gauge possible surface energy flux differences between the four primary landfall regions.

Tropical system 2007172N15088 developed 20 June 2007 in the Bay of Bengal. It strengthened to a tropical depression and made landfall on the east coast of India near Ethamukkala, Andhra Pradesh. After intially weakening, it regained strength in central India while moving northwest on 23 June. The wind was recorded at 20 kts and the pressure at 1007 hPa.

Cyclone Wylva developed 14 February 2001 in the Gulf of Carpentaria. It reached tropical storm strength at 41 kt winds before passing near Robinson River Airport in the Northern Territory of Australia. The pressure was steady for about 2 days post-landfall, then began dropping as Wylva moved west (minimum central pressure of 988 hPa). HURSAT (http://www.ncdc.noaa.gov/oa/rsad/hursat/) visible satellite images for each TCMI at the time of intensification are shown in Figure 3.3.

Model setup

HYDRUS-1D (http://www.pc-progress.com/en/Default.aspx?h1d-description) is a finite element model for simulating the 1-dimensional movement of water, heat, and solutes in soil. It numerically solves the Richards' equation for water flow and advection dispersion equations for heat and solutes. The heat transport equation includes heat flow by conduction, convection, and vapor phase, and takes into account soil water content (Saito *et al*. 2006).

Each model run simulates the water and energy balance of a TCMI region in the two weeks antecedent to the intensification event to produce LHF, SHF, and soil temperature time series. Note that HYDRUS produces time series for one specified location. Therefore, the heat flow and meteorological boundary conditions are taken from assimilated re-analysis data area-averaged means (a 6°x6° geographical area centered on the storm during intensification as indicated by the best track data). Research has shown that the cyclonic, convergent inflow is within a 4°-6° radius of the TC center and the potential vorticity signature is well within a 500 km radius (Frank 1977, Evans and Hart 2003).

Three-hourly near-surface air temperature (°C), near surface wind speed (km d^{-1}), solar radiation flux (MJ m^{-2} d^{-1}), 0-10 cm soil temperature (°C), and 40-100 cm soil temperature (°C) are obtained from Global Land Data Assimilation System (GLDAS-2 NOAH model experiment, http://ldas.gsfc.nasa.gov/gldas/). Near-surface relative humidity (%) and precipitation rate or influx (mm d^{-1}) are obtained from Modern Era Retrospective-Analysis for Research and Applications (MERRA, https://gmao.gsfc.nasa.gov/merra/). Natural Resources Conservation Service (NRCS, http://soils.usda.gov) provides information on regional soil types. A description of the case studies is shown in Table 3.1. TCMI occurrence is most common in Australia and least common in the US (Andersen and Shepherd 2013).

Water flow and heat transport are simulated for a 100 cm depth of soil. It has been shown that vapor flow is important to consider in arid and semiarid regions (Scanlon *et al*. 2003) and is accounted for along with water flow:

$$\frac{\partial \theta(h)}{\partial t} = \frac{\partial}{\partial x}\left[(C + C_{vh})\left(\frac{\partial h}{\partial x} + 1\right) + (C_{LT} + C_{vT})\frac{\partial T}{\partial x}\right] - S(h) \qquad \text{(Eq. 3.2)}$$

where θ is the total volumetric water content ($cm^3\ cm^{-3}$), x is depth (cm), T is temperature (K), C is the isothermal hydraulic conductivity of the liquid phase ($cm\ K^{-1}$), C_{LT} is the thermal hydraulic conductivity of the liquid phase ($cm^2\ C^{-1}\ K^{-1}$), C_{vh} is the isothermal vapor hydraulic conductivity ($cm\ K^{-1}$), and C_{vT} is the thermal vapor hydraulic conductivity ($cm^2\ C^{-1}\ K^{-1}$). Heat flow with vapor transport is calculated as:

$$C_p(\theta)\frac{\partial T}{\partial t} + L_0\frac{\partial \theta_v}{\partial t} = \frac{\partial}{\partial x}\left(\lambda(\theta)\frac{\partial T}{\partial x}\right) - C_w q\frac{\partial T}{\partial x} - C_v\frac{\partial q_v T}{\partial x} - L_0\frac{\partial q_v}{\partial x} \qquad \text{(Eq. 3.3)}$$

where C_p is volumetric heat capacity of the porous medium ($kg\ cm^{-1}\ K^{-2}\ C^{-1}$), θ is volumetric water content ($cm^3\ cm^{-3}$), θ_v is volumetric water vapor content ($cm^3\ cm^{-3}$), L_0 is the volumetric latent heat of vaporization of liquid water ($kg\ cm^{-1}\ K^{-2}$), C_w is volumetric heat capacity of the liquid phase ($kg\ cm^{-1}\ K^{-2}\ C^{-1}$), q is Darcian fluid flux density ($cm\ K^{-1}$), and q_v is the vapor flux density ($cm\ K^{-1}$). The simulation time is 14 days with 112 time-variable boundary records and 112 meteorological records specifying an energy balance boundary condition. The van Genuchten–Mualem soil hydraulic model is used with no hysteresis. The water flow parameters are chosen according to the soil textural class (e.g., sand, clay, or loam). The water flow boundary conditions are atmospheric with surface runoff (upper) and zero pressure head gradient or free drainage (lower), assuming the water table is well below the simulated soil profile. The heat transport parameters and thermal conductivity used are from the HYDRUS soil catalog (adapted from Carsel and Parrish 1988). The heat transport boundary conditions are temperature (upper) and zero gradient (lower). Solar radiation flux, solar radiation-based cloudiness factor, TCMI location latitude and altitude, and relative humidity are selected as meteorological parameters. For the soil profile, initial pressure head is set to -100 uniformly (approximately field

capacity). The surface LHF term is:

$$E = \frac{\rho_s - \rho_a}{r_a + r_s} \quad \text{(Eq. 3.4)}$$

where ρ_s is the water vapor density at the soil surface (kg m^{-3}), ρ_a is the atmospheric vapor density (kg m^{-3}), r_a is the aerodynamic resistance to water vapor flow (s m^{-1}), and r_s is the soil surface resistance to water vapor flow (s m^{-1}). Further information on numerical solutions and equations are provided in the HYDRUS-1D manual by Šimůnek *et al*. (2009).

3.3 Results

HYDRUS

The soil temperature and sensible and latent heat fluxes from the model runs are used to assess the surface conditions prior to the tropical cyclone. The soil temperature profiles for bare soil show that the surface is most susceptible to diurnal temperature variations (Figure 3.4). In southeastern China, northern Australia, and central India, the temperatures slightly decrease with time, while soil temperatures in the south-central US increase. The US and Australia have the greatest diurnal fluctuations and highest maximum temperatures. The reason for this observation may be related to high solar radiation during the day (summertime TCMI occurrence) and radiational cooling at night (clear skies). In Australia and India, deeper soil remains warmer on average compared to the other cases owing to the tropical climate. In all regions, the daily maximum surface temperature equals or surpasses the 26.5 ºC SST threshold: 26.5 ºC in China, 37.7 ºC in the US, 39.9 ºC in Australia, and 33.7 ºC in India.

SHF time series for each region are shown in Figure 3.5. Note that the model output is in incremental time steps, therefore the time series plots undergo some smoothing to generate 3-

hourly data. SHF magnitudes over China and India are very low, less than 30 W m^{-2} for the duration of the simulations. For much of the time, SHF is negative implying that the ground temperature is relatively cooler than the air. This is not surprising as Typhoon Nat occurred in early autumn and the Indian tropical system occurred during the wet monsoon season. TS Erin occurred during the hottest month of the year, therefore the US features high daytime SHF (up to 220 W m^{-2}). While Australia exhibited the highest soil temperatures, the SHF trails the US with daily values reaching 50-150 W m^{-2}.

The HYDRUS LHF time series and MERRA total precipitation flux (mm d^{-1}) are shown in Figure 3.6. In the regions where intensification is to occur, LHF is highest in the afternoons/evenings and lowest in the mornings. As solar radiation warms the boundary layer throughout the day, evaporation increases along with LHF. For these case studies, the LHF values are consistently higher in China and India. In the US case, LHF is more variable over time and spikes after precipitation events. In the US and Australia, the trend of LHF follows most closely to the trend of precipitation due to drier ambient conditions. The daily maximums for all regions often reach 200 W m^{-2} or greater. The soil texture does not appear to have a significant effect on the LHF magnitudes across regions, however, the diurnal changes are sharper over Australia. Taken together with SHF, it is apparent that the US and Australia study regions have both moderately high heat and moisture fluxes.

The total 2-week mean LHF indicates there is a ~70 W m^{-2} area-averaged threshold for TCMI occurrence consistent with previous findings (Andersen and Shepherd 2013) (Figure 3.7). The total 2-week maximum LHF values indicate daytime fluxes reach 300 W m^{-2} or higher over the inland intensification regions. With the exception of Nat, the TCMIs intensified during the nighttime hours and likely encountered the residual effects of daytime surface fluxes.

Specifically, the high daytime fluxes increase the low-level atmospheric moisture which is subsequently swept into the TC when it moves over.

Land vs. ocean

HYDRUS estimates of 3-hourly land surface LHF antecedent to TCMI events respond to the diurnal pattern of the boundary layer with maximum values occurring in the daytime. The magnitude of LHF is better understood with a comparison of values over land versus tropical ocean. LHF within TCs are not precisely known due to the lack of accurate observations. However, remote sensing and algorithms have been used to calculate reasonable estimates (Guimond *et al.* 2011). Note that in this study, LHF magnitudes over an area *prior to the storm* are of greater interest than those *within the storm* since the goal is to determine how favorable the environment is leading up to the TC.

According to Zhang and Rossow (1997), the mean annual LHF peaks around 115-125 W m^{-2} near 15°N/S. Trenberth and Fasullo (2007) estimate that the background LHF over the tropical ocean is approximately 120 W m^{-2}. High-resolution satellite-derived LHF estimates of the pre-TC ocean environment have been found to be 100-200 W m^{-2} (Liu *et al*., 2011). In the western North Pacific, TC LHF maxima have been estimated between 150-190 W m^{-2} (Gao and Chiu 2010). According to the HYDRUS results, daytime values of LHF over the study regions of southeastern China, south-central US, northern Australia and central India reach well above these estimates.

To facilitate a meaningful comparison, MERRA LHF over ocean pre-storm (6°x6° region adjacent to coast where TC is to form or strengthen) and over land (same 6°x6° region used for HYDRUS runs) are analyzed. “Pre-storm” is considered the 3 days prior to the TC making an appearance in the region. HYDRUS has slightly lower 3-day *mean* LHF in 3 of 4 intensification

regions when compared to the same land region from the MERRA dataset (Figure 3.8, left). This is likely due to the fact that HYDRUS is initialized and run with area-averaged conditions, while MERRA means are calculated from x-y gridded LHF values. The two datasets match within approximately 45 W m^{-2} for all regions. When comparing HYDRUS land vs. MERRA ocean fluxes, the pre-storm means are similar in magnitude with the exception of TCMI Wylva. Prior to Wylva, the ocean area exhibited about a 60% greater flux than the land area. Australia's proximity to the equator and the timing of the TCMI (i.e., hottest month of the year) might suggest that the offshore sea-surface temperatures are relatively higher than the other three regions and lead to enhanced LHF.

The pre-storm *maximum* values reveal the same underestimation of LHF by HYDRUS in the inland regions (up to 140 W m^{-2} in Australia). Despite this bias, the HYDRUS inland fluxes are remarkably higher than the ocean fluxes (> 200%) in China and India. In the US and Australia, the land and ocean fluxes are nearly equal. Near zero nighttime values over land lower the mean, while the daytime fluxes are much higher and are quantified by the pre-storm maximum values. The diurnal trend is subdued over the ocean where evaporation is relatively continuous.

The results indicate that the land surface is capable of producing a nearly equal or greater magnitude LHF as the ocean during the daytime hours closely preceding a TC. Due to the area-averaging method used with HYDRUS, the moisture fluxes produced are likely on the conservative side. Considering LHF is a primary contributor to TC formation and intensification, the land surface may play an important role in aiding the maintenance and intensification of TCs when soils are abundantly moist and LHF is high.

3.4 Discussion and conclusions

Tropical cyclones (TCs) often weaken or transition to extratropical cyclones once reaching land. However, there are instances in which a TC has remained a warm-core structure and intensified inland away from the primary oceanic energy source (Arndt *et al*. 2009, Dong *et al*. 2010, Evans *et al*. 2011, Kellner *et al*. 2012, Andersen and Shepherd 2013). Building upon the work of Andersen and Shepherd (2013), four tropical cyclone maintenance or intensification (TCMI) events were chosen as case studies to run HYDRUS-1D, a water and heat flow model. The surface energy balance was simulated for each intensification region leading up to the cyclone to quantify the available heat and moisture fluxes and determine if patterns are related to soil texture.

Time series were generated two weeks prior to each TCMI event for a bare soil configuration over a region centered on the TCMI location at the time of inland intensification. Soil temperature and LHF were generally high in each region with China and India exhibiting the highest LHF and lowest SHF. The soil texture does not appear to have a significant effect on the LHF magnitudes across regions. While TCMIs are most common over Australia, the LHF over the study period is not noticeably greater over sandy soil than over clay (China and India) or loam (US). However, the diurnal changes are sharper over Australia and the high LHF is accompanied by high SHF. This agrees with the notion of "sudden energy release" when the sandy soil is wetted. For saturated soils, hydraulic conductivity is significantly greater for coarse-textured soils than clays or loams (Radcliffe and Šimůnek 2010). The US region exhibits a similar trend with relatively high LHF and SHF, yet TCMIs are much less common (Andersen and Shepherd 2013). TCMI frequency in Australia is likely a function of latitude, total landfalls, terrain characteristics, and atmospheric conditions.

For all HYDRUS runs, the total 2-week maximum LHF values are comparable to or exceed typical ocean LHF magnitudes. The total 2-week mean LHF indicates there is a ~70 W m^{-2} area-averaged threshold for TCMI occurrence. MERRA re-analysis 3-day (pre-storm) LHF were utilized for a land versus ocean comparison. The pre-storm mean LHF prior to the TC reveal that the oceanic LHF was higher than the land LHF in 3 of 4 regions. Considering that LHF is diminished at nighttime over land, the daytime flux values are remarkably high. The 3-day maximum LHF values inland are well above those over the ocean in the China and India intensification regions, while LHF magnitudes ocean vs. land were nearly equal over the US and Australia regions. This suggests that LHF maxima over land have a similar magnitude to those found over the ocean prior to the appearance of a TCMI and provides plausibility of the *brown ocean* effect. While HYDRUS provides a unique avenue to assessing the surface energy balance by including liquid water and vapor transport in soils, the 1D design is a limitation to exploring the spatial distribution of LHF. It may be concluded, however, that the daytime flux magnitudes output by HYDRUS are underestimations due to the area-averaging method.

Further analysis is needed to determine the relative importance of short-term soil moisture anomalies to other contributing factors of TC intensification. Although Evans *et al.* (2011) examined the seasonal soil moisture signal influence on TS Erin, precipitation recycling and soil moisture memory warrant investigation in other landfall regions where the land surface-atmospheric feedback may be stronger or weaker. Additionally, it was suggested that anomalously wet soils encouraged moisture transport from the Gulf (Evans *et al.* 2011). Analysis of synoptic-scale features for additional TCMIs could determine if this is a common trait. A thorough investigation of soil moisture patterns, timing of rainfall events, and structure and speed of TCs in relation to intensification potential would be beneficial.

Future studies may extend this research by using a larger sample size to compare TCMIs within and across regions or add null cases to better understand differences between intensifying and weakening TCs. This study and previous works are primarily feasibility studies for the soil moisture-cyclone feedback hypothesis. High spatial and temporal resolution modeling would provide more refined evidence of the heat and moisture transport to the TC. Additionally, point observations from meteorological stations are ideal input where available and could lead to more precise results for multiple TCMI events. A hurricane simulation model coupled with a sophisticated soil model can simulate a TCMI event and lead to better understanding of the *brown ocean* effect.

3.5 References

Andersen, T.K., and J.M. Shepherd (2013). A spatio-temporal analysis of tropical cyclone maintenance or intensification inland. *International Journal of Climatology*. DOI: 10.1002/joc.3693.

Arndt, D.S., J.B. Basara, R.A. McPherson, B.G. Illston, G.D. McManus, and D. B. Demko (2009). Observations of the overland reintensification of Tropical Storm Erin (2007). *Bulletin of the American Meteorological Society* **90,** 1079-1093. DOI: 10.1175/2009BAMS2644.1.

Barcikowska, M., F. Feser, and H. von Storch (2012). Usability of best track data in climate statistics in the western North Pacific. *Monthly Weather Review* **140**, 2818–2830. DOI: 10.1175/MWR-D-11-00175.1.

Bosilovich, M.G., and W.-Y. Sun (1999). Numerical simulation of the 1993 midwestern flood: Land atmosphere interactions. *Journal of Climate* **12,** 1490-1505.

Carsel, R.F., and R.S. Parrish (1988). Developing joint probability distributions of soil water retention characteristics. *Water Resources Research* **24**, 755-769. DOI: 10.1029/WR024i005p00755.

Chang, H., D. Niyogi, A. Kumar, C.M. Kishtawal, J. Dudhia, F. Chen, U.C. Mohanty, and M. Shepherd (2009). Possible relation between land surface feedback and the post-landfall structure of monsoon depressions. *Geophysical Research Letters* **36**, 1–6. DOI: 10.1029/2009GL037781.

Chen, L.-S. (2012). Research progress on the structure and intensity change for the landfalling tropical cyclones. *Journal of Tropical Meteorology* **18**, 113–118. DOI: 10.3969/j.issn.10068775.2012.02.001.

Clark, C.A., and R.W. Arritt (1995). Numerical simulations of the effect of soil moisture and vegetation cover on the development of deep convection. *Journal of Applied Meteorology* **34,** 2029-2045. DOI: 10.1175/1520-0450(1995)034&lt.

Dong, M., L. Chen, Y. Li, and C. Lu (2010). Rainfall reinforcement associated with landfalling tropical cyclones. *Journal of Atmospheric Science* **67,** 3541-3558. DOI: 10.1175/2010JAS3268.1.

Emanuel, K., J. Callaghan, and P. Otto (2008). A hypothesis for the redevelopment of warm-core cyclones over northern Australia. *Monthly Weather Review* **136**, 3863–3872. DOI: 10.1175/2008MWR2409.1

Evans, J.L., and R.E. Hart (2003). Objective indicators of the life cycle evolution of extratropical transition for Atlantic tropical cyclones. *Monthly Weather Review* **131**, 909-925.

Evans, C., R.S. Schumacher, and T.J. Galarneau (2011). Sensitivity in the overland reintensification of Tropical Cyclone Erin (2007) to near-surface soil moisture characteristics. *Monthly Weather Review* **139,** 3848–3870. DOI: 10.1175/2011MWR3593.1.

Frank, W.M. (1977). The structure and energetics of the tropical cyclone. *Monthly Weather Review* **105**, 1119-1135.

Gao, S., and L.S. Chiu (2010). Surface latent heat flux and rainfall associated with rapidly intensifying tropical cyclones over the western North Pacific. *International Journal of Remote Sensing* **31,** 4699-4710. DOI: 10.1080/01431161.2010.485149.

Gray, W. M. (1968). Global view of the origin of tropical disturbances and storms. *Monthly Weather Review* **96**, 669-700.

Guimond, S.R., M.A. Bourassa, and P.D. Reasor (2011). A latent heat retrieval and its effects on the intensity and structure change of Hurricane Guillermo (1997). Part I: The algorithm and observations. *Journal of Atmospheric Science* **68,** 1549-1567. DOI: 10.1175/2011JAS3700.1.

Kellner O., D. Niyogi, M. Lei, and A. Kumar (2012). The role of anomalous soil moisture on the inland reintensification of Tropical Storm Erin (2007). *Natural Hazards* **139**, 1573-1600.

Kishtawal, C.M., D. Niyogi, A. Kumar, M.L. Bozeman, and O. Kellner (2012). Sensitivity of inland decay of North Atlantic tropical cyclones to soil parameters. *Natural Hazards* **63**, 1527-1542. DOI: 10.1007/s11069-011-0015-2.

Kleinschmidt, E., Jr. (1951). Gundlagen einer Theorie des tropischen Zyklonen. Archiv fur Meteorologie, *Geophysik und Bioklimatologie*, Serie A, **4**, 53-72.

Knapp, K.R., M.C. Kruk, D.H. Levinson, H.J. Diamond, and C.J. Neumann (2010). The International Best Track Archive for Climate Stewardship (IBTrACS): Unifying tropical cyclone best track data. *Bulletin of the American Meteorological Society* **91**, 363-376. DOI: 10.1175/2009BAMS2755.1.

Liu, J., J.A. Curry, C.A. Clayson, and M.A. Bourassa (2011). High-resolution satellite surface latent heat fluxes in North Atlantic Hurricanes. *Monthly Weather Review* **139,** 2735-2747. DOI: 10.1175/2011MWR3548.1.

Liu, C.-X., Q.-L. Wan, F. Liao, and Z.-K. Zhao (2012). Surface observations in the tropical cyclone environment over the South China Sea. *Journal of Tropical Meteorology* **18,** 263-274. DOI: 10.3969/j.issn.1006-8775.2012.02.015.

Lynn, B.H., W.-K. Tao, and P.J. Wetzel (1998). A study of landscape–generated deep moist convection. *Monthly Weather Review* **126,** 928-942.

Malkus, J.S., and H. Riehl (1960). On the dynamics and energy transformations in steady-state hurricanes. *Tellus* **12**, 1-20.

Miller, B.I. (1958). On the maximum intensity of hurricanes. *Journal of Meteorology* **15**, 184-195.

Radcliffe, D.E., and J. Šimůnek (2010). *Soil physics with HYDRUS: Modeling and applications*. CRC Press, 373 pp.

Saito, H., J. Šimůnek, and B.P. Mohanty (2006). Numerical analysis of coupled water, vapor, and heat transport in the vadose zone. *Vadose Zone Journal* **5,** 784-800. DOI: 10.2136/vzj2006.0007.

Scanlon, B., K. Keese, R. C. Reedy, J. Šimůnek, and B. Andraski (2003). Variations in flow and transport in thick desert vadose zones in response to paleoclimatic forcing (0 – 90 kyr): Monitoring, modeling, and uncertainties. *Water Resources Res*search **39**, 1-17. DOI: 10.1029/2002WR001604.

Shen, W., I. Ginis, and R.E. Tuleya (2002). A numerical investigation of land surface water on landfalling hurricanes. *Journal of Atmospheric Science* **59**, 789-802.

Trenberth, K.E., and J. Fasullo (2007). Water and energy budgets and hurricanes and implications for climate change. *Journal of Geophysical Research* **112,** 1-10. DOI: 10.1029/2006JD008304.

Tuleya, R.E. (1994). Tropical storm development and decay: Sensitivity to surface boundary conditions. *Monthly Weather Review* **122**, 291–304.

Zhang, Y.-C., and W.B. Rossow (1997). Estimating meridional energy transports by the atmospheric and oceanic general circulations using boundary fluxes. *Journal of Climate* **10,** 2358-2373.

Table 3.1: Description of the four case studies for HYDRUS runs. The last day of each simulation is the time of intensification. 'Pressure' refers to minimum central pressure and 'wind speed' refers to maximum sustained wind speed.

	Case 1	**Case 2**	**Case 3**	**Case 4**
TCMI Case	Typhoon Nat	Tropical Storm Erin	Cyclone Wylva	2007172N15088
Region	Southeast China *25-31N, 114-120E*	South-Central US *33-39N, 96-102W*	Northcentral Australia *16-22S, 128-134E*	Central India *15-21N, 75-81E*
Simulation Period	20 Sep–3 Oct 1991	6 Aug–19 Aug 2007	5 Feb–18 Feb 2001	10 Jun–23 Jun 2007
Landfall	1 Oct 1200 UTC	16 Aug 1200 UTC	16 Feb 1200 UTC	22 Jun 0600 UTC
Intensification	Pressure dropped 4 hPa in 6 hrs	Pressure dropped 12 hPa & wind speed increased 30 kts in 12 hrs	Pressure dropped 7 hPa in 18 hrs	Pressure dropped 3 hPa & wind speed increased 5 kts in 6 hrs
Soil	Ultisols (red clay)	Mollisols (organic and clay)	Entisols (sand)	Alfisols (clay)
Climate	Humid subtropical	Humid subtropical	Desert	Semi-arid to humid subtropical

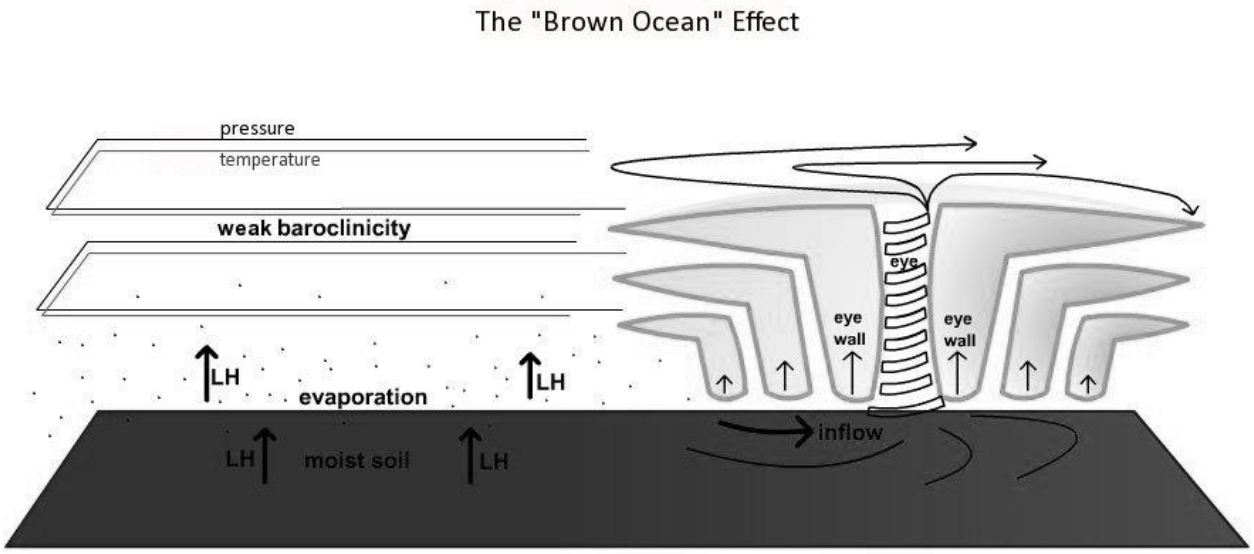

Figure 3.1: Schematic of the *brown ocean* effect. Anomalously wet soil moisture conditions enhance evaporation and latent heat release. In a weakly baroclinic environment, the energy can help to sustain or intensify an inland tropical cyclone.

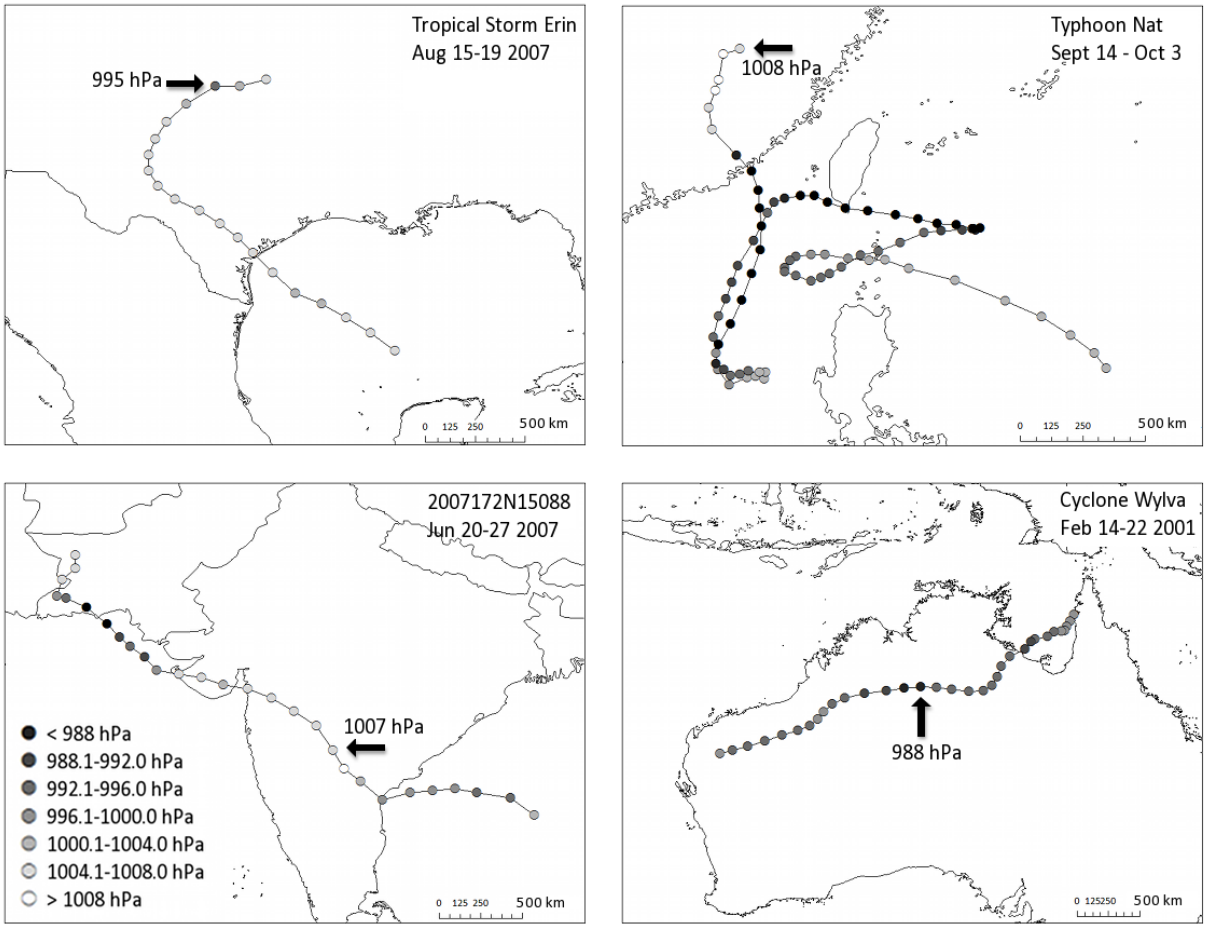

Figure 3.2: TCMI case studies for HYDRUS-1D model runs. Each is the strongest intensification event (i.e., greatest pressure drop inland) originating from its respective hurricane basin between 1979-2008 based on work by Andersen and Shepherd (2013). The arrow denotes the point of intensification.

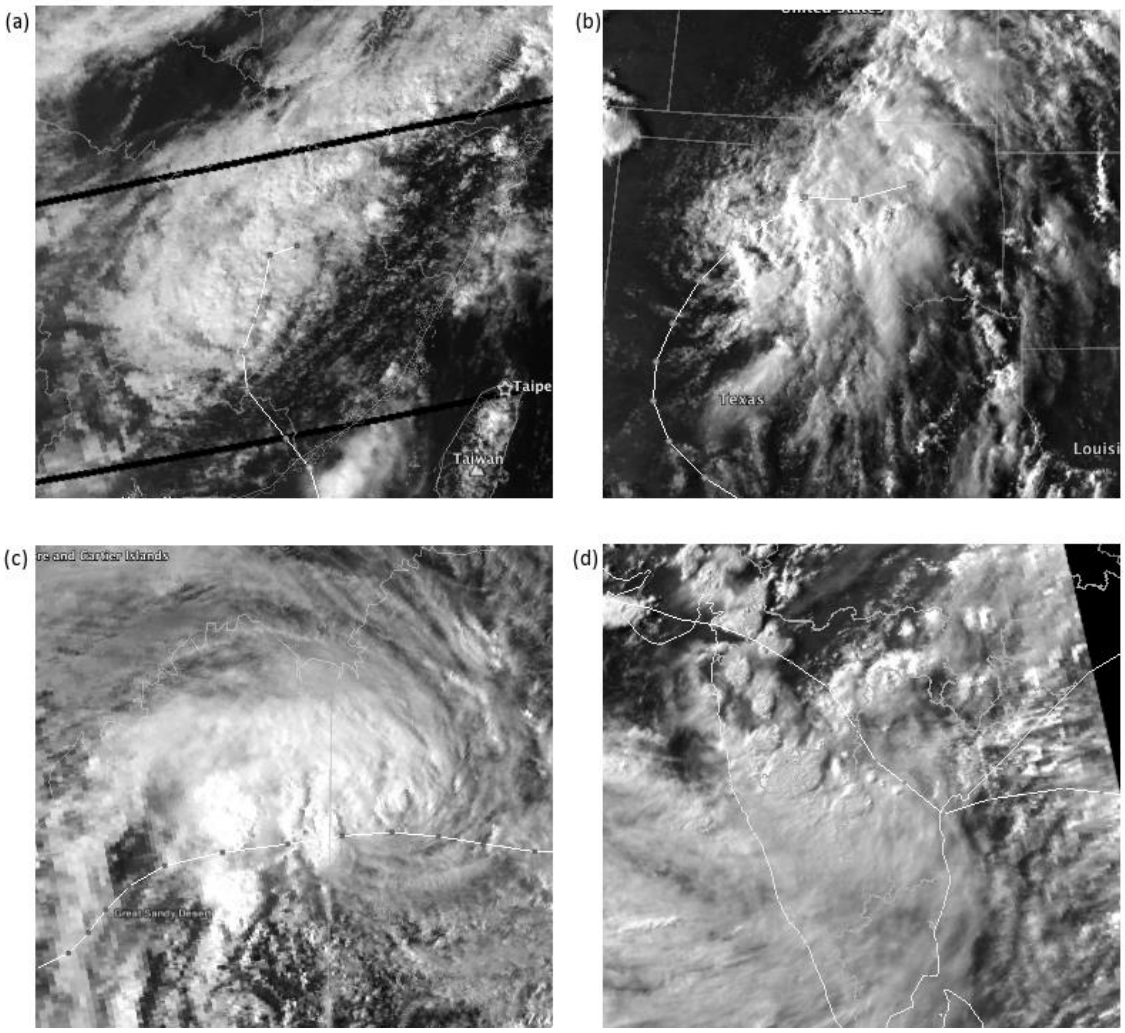

Figure 3.3: HURSAT visible satellite images for (a) Typhoon Nat (1991), (b) Tropical Storm Erin (2007), (c) Cyclone Wylva (2001), and (d) 2007172N15088.

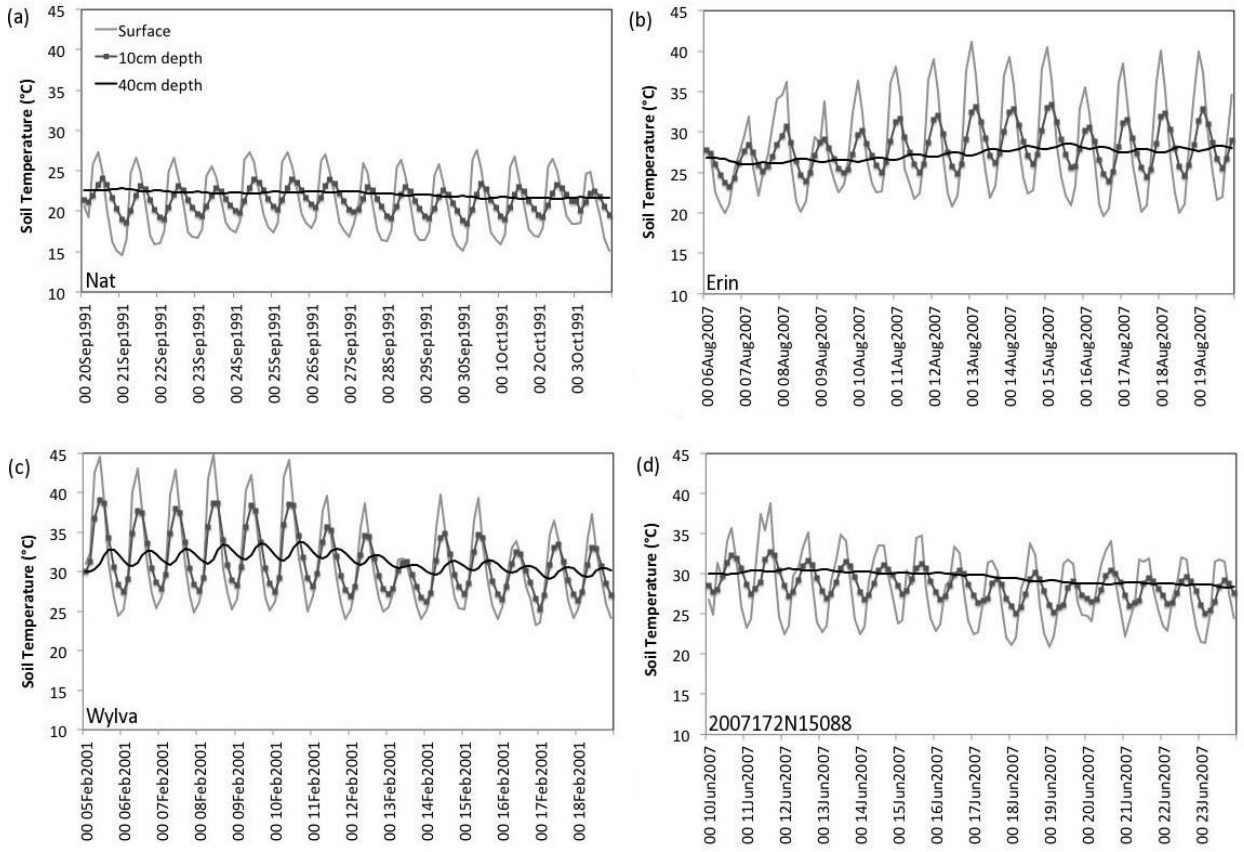

Figure 3.4: HYDRUS-generated soil temperature (°C) at the surface, 10 cm, and 40 cm depths for (a) Typhoon Nat (China), (b) Tropical Storm Erin (US), (c) Cyclone Wylva (Australia) and (d) tropical system 2007172N15088 (India) over bare soil.

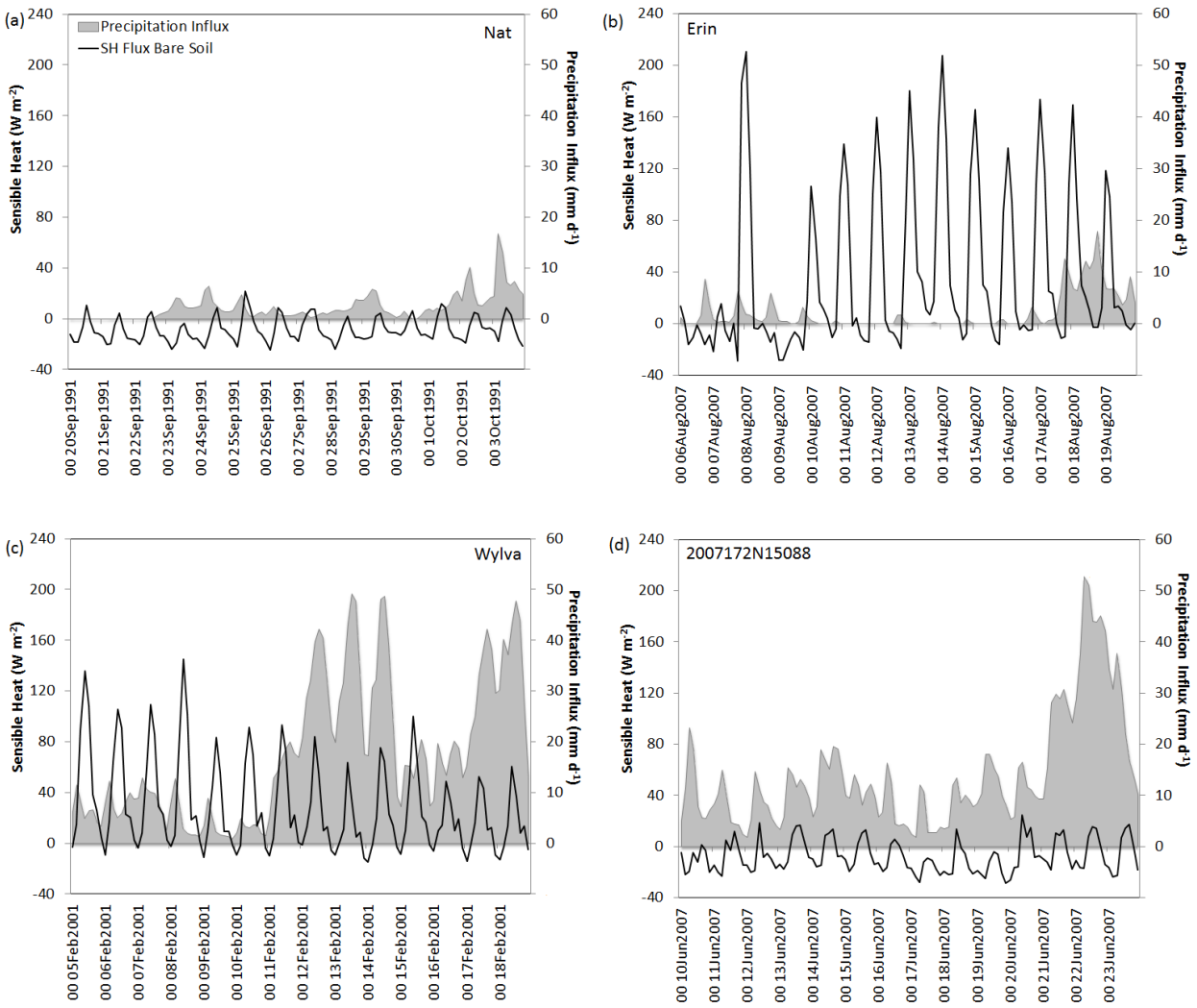

Figure 3.5: HYDRUS-generated surface sensible heat flux (W m^{-2}) over two weeks prior to (a) Typhoon Nat, (b) Tropical Storm Erin, (c) Cyclone Wylva and (d) tropical system 2007172N15088 for bare soil (solid line) simulations. MERRA precipitation flux (mm d^{-1}) is plotted for reference.

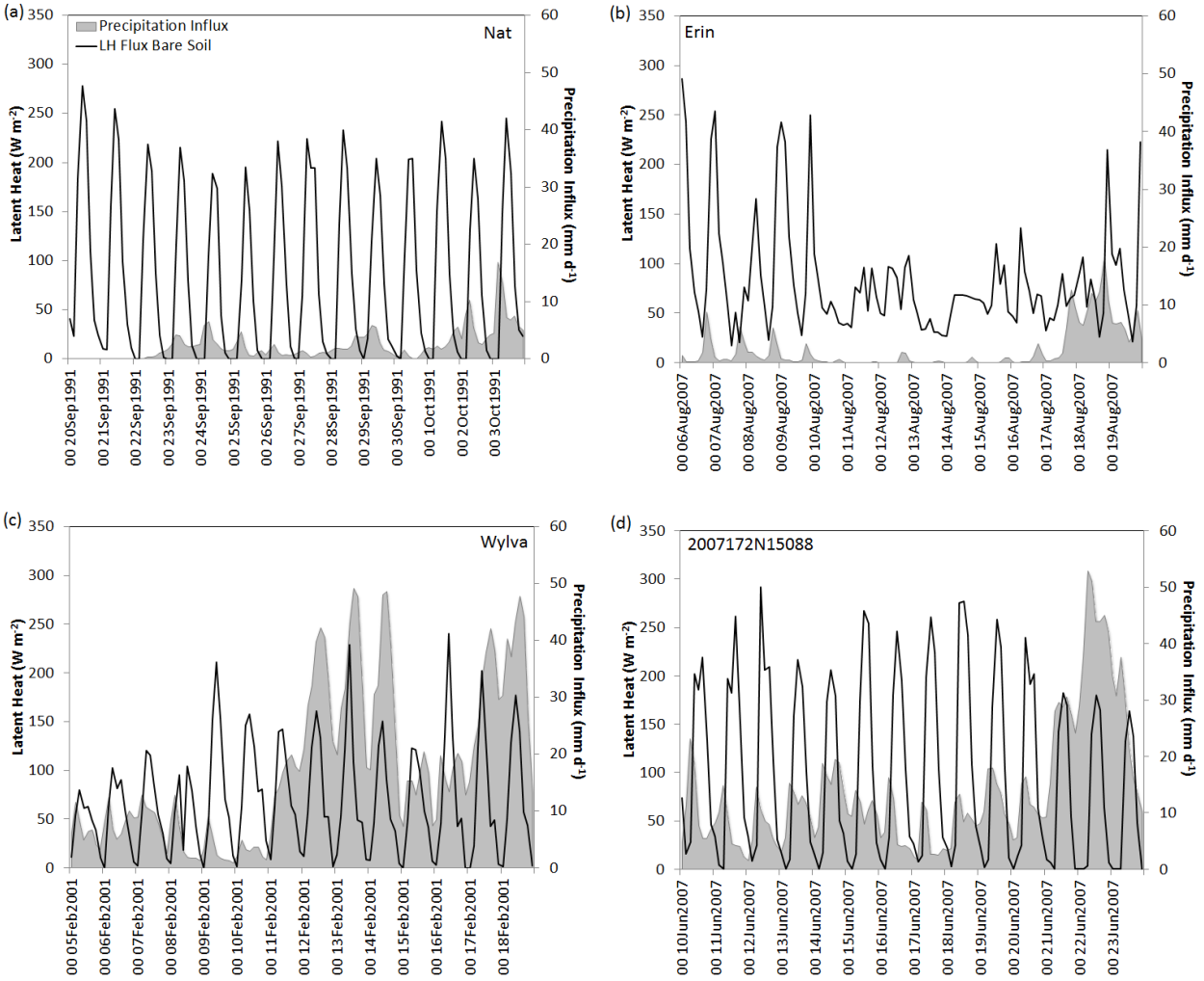

Figure 3.6: HYDRUS-generated surface latent heat flux (W m^{-2}) two weeks prior to (a) Typhoon Nat, (b) Tropical Storm Erin, (c) tropical system 2007172N15088 and (d) Cyclone Wylva for bare soil (solid line) simulations. MERRA precipitation influx (mm d^{-1}) is plotted for reference.

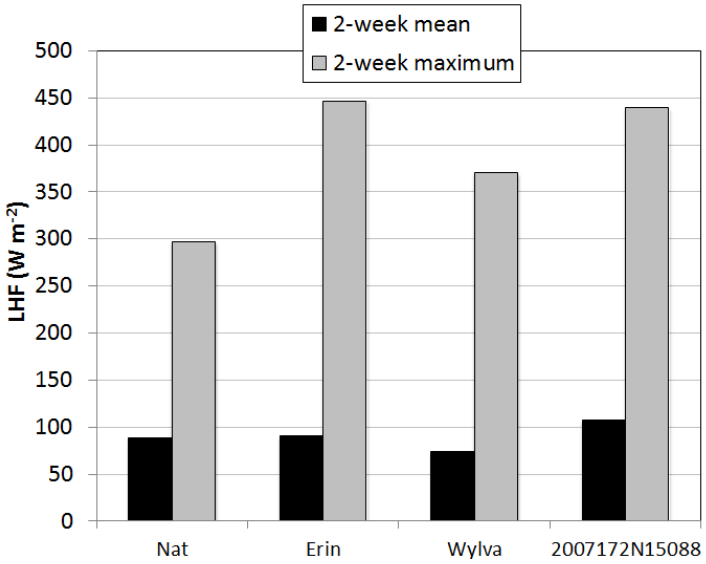

Figure 3.7: The 2-week mean and maximum LHF (W m^{-2}) antecedent to the TCMI for HYDRUS bare soil simulations.

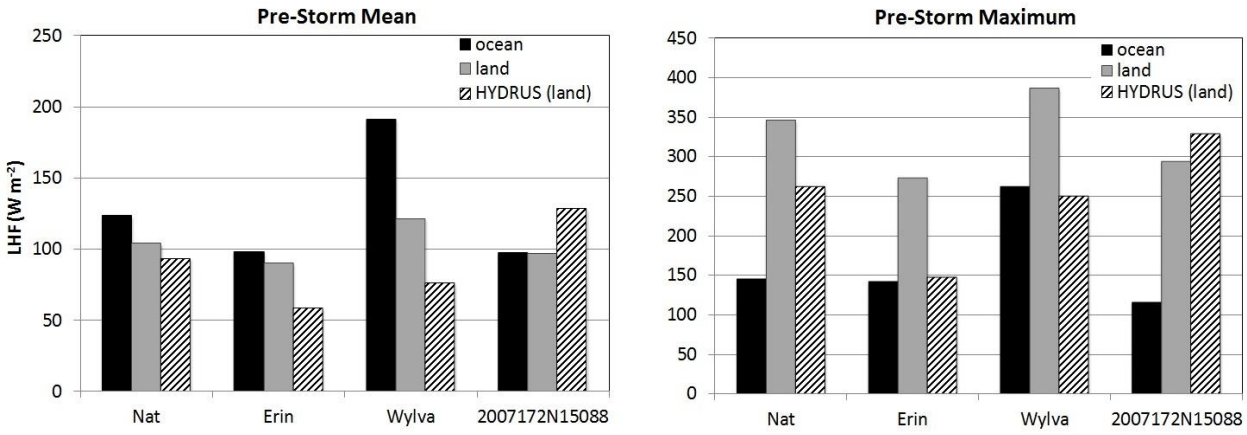

Figure 3.8: Three-day mean LHF over ocean (MERRA) and land (MERRA and HYDRUS) (left) and 3-day maximum LHF over ocean (MERRA) and land (MERRA and HYDRUS) (right) along TCMI tracks.

CHAPTER 4

3D MESOSCALE MODEL-BASED ASSESSMENT OF THE SOIL MOISTURE FEEDBACK ON AN INLAND TROPICAL CYCLONE[3]

[3] Andersen, T.K., and J.M. Shepherd (2013). 3D mesoscale model-based assessment of the soil moisture feedback on an inland tropical cyclone. Submitted to *Atmospheric Research* 6/7/13.

Abstract

The *brown ocean* effect theorizes that anomalously wet soils energize tropical cyclones (TCs) where ocean forcing is removed via enhanced upward latent heat flux (LHF). To test the theory, the Weather Research and Forecast model (WRF-ARW) is used to determine the sensitivity of Cyclone Abigail (2001) to varying soil moisture conditions. The chosen domain is a 275x325 grid at 8 km grid spacing over northern Australia. Control, dry and wet simulations are run with parameterizations similar to ocean-based TC studies. Results indicate that a decrease in initial soil moisture results in a weaker cyclone with less precipitation, reduced LHF, higher pressure, and weaker winds while the opposite is found when increasing the initial soil moisture. The output from the control run was more similar to the wet run than to the dry run which highlights the anomalously wet conditions during Cyclone Abigail's intensification. The findings suggest that WRF captures land surface feedbacks related to landfalling tropical systems, specifically, that soil moisture content and associated moisture fluxes influence cyclone intensity and structure.

4.1 Introduction

Numerical weather models are valuable tools for studying the feedbacks between the land surface and landfalling tropical cyclones (TCs). Evans *et al*. (2011) utilized the Weather Research and Forecast (WRF-ARW) model to simulate the re-intensification of Tropical Storm Erin (2007) over Oklahoma. A control simulation and 8 sensitivity simulations were run with varying soil moisture conditions. They found that the final intensity of the vortex was linked to maintenance of planetary boundary layer (PBL) moisture over preexisting wet soil. Lin *et al.* (2010) studied the landfall of Hurricane Isabel over the complex terrain of the Appalachian Mountains using WRF coupled with the Advanced Circulation Model. The model accurately reproduced orographically enhanced rainfall and the general wind field, however, wind maxima were displaced. Similarly, Xie and Zhang (2012) found that accurate TC track forecasts are essential in determining flood potential in Taiwan due to topographical forcing. Zhang *et al.* (2011) used WRF to simulate land surface effects on Typhoon Sepat (2007) in China and found that the model successfully reproduced the typhoon track and rainfall. Sensitivity experiments revealed that sensible and latent heat fluxes (LHF) maintained the cyclone and spiral structure over land. Moreover, the distribution and intensity of the rain field was dependent on accurate soil moisture content initialization (Zhang *et al.* 2011). In a sensitivity study of North Atlantic TCs to soil parameters, Kishtawal *et al.* (2012) found that the intensities of hurricanes Rita and Katrina were impacted by changes in surface roughness and soil heat capacity. However, the impacts were limited compared to the observational analysis and suggest a need for improvement in modeled surface feedbacks.

Studies have concluded that numerical models represent hurricane track and intensity post-landfall reasonably well (Lin *et al.* 2010, Evans *et al.* 2011). However, the model

configuration and initializing data should be considered carefully. According to Bozeman *et al.* (2012), HWRF model track and intensity forecasts are sensitive to land surface parameterization, initial boundary conditions, and PBL scheme. Similarly, Lin *et al.* (2010) found that initial conditions greatly impact subsequent storm development. In a test of suitable model parameterization schemes for Indian Ocean TCs, Osuri *et al.* (2012) report that of six experiments, the Yonsei University (YSU) PBL scheme in combination with the Kain-Fritsch (KF) convective scheme produce the least amount of intensity error. Additionally, the KF scheme performs better than Betts Miller and Janjic (BM) or Grell and Devenyi (GD) in 24- and 48-hour track forecasts. Rao and Tallapragada (2012) found that HWRF is superior to WRF-ARW and NCAR/Penn State University Mesoscale model version 5 (MM5) in simulating TCs in the Bay of Bengal (BB). HWRF skill is attributed to the specialized vortex initialization, a synthetic vortex unique to BB cyclones, grid point statistical interpolation, and two-way moveable nest. Likewise, Dodla *et al.* (2011) found HWRF performed better than WRF-ARW and WRF-NMM in two-way interactive nested domain simulations of Hurricane Katrina.

While approaching land, TC wind speed may be reduced as a result of momentum loss due to land roughness. However, the radial wind component may increase in the PBL producing inflow and enhanced moisture convergence (Zhu 2008, Au-Yeung and Chan 2010). Likewise, higher moisture availability over land can help to sustain TCs by increasing condensation and latent heat supply (Tuleya and Kurihara 1978, Tuleya 1994). Studies have found that moisture distribution along the coast, land roughness variation, and small-scale surface features are important factors influencing TC intensity and track post-landfall (Zhu 2008, Au-Yeung and Chan 2010, Bozeman *et al*. 2012). Soil heat capacity and conductivity are also important characteristics that influence the surface temperature and cyclone decay process (Tuleya 1994,

Kishtawal *et al.* 2012). Over northern Australia, it has been suggested that large vertical heat fluxes from recently wetted, hot, sandy soil help to intensify inland-moving TCs (Emanuel *et al.* 2008). In India, overland monsoon depressions have been observed to maintain intensity longer if the area received prior rainfall (Chang *et al.* 2009).

The possible soil moisture-TC feedback, or *brown ocean* effect, hypothesizes that anomalously wet soils energize TCs where ocean forcing is removed via enhanced upward latent heat flux (LHF) (Andersen and Shepherd 2013). This inland phenomenon is referred to as Tropical Cyclone Maintenance or Intensification (TCMI). Andersen *et al.* (2013) found that TCMI events are associated with a surface LHF upwards of 200 W m^{-2}. When comparing similar-tracking TCs, TCMI regions tend to exhibit average or above average LHF during TCMI occurrence than during TC decay.

The current objective builds upon the *brown ocean* framework by testing the response of an inland-tracking tropical cyclone over Australia, in terms of intensity, precipitation, atmospheric moisture, and energy, to soil moisture conditions using the WRF-ARW model. Emanuel *et al.* (2008) was the first to study the TC response to soil moisture in Australia by using a coupled soil and hurricane model. Along with Andersen *et al*. (2013), the feasibility of the hypothesis has been established. Here, the research is extended to identify surface and low-level atmospheric reactions to modified soil moisture. A simulation period of 30-h will aid in understanding soil moisture interactions, flux magnitudes, and storm evolution prior to and during cyclone intensification. A control case is compared to "dry" and "wet" cases to determine if soil moisture content alone influences the results. Section 4.2 describes the selected case study, section 4.3 provides information on the model, initialization and methodology, section 4.4 summarizes the results, followed by a discussion and conclusions in section 4.5.

4.2 Case study

Cyclone Abigail began as an area of low pressure in the Coral Sea on 22 February. Two pressure centers merged and tracked westward. Just before making landfall at eastern Australia, the system intensified. At 0000 UTC on 24 February, the system made landfall near Cairns and subsequently weakened. The highest recorded wind speed was 65 kts. Abigail redeveloped and intensified over land twice. The first was around 1 March 0600 UTC when the pressure dropped to 998 hPa. Emanuel *et al.* (2008) used a simple soil model coupled to a hurricane model to study this time period of Abigail. The second intensification occurred around 3 March 0000 UTC at which time the pressure dropped to 992 hPa (Figure 4.1). The latter time period is the focus of this paper. Thermal wind analysis indicates Abigail maintained a warm-core for the duration of both intensification periods (Andersen and Shepherd 2013). The tropical cyclone structure and rainbands are apparent in HURSAT visible satellite imagery (Figure 4.2). Near Halls Creek, a clear eye formed 1 March 1700 UTC and was apparent until 3 March 0600 UTC (Figure 4.3). Meteorological observations from Halls Creek during Abigail's passing are shown in Figure 4.4. The 6-hourly precipitation peaks at 0.83" and the wind direction changes around 2 March. The low pressure center can be seen on the Bureau of Meteorology (BOM) surface analyses (Figure 4.5).

4.3 Model setup and methodology

WRF-ARW is a fully-compressible, non-hydrostatic system of equations that can generate fine-scale atmospheric structures. The Mesoscale and Microscale Meteorology Division of the National Center for Atmospheric Research (NCAR) maintains the software framework, ARW dynamic solver, the WRF Preprocessing System (WPS), physics packages, and graphics programs. The WRF modeling system flow chart is shown in Figure 4.6.

In this research, WRF version 3.5 is configured for a single processor with basic nesting and compiled for a real data simulation. WPS version 3.5 is used to define the simulation domain, interpolate terrestrial data, and degrib and interpolate meteorological data. A single simulation domain spanning 275x325 horizonal grid points at 8 km resolution and 34 vertical levels is utilized (Figure 4.7). The initial and boundary conditions are provided by NCEP FNL (Final) Operational Global Analysis 1.0°x1.0° data. The product is prepared every 6 hours from the Global Data Assimilation System (GDAS). The data are available on the surface and 26 pressure levels between 1000-10 hPa. According to Evans *et al.* (2011), 1° data are useful for mesoscale studies of soil moisture impacts on vortices. Higher resolution data can introduce unrealistic convective-scale feedbacks. The simulation time begins 2 March 2001 0000 UTC (24 hours before intensification) and ends 3 March 2001 0600 UTC.

The physics and dynamics options selected are similar to those in ocean-based TC studies (Evans et al. 2011). Shortwave radiation is represented by the Dudhia scheme which allows for simple downward integration. The Rapid Radiative Transfer Model (RRTM) is chosen for longwave radiation. It accounts for multiple bands, trace gases, and microphysics species. Microphysics is simulated with the Purdue-Lin scheme which has ice, snow, and graupel processes (Chen and Sun 2002). The Unified Noah land surface model is used for surface physics (Chen and Dudhia 2001). It includes soil temperature and moisture in four layers, fractional snow cover and frozen soil physics. The Yonsei University (YSU) scheme is used for PBL physics (Hong *et al*. 2006). It is a non-local-K scheme with an explicit entrainment layer and parabolic K profile in unstable mixed layer. The fifth-generation Pennsylvania State University-National Center for Atmospheric Research Mesoscale Model (MM5) similarity scheme, based on Monin-Obukhov with Carlson-Boland viscous sublayer, is used for surface

layer physics (Skamarock *et al.* 2008). The Kain-Fritsch (KF) cumulus option, a deep and shallow convection sub-grib scheme, is utilized since convection is not explicitly handled in the model (Kain and Fritsch 1990). The KF scheme has been identified as superior to alternative convective schemes for TCs in many studies (Prater and Evans 2002, Ma and Tan 2009, Deshpande *et al.* 2012). A summary of the model configurations are shown in Table 4.1.

For this study, a control run and two sensitivity tests are utilized. The control run is used to verify the model, identify discrepancies with historical records, and represent the standard soil moisture scenario for the case study. Similar to Kellner *et al.* (2012), the sensitivity tests are a "dry" run (50% reduced soil moisture content) and a "wet" run (50% increased soil moisture content) at initialization. The equations to modify the values are:

$$SM_{wet} = SM_{ctrl} + (0.5 * SM_{ctrl}) \qquad 0.00 < SM_{ctrl} < 0.65 \qquad \text{(Eq. 4.1)}$$

$$SM_{dry} = SM_{ctrl} - (0.5 * SM_{ctrl}) \qquad 0.00 < SM_{ctrl} < 0.65 \qquad \text{(Eq. 4.2)}$$

Using a percentage allows for the majority of the gridpoint values to decrease (increase) while still maintaining extremes. In order to prevent the modified values from exceeding 100%, a 0.65 threshold was implemented (note: no control values over land masses were excluded as all were below the threshold). All other parameters remain the same for the three cases. The simulations are compared quantitatively and qualitatively in terms of surface LHF, precipitation, total precipitable water (PW), minimum central pressure, wind fields, and Convective Available Potential Energy (CAPE).

4.4 Results

Control run

WRF-generated total precipitation (mm) during the intensification of Abigail for the control run, a HURSAT infrared (IR) image depicting cloud-top temperature (ºC), and Modern

Era Retrospective-Analysis for Research and Applications (MERRA) total precipitation flux (10^{-3} kg m^{-2} s^{-1}) are shown in Figure 4.8. The extent and rotation of the cyclone are evident in the control simulation along with the precipitation maxima near the eyewall. WRF was not able to clearly distinguish the north and south convective clusters nor did it capture the central eye. A similar study by Kellner *et al.* (2012) found that distinct TC features found in NEXRAD radar were not captured in WRF simulations. The simulated precipitation maximum reaches well over 300 mm at some gridpoints, while MERRA shows a maximum around 178 mm.

At the time of intensification, Abigail was characterized by a minimum central pressure of 992 hpa and winds at 25 kts (Figure 4.9). The model indicates a wind speed increase and pressure lowering near the actual intensification time (highlighted). The simulated pressure (997 hPa) and wind speed (14 kts) are similar to observations, but indicate an overall weaker cyclone. Intensity differences may be attributed to spinup time, boundary conditions, or spatial resolution. The cyclone center is modeled approximately 50-100 km southwest of IBTrACS hurricane track records during the period of intensification (Figure 10). WRF-generated sea-level pressure (SLP) tendency shows a 12-hour pressure decrease within the cyclone, and rising pressure over the rest of the domain (Figure 4.10).

Modified soil moisture

Sensitivity experiments using perturbed soil moisture content initialization are useful for determining the relative influence of surface energy fluxes on cyclone evolution. It is theorized that drier soils and weak upward moisture flux result in a weaker cyclone than a case with more heavily saturated soils. To test this hypothesis, two experiments are performed: a “dry run” with initial soil moisture content 50% less than the control run and a “wet run” with soil moisture

content 50% greater than the control run (Figure 4.11). Coastal Northern Territory contains the wettest soil in the domain. A smaller pocket of moisture can be seen in the southwest corner.

The surface LHF is closely tied with soil moisture (Figure 4.12). In areas where soil moisture increased substantially, the LHF also increased. In the wet run, LHF reaches 200 W m^{-2} near the cyclone center and is consistent with thresholds identified in previous work (Andersen *et al.* 2013). In the dry run, values are considerably lower and the southwestern moisture pocket disappears. The highest flux values remain near the coast in all scenarios. Cyclones preceding Abigail took similar tracks and may have set the stage for large amounts of energy release.

Precipitation characteristics reveal information about the structure and intensity of the cyclone. As compared to the control run, dry soil has reduced total precipitation (mm), less "wrap-aroundness" near the cyclone center, and a more disorganized structure. While the changes in the wet run precipitation are more subtle, wetter soil did produce higher total precipitation and tighter rotation than the control simulation (Figure 4.13). The thin convective cells to the southeast of the center (20ºS, 130ºE) are diminished substantially in the dry run.

Atmospheric moisture and energy distribution provide insight into the precipitation trends. PW increases in the 12 hours leading up to cyclone intensification, however, differences between dry, control, and wet runs are not significant (not shown). PW is a measure of the total atmospheric column of moisture and may not capture subtle differences at the low levels. Equivalent potential temperature (θ_e), or moist static energy, can be used to identify areas of temperature and moisture advection. High values indicate instability and positively buoyant air parcels. θ_e "ridges" often encourage thermodynamically-induced thunderstorms and mesoscale convective systems. During Abigail, high values of θ_e are seen over west-central Australia (Figure 4.14, top). A θ_e gradient is aligned with Abigail along the southeast quadrant of the

cyclone. Similarly, surface dew point (T_d) is an indication of instability when values are high (above 70º F). A tongue of moisture pushing south along Abigail's westward track is apparent in Figure 4.14 (bottom). A secondary moist air mass is located in central Australia near Alice Springs. The θ_e and T_d over land reach ocean-strength magnitudes and indicate that Abigail encountered an inland moisture source, or possible *brown ocean*.

Surface CAPE (J kg^{-1}) at eta level 1(1000 hPa) indicates moderate convection along the coasts and is highest for the wet run (Figure 4.15, top). Over-ocean values are extremely high just to the north of Abigail. CAPE is an indication of updraft strength and signifies that vertical motion is strongest in the wet soil scenario. The dry run has greater surface CAPE than the wet run at slightly higher levels (not shown). Generally, dry soil allows the planetary boundary layer (PBL) to grow to greater depths, which reduces thermodynamic instability. Wet soils tend to produce a moist, shallow PBL with higher CAPE (Lanicci *et al.* 1987, Segal *et al.* 1995, Alonge *et al.* 2007). However, the relationship is dependent on the season and synoptic patterns (Frye and Mote 2010). In this case, the dry run has a deeper PBL and vertically extended CAPE, while the wet run has a shallow PBL with CAPE concentrated near the surface (Figure 4.15, bottom).

Surface and low-level wind fields can be used to assess the shear environment of a cyclone. TCs favor low shear in order to develop symmetric warm-core structures. However, a limited amount of shear can benefit divergence aloft. Simulated surface 10 m wind fields are shown in Figure 4.16 (top). As expected in the southern hemisphere, the strongest winds are located to the east of the cyclone track. The surface pressure deepens from the dry to wet runs (i.e., dry = 1000 hPa, control = 999 hPa, wet = 998 hPa). Simulated 850 hPa wind speeds decrease in the dry run, but do not significantly increase in the wet run (Figure 4.16, bottom). The control and wet runs particularly exhibit intensification in the southeast quadrant of the TC

compared to the dry run. There does not appear to be any directional or speed shear that would affect the system.

4.5 Discussion and conclusions

Landfalling tropical cyclones often weaken or transition to extratropical systems owing to loss of moisture, wind shear, temperature gradients, frictional effects, and other baroclinic and topographical features. However, some TCs maintain their warm-core structures despite the generally unfavorable conditions over land outside the tropics, referred to as Tropical Cyclone Maintenance or Intensification (TCMI). Previous work has identified the feasibility of anomalously moist soil acting as a substitute for the ocean environment by providing the necessary upward moisture flux to keep the TC "heat engine" in motion (Emanuel *et al.* 2008, Evans *et al.* 2012, Kellner *et al.* 2012, Kishtawal *et al.* 2012, Andersen and Shepherd 2013, Andersen *et al.* 2013).

To test the proposed land surface-atmospheric feedback (i.e., *brown ocean* framework), WRF-ARW was used to simulate Cyclone Abigail (2001), a TC that intensified over northern Australia. The physics and dynamics options in the model set-up were similar to those used in ocean-based studies. WRF was able to reproduce a cyclone in the same region as Abigail with similar wind and pressure values, albeit slightly weaker. Sensitivity tests of the cyclone to the soil moisture regime were performed using 50% reduced and 50% increased soil moisture content at initialization. Spatial and temporal analyses surface and low-level parameters indicate that the wet run produced a stronger, more organized cyclone in a convectively unstable environment. Wet soil increases the surface LHF in northern Australia and leads to a shallow, moist boundary layer with moderate-strong surface-based CAPE. The low-level winds are strongest in the southeast quadrant of the cyclone, where forward speed and clockwise rotation

reinforce each other. There are no signs of other wind maxima that would unfavorably effect the TC (i.e., wind shear is minimal).

Results from this objective support the *brown ocean* framework by showing that soil moisture conditions have an impact on cyclone intensity and structure when using a numerical weather model. Considering the output from the control run and wet run were similar in many respects, it may be inferred that Cyclone Abigail intensified under relatively wet conditions. Future work may extend this research by simulating many cases over one or more landfall regions. Additionally, at resolutions of 5 km or finer, convection is explicitly resolved and would benefit tropical cyclone analysis.

4.6 References

Alonge, C.J., K.I. Mohr, and W.-K. Tao (2007). Numerical studies of wet versus dry soil regimes in the West African Sahel. *Journal of Hydrometeorology* **8**, 102–116. doi: 10.1175/JHM559.1

Andersen, T.K., and J.M. Shepherd (2013). A global spatio-temporal analysis of inland tropical cyclone maintenance or intensification. *International Journal of Climatology*, 1-12. doi: 10.1002/joc.3693

Andersen, T.K., D.E. Radcliffe, and J.M. Shepherd (2013). Quantifying surface energy fluxes in the vicinity of inland-tracking tropical cyclones. *Journal of Applied Meteorology and Climatology*, in review.

Au-Yeung, A.Y.M., and J.C.L. Chan (2010). The effect of a river delta and coastal roughness variation on a landfalling tropical cyclone. *Journal of Geophysical Research-Atmospheres* **115**, D19121. doi: 10.1029/2009JD013631

Bozeman, M.L., D. Niyogi, S. Gopalakrishnan, F. Marks, X. Zhang, and V. Tallapragada. (2012). An HWRF-based ensemble assessment of the land surface feedback on the post-landfall intensification of Tropical Storm Fay (2008). *Natural Hazards* **63**, 1543-1571. doi: 10.1007/s11069-011-9841-5

Chang, H.-I., D. Niyogi, A. Kumar, C.M. Kishtawal, J. Dudhia, F. Chen, U.C. Mohanty, and M. Shepherd (2009). Possible relation between land surface feedback and the post-landfall structure of monsoon depressions. *Geophysical Research Letters* **36**, 1-6.

Chen, F., and J. Dudhia (2001). Coupling an advanced land-surface/hydrology model with the Penn State–NCAR MM5 modeling system. Part I: Model description and implementation. *Monthly Weather Review* **129**, 569–585.

Chen, S.-H., and W.-Y. Sun (2002). A one-dimensional time dependent cloud model. *Journal of the Meteorological Society of Japan* **80**, 99–118. doi: 10.2151/jmsj.80.99

Deshpande, M.S., S. Pattnaik, and P.S. Salvekar (2012). Impact of cloud parameterization on the numerical simulation of a super cyclone. *Annales Geophysicae* **30**, 775-795. doi: 10.5194/angeo-30-775-2012

Dodla, V.B., S. Desamsetti, and A. Yerramilli (2011). A comparison of HWRF, ARW and NMM models in Hurricane Katrina (2005) simulation. *International Journal of Environmental Research and Public Health* **8**, 2447-2469. doi: 10.3390/ijerph8062447

Emanuel, K., J. Callaghan, and P. Otto (2008). A hypothesis for the redevelopment of warm-core cyclones over northern Australia. *Monthly Weather Review* **136,** 3863–3872. doi: 10.1175/2008MWR2409.1

Evans, C., R.S. Schumacher, and T.J. Galarneau (2011). Sensitivity in the overland reintensification of Tropical Cyclone Erin (2007) to near-surface soil moisture characteristics. *Monthly Weather Review* **139**, 3848–3870. doi: 10.1175/2011MWR3593.1

Frye, J.D., and T.L. Mote (2010). The synergistic relationship between soil moisture and the low-level jet and its role on the pre-storm environment in the southern Great Plains. *Journal of Applied Meteorology and Climatology* **49**, 775–791. doi: 10.1175/2009JAMC2146.1

Hong, S.-Y., Y. Noh, and J. Dudhia (2006). A new vertical diffusion package with an explicit treatment of entrainment processes. *Monthly Weather Review* **134**, 2318–2341.

Kain, J.S., and J.M. Fritsch (1990). A one-dimensional entraining/detraining plume model and its application in convective parameterization. *Journal of Atmospheric Science* **47**, 2784–2802.

Kellner, O., D. Niyogi, M. Lei, and A. Kumar (2012). The role of anomalous soil moisture on the inland reintensification of Tropical Storm Erin (2007). *Natural Hazards* **63**, 1-27. doi: 10.1007/s11069-011-9966-6

Kishtawal, C.M., D. Niyogi, A. Kumar, M.L. Bozeman, and O. Kellner (2012). Sensitivity of inland decay of North Atlantic tropical cyclones to soil parameters. *Natural Hazards* **63**, 1527-1542.

Lanicci, J.M., T.N. Carlson, and T.T. Warner (1987). Sensitivity of the Great Plains severe-storm environment to soil-moisture distribution. *Monthly Weather Rev*iew **115**, 2660-2673.

Lin, N., J.A. Smith, G. Villarini, T.P. Marchok, and M.L. Baeck (2010). Modeling extreme rainfall, winds, and surge from Hurricane Isabel (2003). *Weather and Forecasting* **25**, 1342-

Ma, L.-M., and Z.-M. Tan (2009). Improving the behavior of the cumulus parameterization for tropical cyclone prediction: convective trigger. *Atmospheric Research* **92**, 190-211. doi: 10.1016/j.atmosres.2008.09.022

Osuri, K. K., U.C. Mohanty, A. Routray, M.A. Kulkarni, and M. Mohapatra (2012). Customization of WRF-ARW model with physical parameterization schemes for the simulation of tropical cyclones over North Indian Ocean. *Natural Hazards* **63**, 1337-1359.

Prater, B.E., and J.L. Evans (2002). Sensitivity of modeled tropical cyclone track and structure of hurricane Irene (1999) to the convective parameterization scheme. *Meteorology and Atmospheric Physics* **80**, 103-115.

Rao, D.V.B. and V. Tallapragada (2012). Tropical cyclone prediction over Bay of Bengal: A comparison of the performance of NCEP operational HWRF, NCAR ARW, and MM5 models. *Natural Hazards* **63,** 1393-1411.

Segal, M., R.W. Arritt, and C. Clark (1995). Scaling evaluation of the effect of surface characteristics on potential for deep convection over uniform terrain. *Monthly Weather Rev*iew **123**, 383-400.

Skamarock, W.C., and Coauthors (2008). A description of the Advanced Research WRF version 3. NCAR Tech. Note NCAR/TN-4751STR, 125 pp.

Tuleya, R.E. (1994). Tropical storm development and decay: Sensitivity to surface boundary conditions. *Monthly Weather Review* **122**, 291**-**304.

Tuleya, R.E., and Y. Kurihara (1978). A numerical simulation of the landfall of tropical cyclones. *Journal of Atmospheric Science* **35**, 242–257.

Xie, B.G. and F.Q. Zhang (2012). Impacts of typhoon track and island topography on the heavy rainfalls in Taiwan associated with Morakot (2009). *Monthly Weather Review* **140**, 3379-3394.

Zhang, Y., C. Cassardo, C.Z. Ye, M. Galli, and N. Vela (2011). The role of the land surface processes in the rainfall generated by a landfall typhoon: A simulation of the typhoon Sepat (2007). *Asia-Pacific Journal of Atmospheric Sciences* **47**, 63-77.

Zhu, P. (2008). Impact of land-surface roughness on surface winds during hurricane landfall. *Quarterly Journal of the Royal Meteorological Society* **134**, 1051-1057.

Table 4.1: WRF-ARW parameters and configurations.

Model parameter	**Configuration**
Version	WRF-ARW v3.5 (Skamarock *et al.* 2008)
Domain	275 x 325 x 34
Horizontal grid spacing	8 km
Duration	30 h, 0000 UTC 2 Mar–0600 UTC 3 Mar 2001
Initial and Boundary Conditions	6-hourly 1.0°x1.0° NCEP FNL operational analyses
Microphysical Parameterization	Purdue–Lin (Chen and Sun 2002)
Boundary Layer Parameterization	YSU (Hong *et al.* 2006)
Surface Layer Parameterization	MM5 similarity (Skamarock *et al.* 2008)
Land Surface Parameterization	Unified Noah land surface model (Chen and Dudhia 2001)
Longwave Radiation Parameterization	RRTM scheme (Mlawer *et al.* 1997)
Shortwave Radiation Parameterization	Dudhia scheme (Dudhia 1989)
Cumulus Parameterization	Kain-Fritsch (Kain and Fritsch 1990)

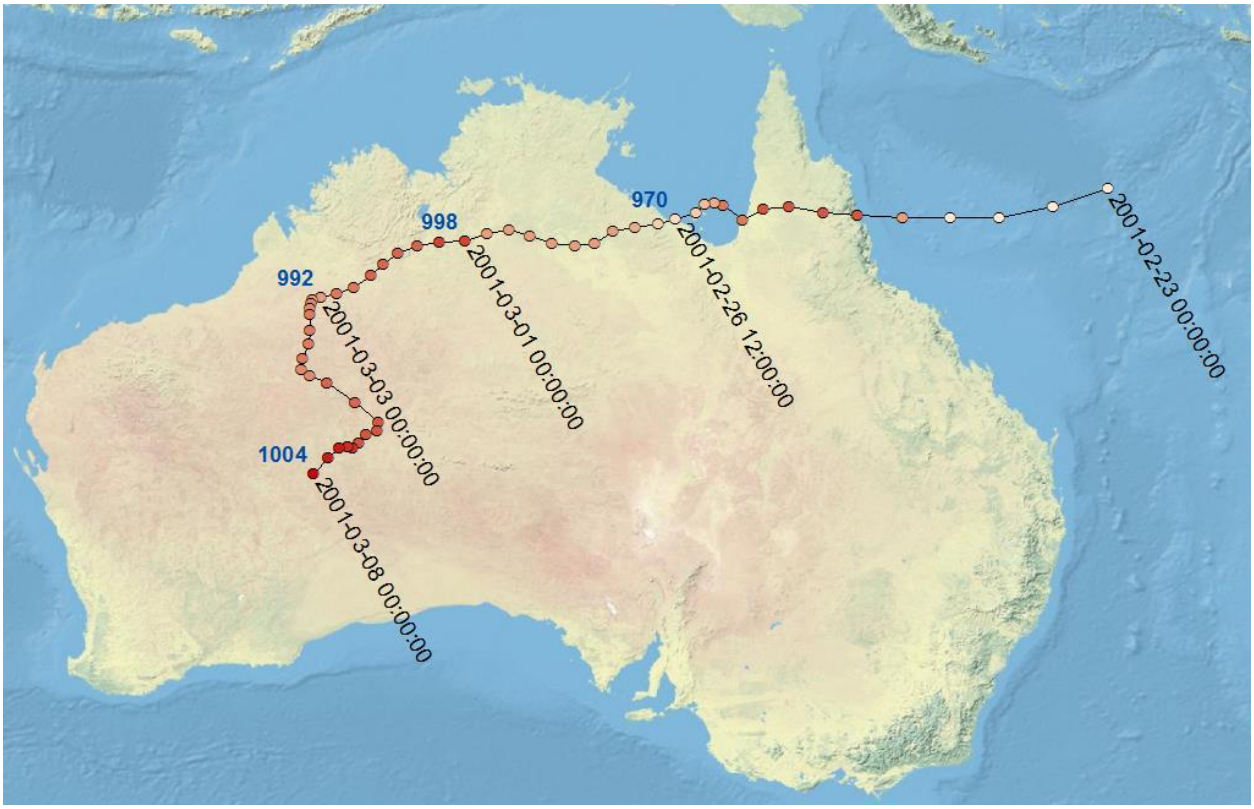

Figure 4.1: Track and intensity of Cyclone Abigail 23 February 2001-8 March 2001. The minimum central pressure (hPa) at landfall, two inland intensifications, and dissipation are displayed.

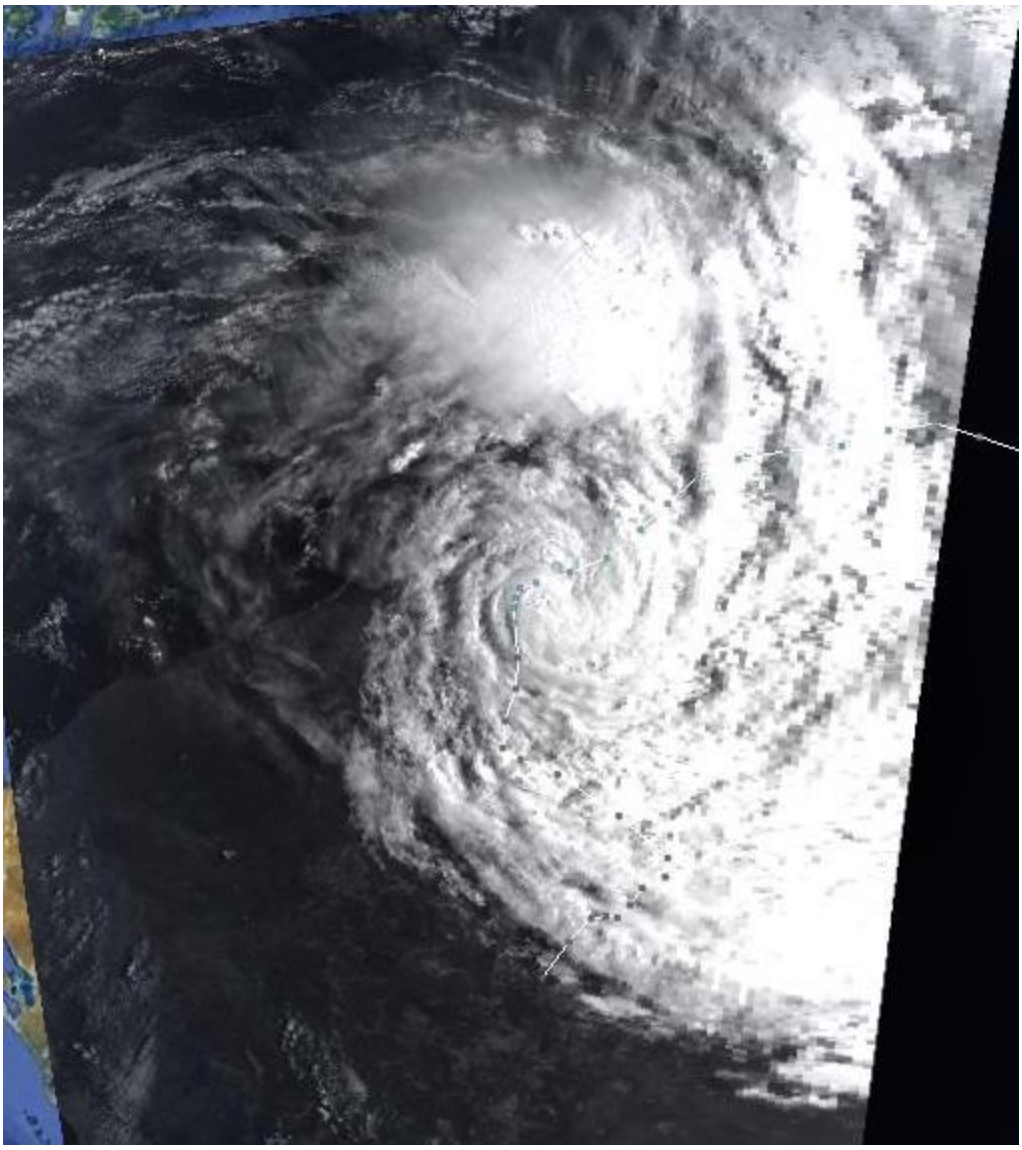

Figure 4.2: HURSAT visible satellite image of Cyclone Abigail 3 March 0100 UTC. It has a characteristic tropical cyclone structure with a low pressure center and spiraling rainbands.

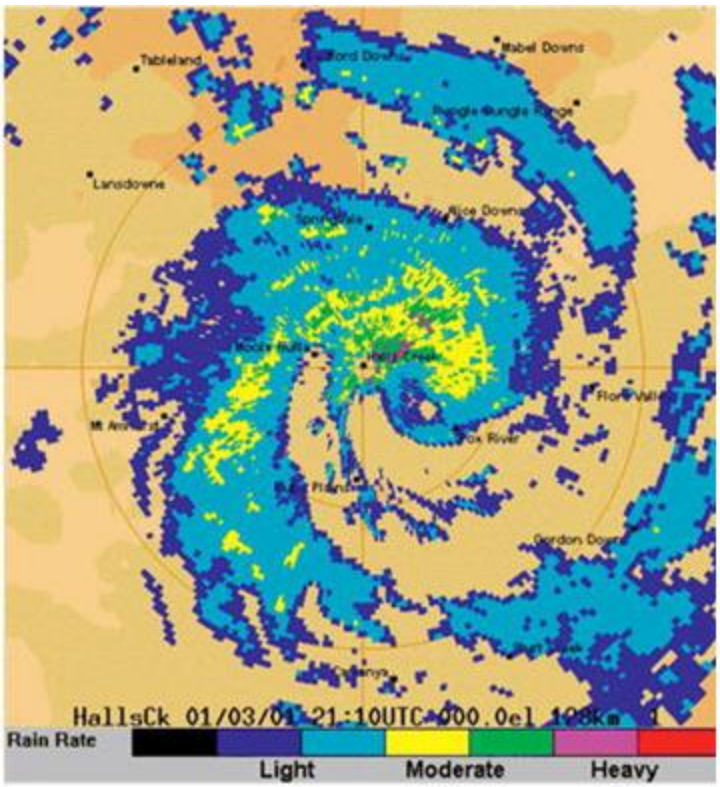

Figure 4.3: Halls Creek radar on 1 March 2001 2110 UTC captured Cyclone Abigail on its westward track. A clearly defined eye is evident (Image Credit: BOM).

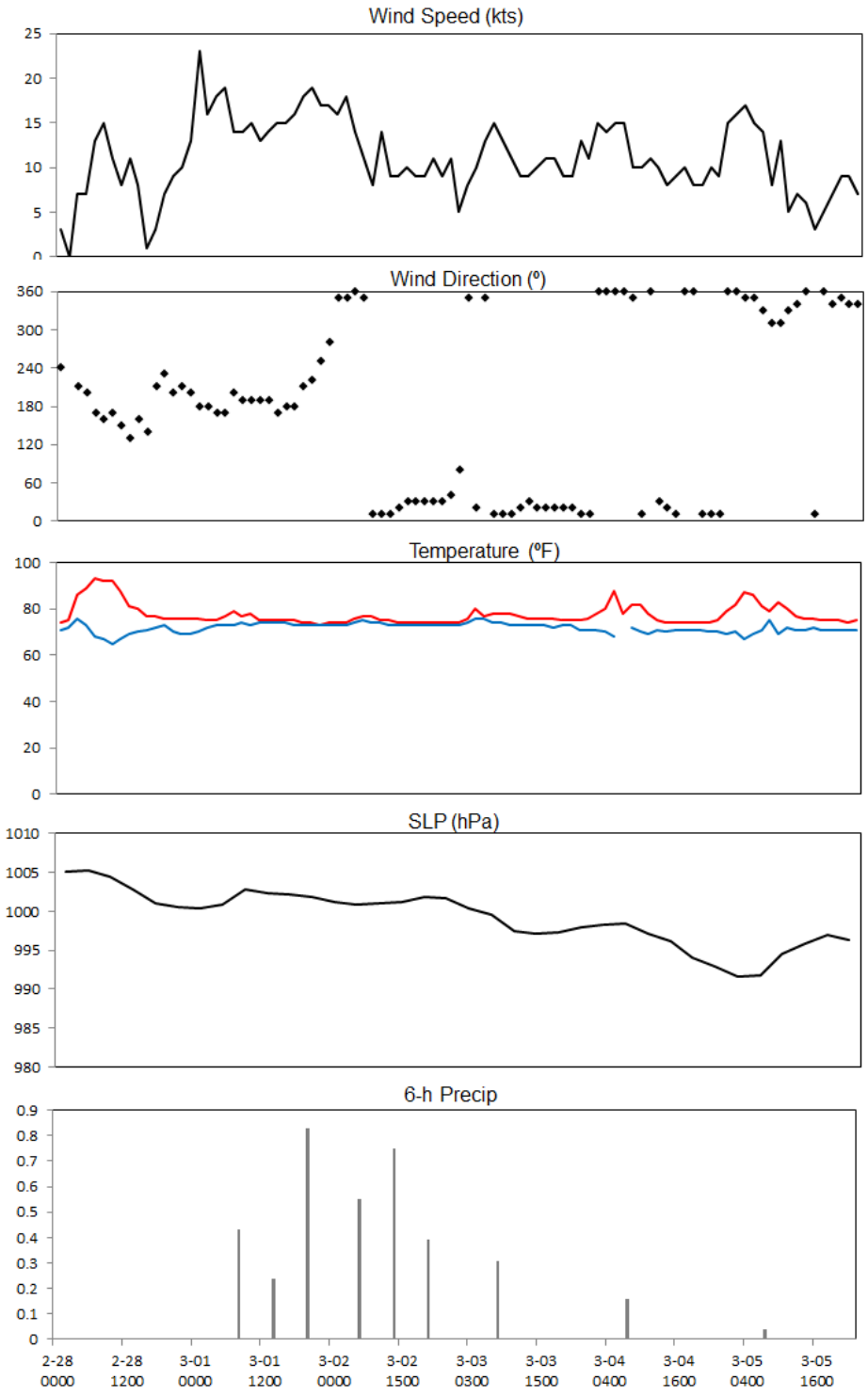

Figure 4.4: Meteorological observations from Halls Creek Airport 28 Feb – 5 March 2001. The passage of Abigail is evident around 2 March.

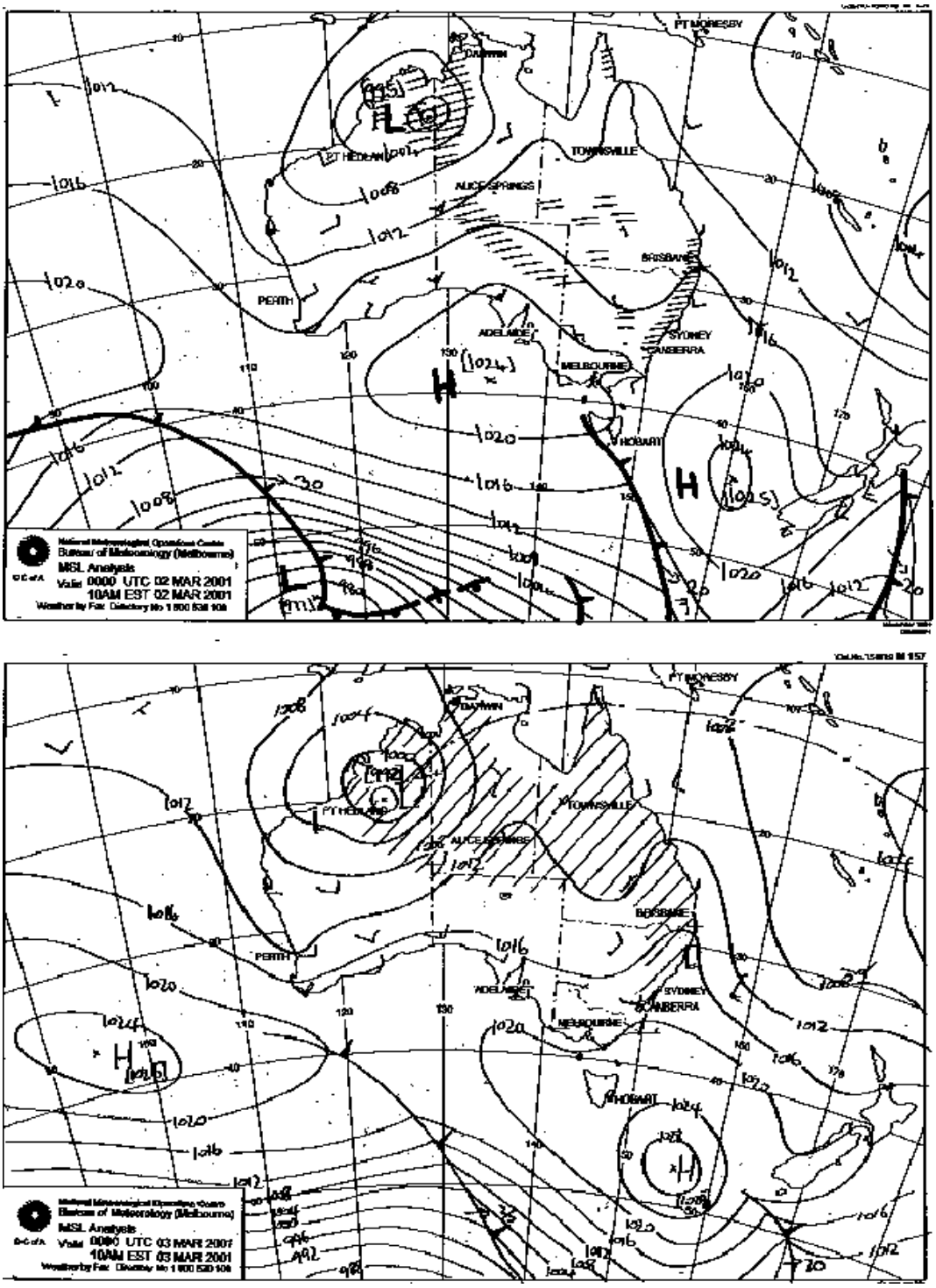

Figure 4.5: BOM surface analyses valid at 0000 UTC 2 March (top) and 0000 UTC 3 March (bottom). The central pressure lowers from 995 to 992 hPa.

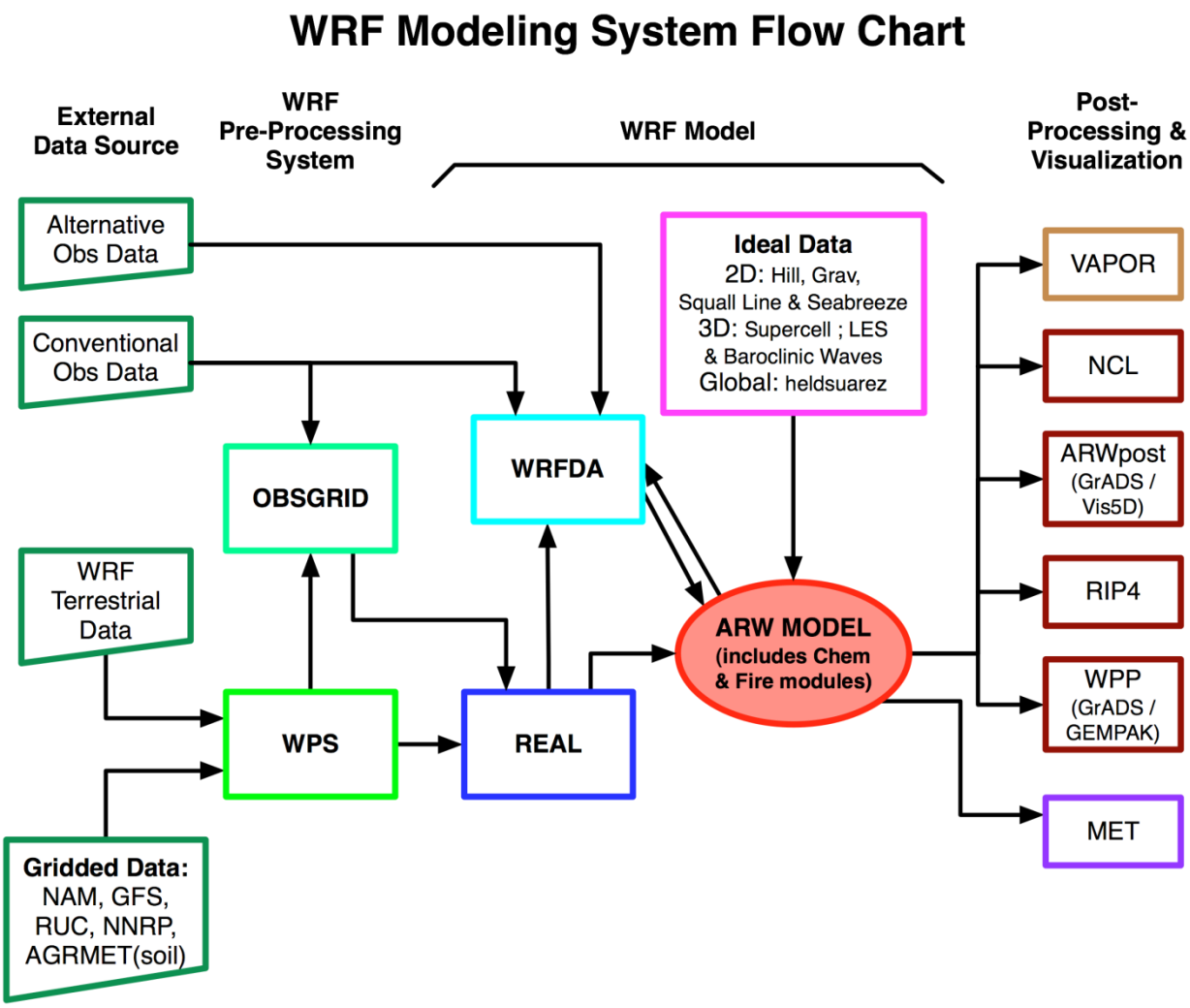

Figure 4.6: WRF modeling system flow chart. The present study uses GFS gridded data, WPS pre-processing, real, ARW model, and NCL post-processing.

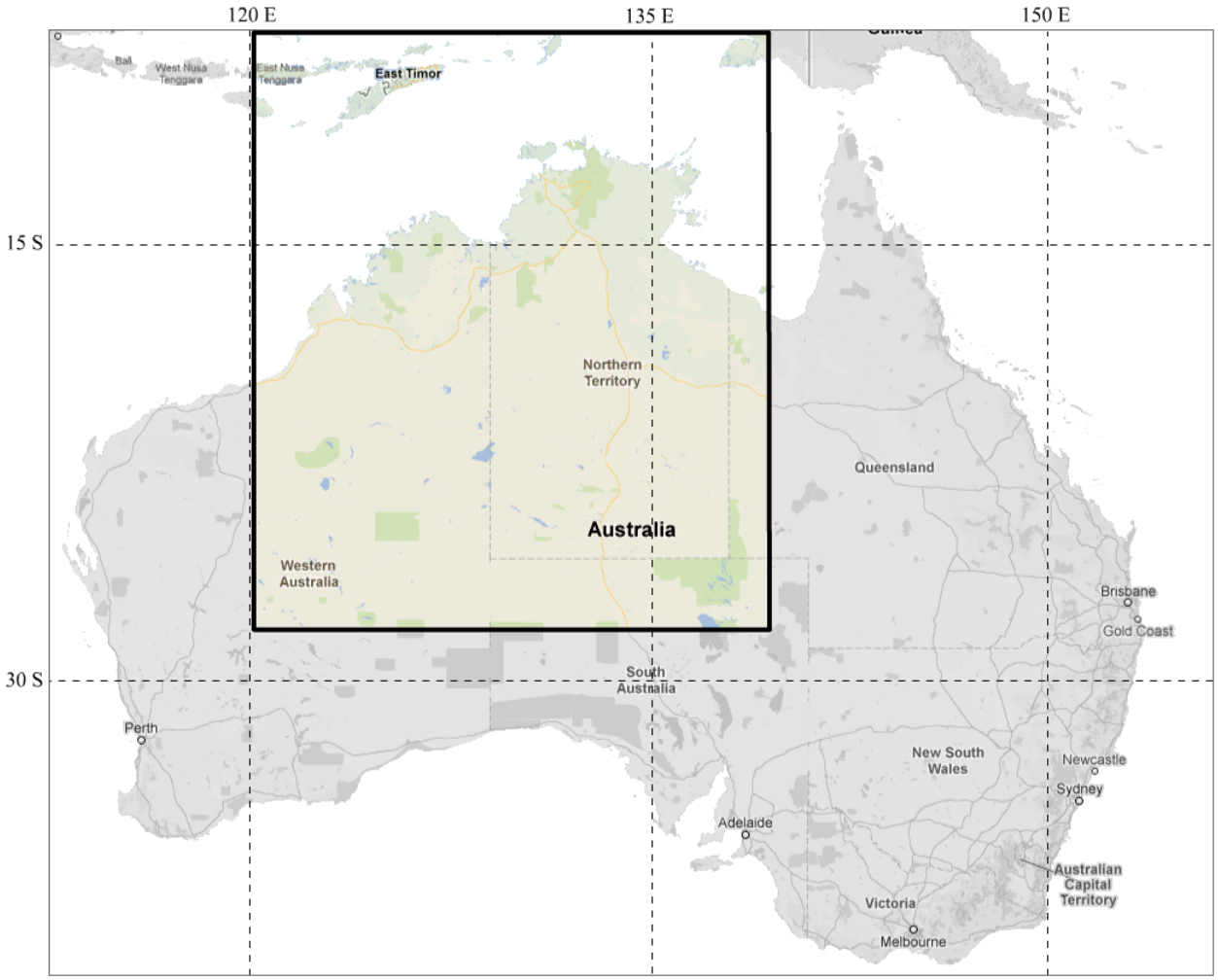

Figure 4.7: The simulation domain is 325x275 grid points over the Northern and Western Territories of Australia (outlined in black).

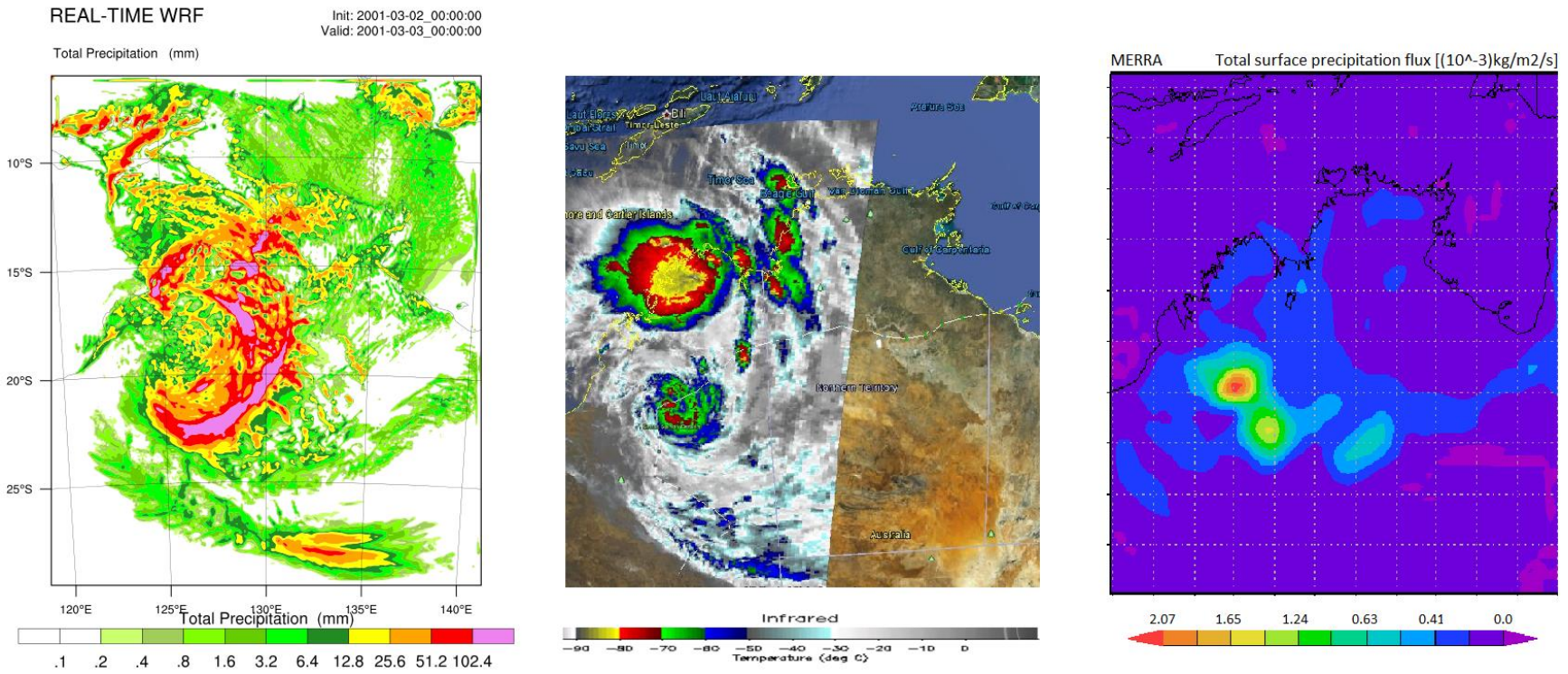

Figure 4.8: Total precipitation valid 3 March 0000 UTC produced by WRF (left), HURSAT IR image with cloud-top temperatures from 3 March 0200 UTC (center), and MERRA total surface precipitation flux 3 March 0000 UTC (right). WRF reproduced the size and shape of the cyclone, and the location of the rain maxima, but did not capture the eye as seen in the satellite image.

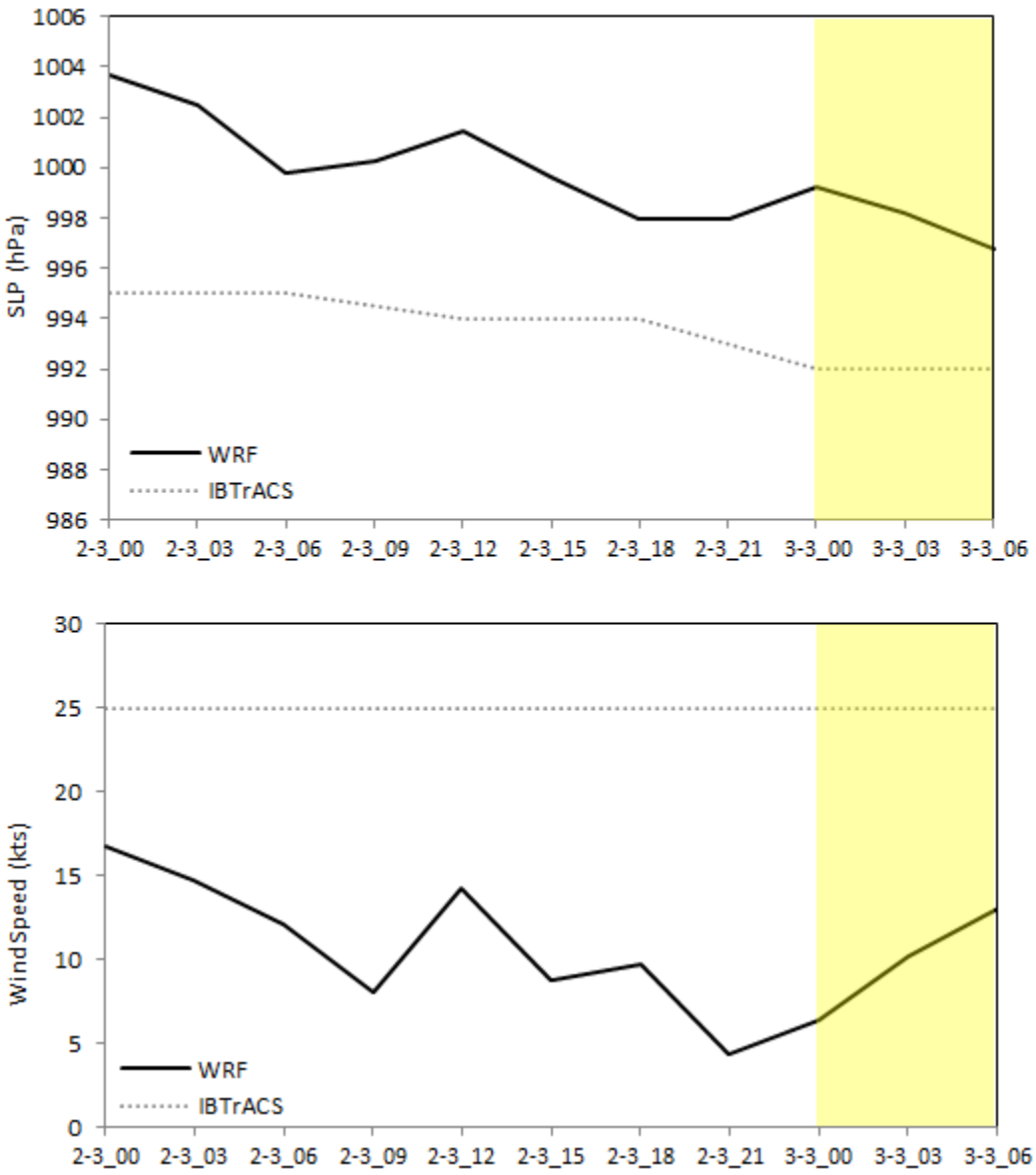

Figure 4.9: Sea-level pressure (hPa) (top) and surface wind speed (kts) (bottom) for the WRF control simulation (solid) and IBTrACS 6-hourly records (dotted) (2 March 0000 UTC to 3 March 0600 UTC). The model indicates a pressure drop and wind speed increase near the actual cyclone intensification time (highlighted).

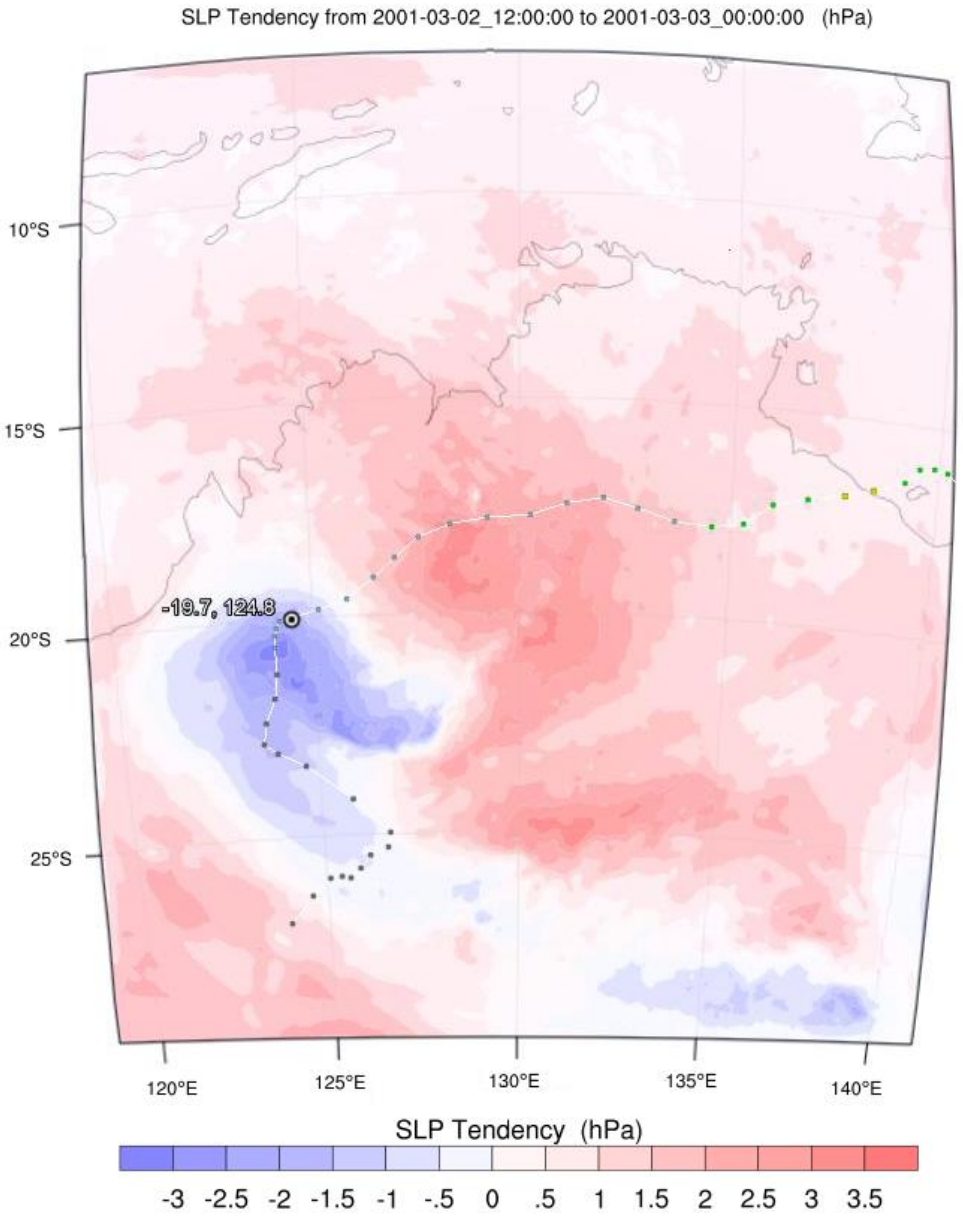

Figure 4.10: Simulated 12-hour SLP tendency with IBTrACS cyclone path overlay. The lowest recorded pressure was at 19.7ºS, 124.8ºE, approximately 50-100 km northeast of the minimum central pressure simulated by WRF.

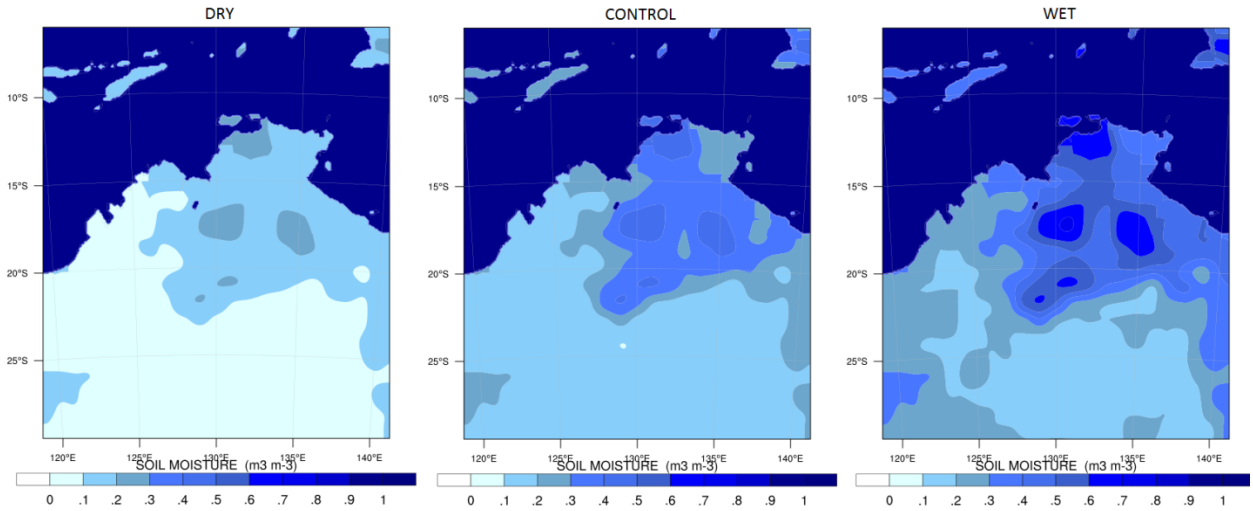

Figure 4.11: Soil moisture initialization (m^3 m^{-3}) for dry (left), control (center), and wet (right) simulations.

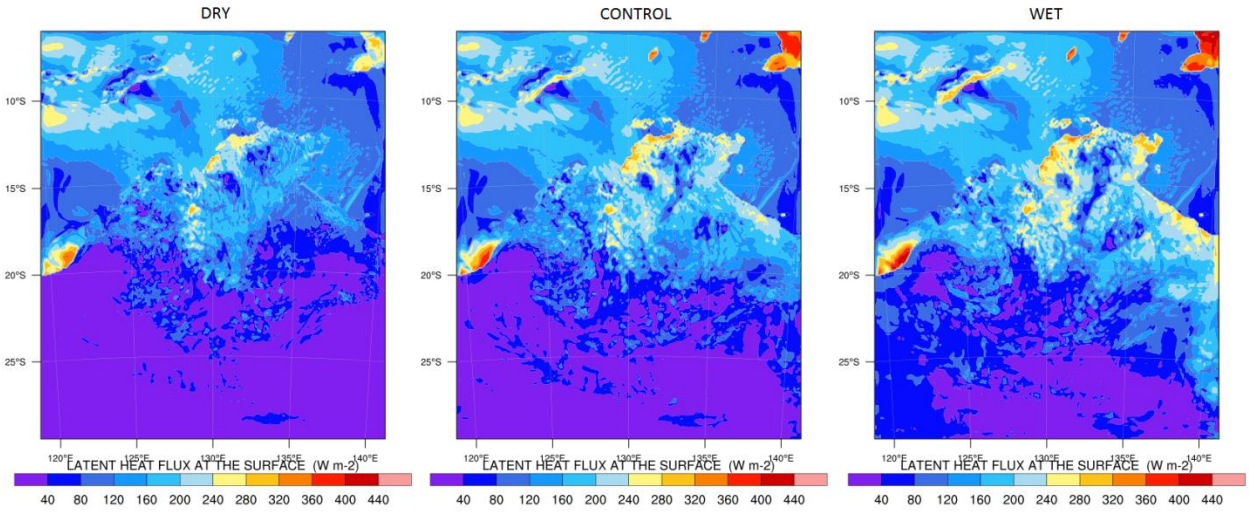

Figure 4.12: Surface latent heat flux (LHF, W m^{-2}) for dry (left), control (center), and wet (right) simulations valid 0000 UTC 3 March 2001.

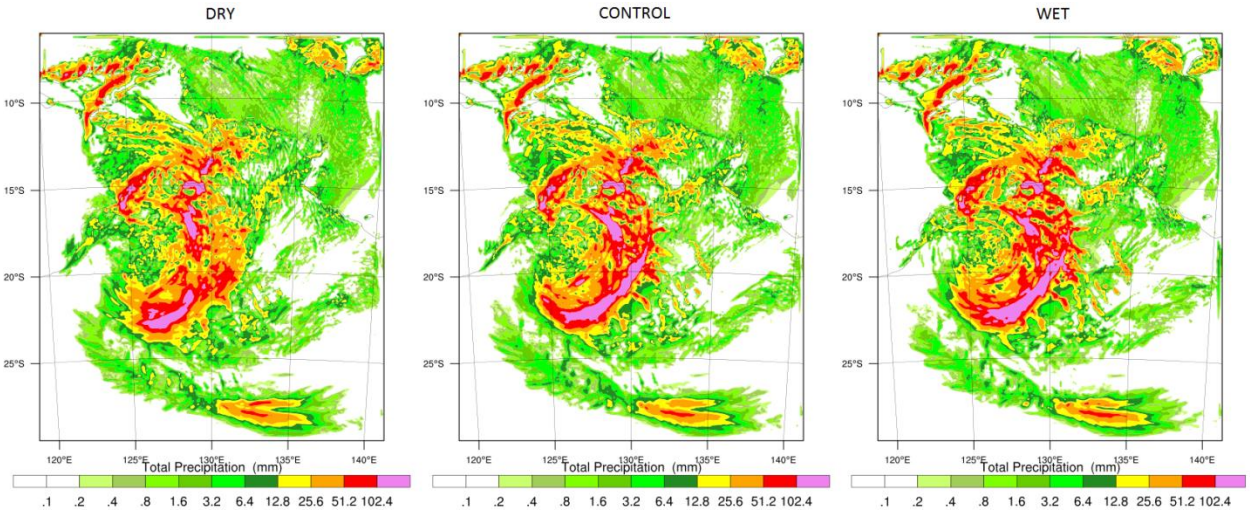

Figure 4.13: Total precipitation (mm) for dry (left), control (center), wet (right) simulations valid 0000 UTC 3 March 2001.

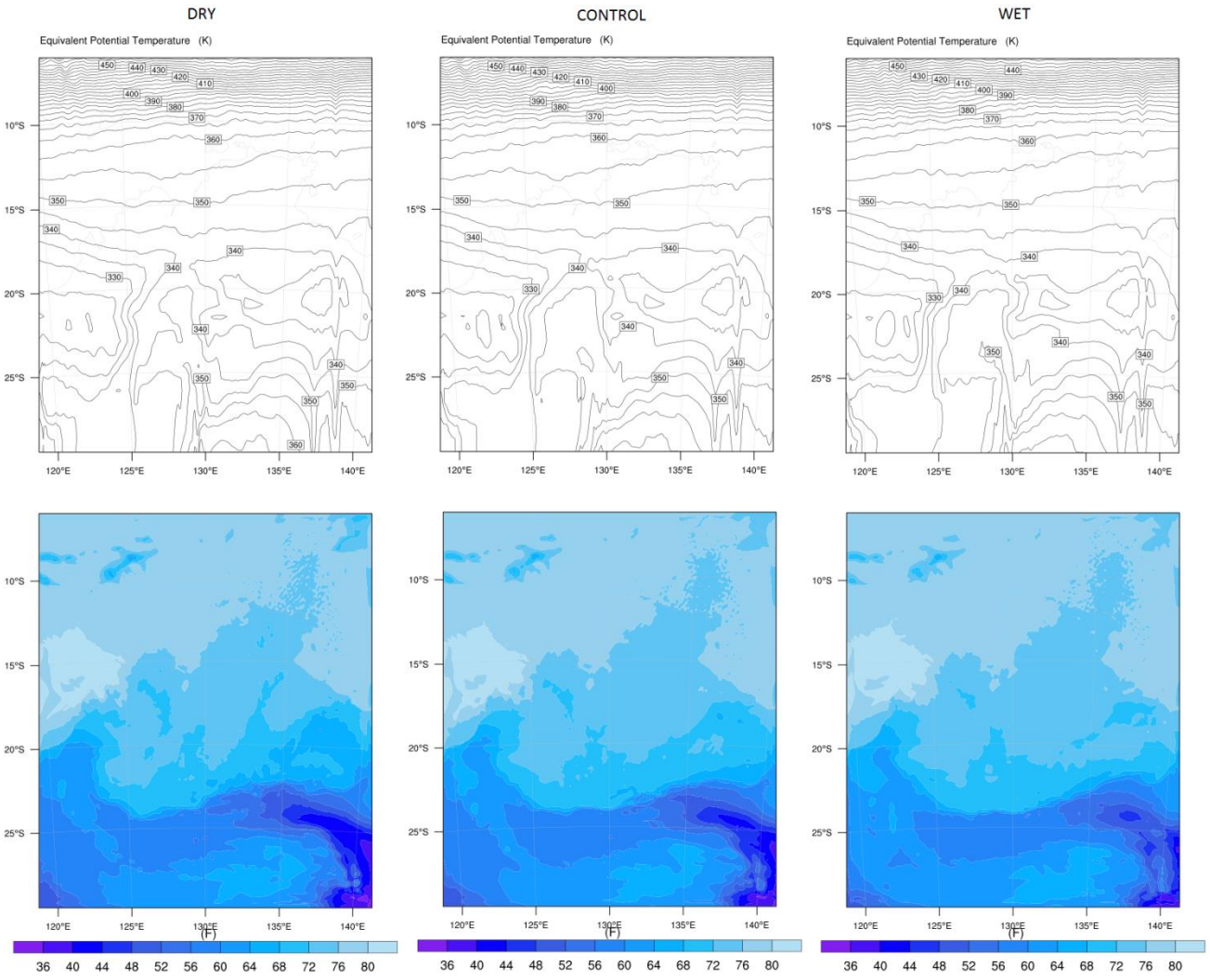

Figure 4.14: Equivalent potential temperature (K) (top) and surface dewpoint temperature (°F) (bottom) for control, dry and wet simulations valid 3 March 2001 0000 UTC. Low-level atmospheric moisture values over land approach the magnitudes of those over the Indian Ocean.

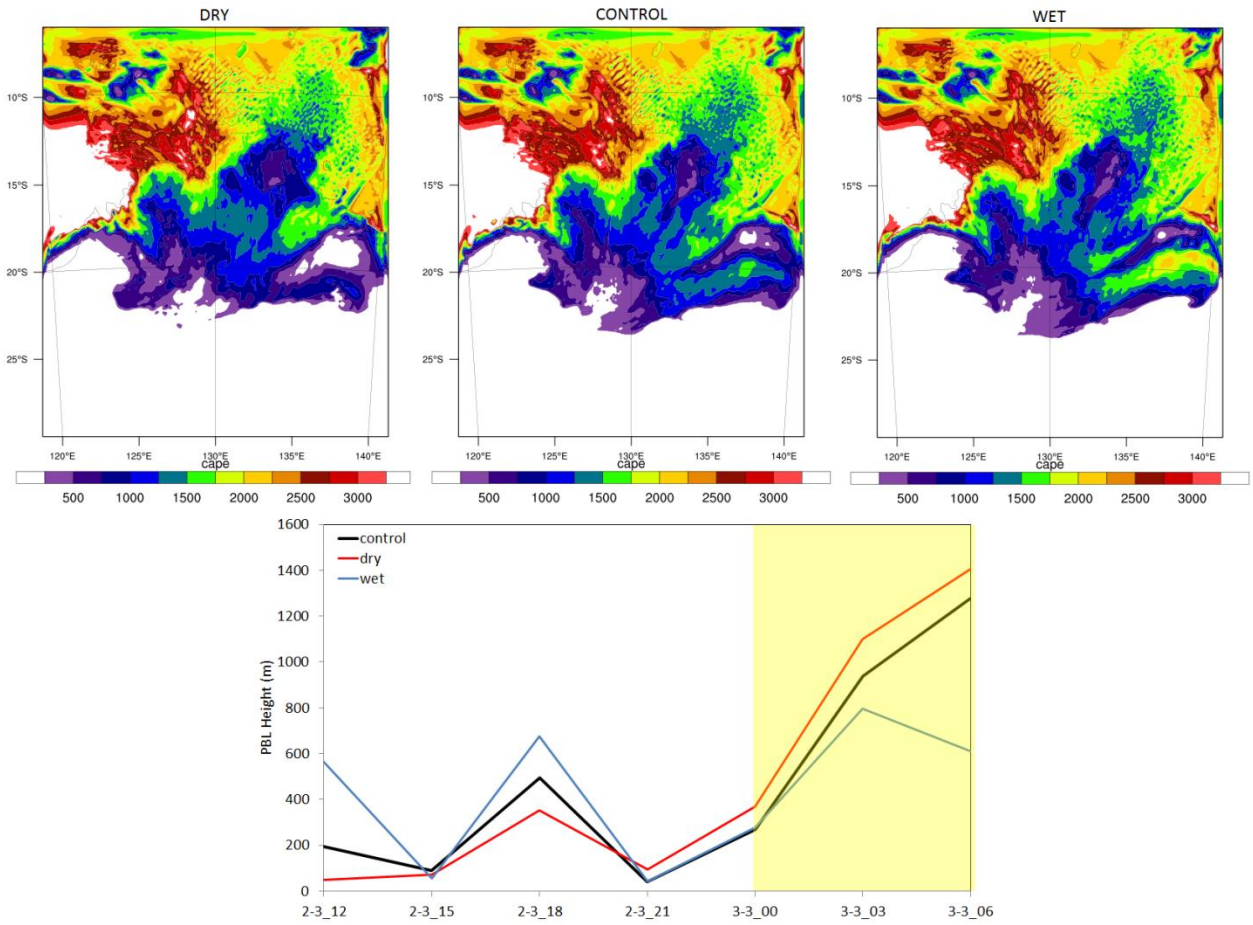

Figure 4.15: CAPE (J kg^{-1}) at eta level 1 (1000 hPa) for dry (left), control (center), and wet (right) simulations valid at 3 March 2001 0000 UTC (top) and PBL height (m) at cyclone center 2 March 1200 UTC to 3 March 0600 UTC (bottom). The period of intensification is highlighted.

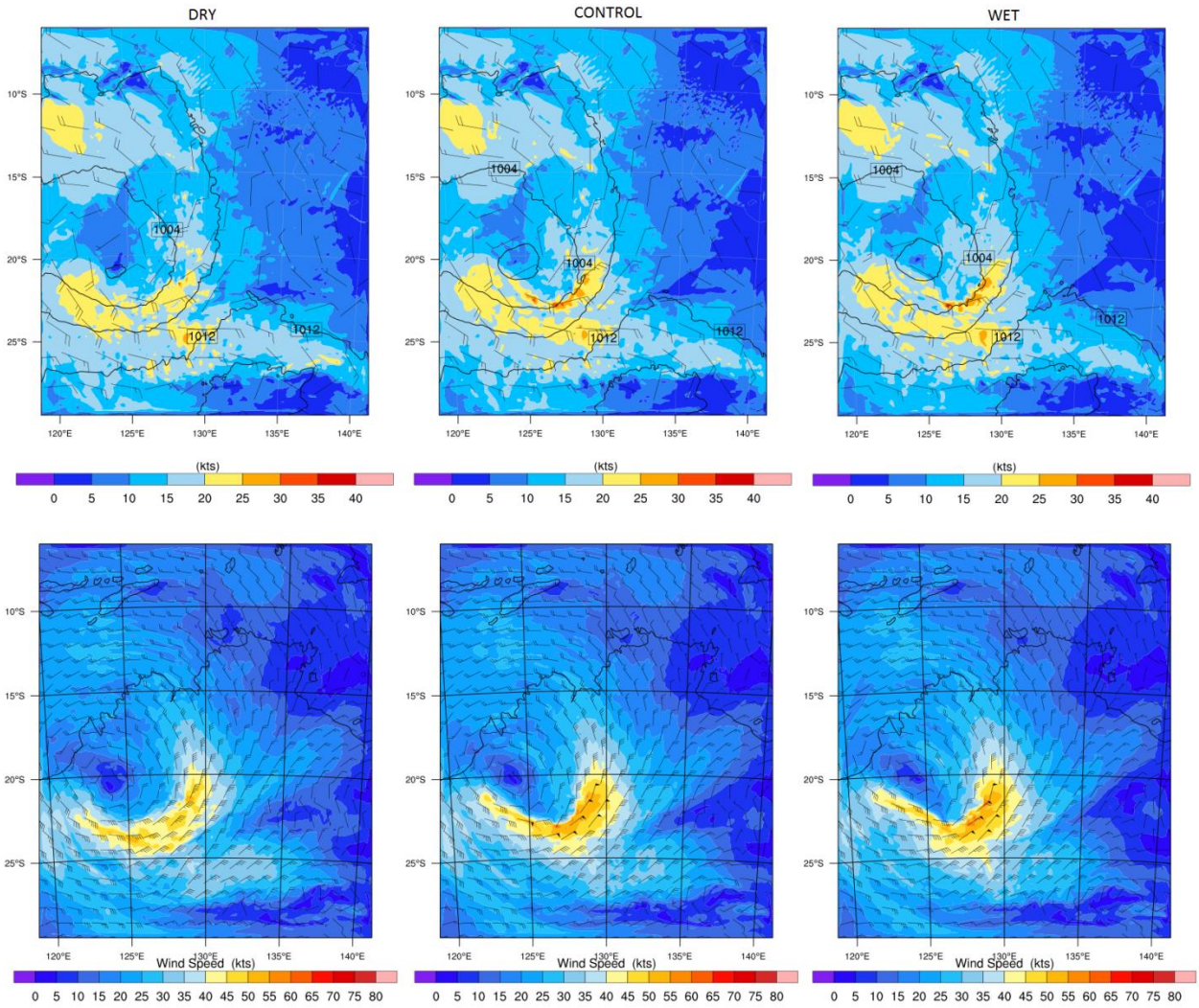

Figure 4.16: Surface wind speed (kts), wind vectors, and sea level pressure (hPa) (top) and 850 hPa wind field (bottom) for dry (left), control (center), and wet (right) simulations valid at 0000 UTC 3 March 2001. The strongest winds are to the east of the cyclone track.

CHAPTER 5

SUMMARY AND CONCLUSIONS

5.1 Overview

An important implication of climate change is the observed acceleration of the global water cycle. The frequency and intensity of tropical cyclones (TCs) is expected to deviate from historical norms. As the risk of stronger TCs increases in the coming decades, it is all the more important to understand the evolution of TCs during and after landfall. The majority of cyclones weaken over land in response to moisture loss, wind shear, friction, and temperature and pressure gradients. Other TCs merge with the midlatitude flow and transition to extratropical cyclones (ETs). In rarer cases, TCs maintain their warm-core structure and tropical characteristics even after moving inland from the coast. In this study, the phenomenon is called Tropical Cyclone Maintenance or Intensification (TCMI). Since the atmosphere is not very conducive to tropical systems over continents, it is theorized that anomalously high soil moisture and upward latent heat flux (LHF) provide the necessary energy to the cyclone to prevent decay in TCMI cases. Investigators at the University of Georgia and Purdue University have termed this the *brown ocean* since the ocean is normally the primary source for the energetics driving tropical systems.

Soil moisture influences the atmosphere via moisture and heat fluxes. The added energy to the lower atmosphere (planetary boundary layer) increases the potential of convective development. Similarly, areas of soil moisture gradients can help initiate thermal circulations. Soil moisture persistence has also been linked to precipitation recycling and is a factor in future

convective activity. In previous studies, it has been suggested that anomalously wet soils encouraged the reintensification of Tropical Storm Erin (2007) over Oklahoma by enhancing latent heating and moist static energy. In Australia and India, TCs and monsoon depressions may be maintained over land after recent heavy rainfall events. In China, large reservoirs, lakes, and wetlands are identified as energy sources for typhoons post-landfall.

To test the *brown ocean* framework, three research objectives were formulated:

1. Differentiate ET from TCMI events inland, (2) address the global spatio-temporal characteristics of TCMIs to produce the first global climatology of inland intensifications and (3) quantify the possible physical mechanistic, geographical, and/or topographical factors associated with TCMIs.
2. Employ the HYDRUS-1D model to simulate the typical surface fluxes over TCMI regions in the weeks leading up to intensification in order to compare the energy potential to ocean heat fluxes.
3. Analyze a historical TCMI event with emphasis on soil moisture interactions, flux magnitudes, and storm evolution using the Weather Research Forecast (WRF-ARW) model.

5.2 Summary

For the first objective, an inland TC database was derived from IBTrACS using spatial analysis. Further, each cyclone was analyzed from landfall to decay to determine those that maintained strength or intensified post-landfall. The results were a total of 17 cold-core (ET), 16 warm-core (TCMI), and 12 neutral/hybrid cyclones globally. Analysis of synoptic conditions at the time of intensification indicates that inland TCs thrive when temperature gradients are weak, while ET is linked to frontal boundaries. The upper-level winds are not significantly different

between ET and TCMI events. A limited amount of wind shear can benefit TCs by increasing storm outflow.

Analysis of surface conditions revealed that soil moisture gradients, and associated LHF, were in the vicinity of the cyclones at the time of intensification. Leading up to each TCMI, the LHF of the region tends to be higher than average. A cyclone may be more likely to intensify inland during the peak of the hurricane season when rainfall events direct precede it or when soil is persistently moist. Intensification regions consistently have higher surface LHF during an intensifying cyclone than during a weakening cyclone in the United States and Australia. These regions may exhibit stronger land surface–atmospheric feedbacks that relate to TC maintenance inland. For all regions, an area-averaged LHF threshold near 70 Wm^{-2} is identified for TCMI occurrence.

For the second objective, HYDRUS-1D is used to simulate the soil profiles, meteorological conditions, and resulting energy fluxes of four intensification regions leading up to TCMI events. Results indicate that soil texture does not have a significant effect on the LHF magnitudes across regions. While TCMIs are most common over Australia, the LHF over the study period is not noticeably greater over sandy soil than over clay (China and India) or loam (US). However, the diurnal changes are sharper over Australia which supports the notion of "sudden energy release" when the sandy soil is wetted. The US region exhibits a similar trend with relatively high LHF and SHF, yet TCMIs are much less common. Australia may experience more total landfalls, smoother terrain, and a more conducive atmosphere. For all HYDRUS runs, the total 2-week maximum LHF values are comparable to or exceed typical ocean LHF magnitudes. The total 2-week mean LHF indicates there is a ~70 W m^{-2} area-averaged threshold for TCMI occurrence. The 3-day maximum LHF values inland are well above those over the

ocean in the China and India intensification regions, while LHF magnitudes ocean vs. land were nearly equal over the US and Australia regions. LHF maxima over land have a similar magnitude to those found over the ocean prior to a TCMI and provides plausibility of the *brown ocean* effect.

For the third objective, the Weather Research and Forecasting model (WRF) is set-up to simulate Cyclone Abigail (2001) as it intensified over northern Australia. The model reproduced the cyclone with realistic wind and pressure characteristics and captured inland intensification at the correct time. The cyclone was slightly more intense than observations and was displaced about 50-100 km to the southwest. Sensitivity tests of the cyclone to the soil moisture regime were performed using dry and wet soil moisture initializations. Quantitative and qualitative analyses of LHF, total precipitation, CAPE, equivalent potential temperature, surface dew point, and low-level wind fields indicate that the wet run produced a stronger, more organized cyclone in a convectively unstable environment. Dry soil reduced the upward moisture flux and subsequently reduced the amount of moist static energy available to the tropical system tracking over.

5.3 Conclusions

Results from this dissertation support the *brown ocean* framework by providing evidence of at least 16 inland tropical cyclone maintenance or intensification phenomena 1979-2008. Almost all of the intensification regions experienced recent rainfall and high moisture fluxes before the TC tracked over. Additionally, the ambient atmospheric conditions were not indicative of extratropical transition. From the three objectives, intensification regions can be characterized by the following:

- 350-500 km inland from the coast in a typical landfall area

- Recent heavy rainfall events
- High soil moisture and upward latent heat flux
- Low-level moisture plumes
- Moderate-high convective potential
- Absence of frontal activity

TCMIs are more likely to occur during the peak of the hurricane season when daily LHF is above the seasonal mean. Although a TCMI may occur over any region, they are most common over Australia despite more overall TCs originating in the western North Pacific. The frequency and path of cyclones as well as the terrain of the Australian region may be favorable factors.

Three primary "ingredients" emerge that increase the likelihood of a TCMI event. First, the continental region over which the TC makes landfall is wetter than normal. Recent precipitation or longer-term soil moisture memory lead to moderate-high upward LHF within 2-3 weeks of the TC. Secondly, the area-averaged LHF should be at least 70 W m^{-2} over the region when the TC is in the vicinity. Third, the atmosphere should be more barotropic than baroclinic, without peripheral weather systems to disturb the warm-core symmetric structure. The strict criteria for identifying "inland" cases have likely resulted in a conservative estimate of TCMI occurrence. TCs closer to the coast may also be vulnerable to soil moisture conditions.

This research is significant for hurricane forecasting and preparedness. Oftentimes a TC is no longer monitored once it is inland and dissipating. However, TC remnants have been observed to reorganize and devastate regions unprepared for the heavy rains, wind, and tornadoes generated by the invigorated cyclone. Extended observation times over land and proper classification of post-landfall TC types can help minimize damage and loss of life. Future

studies may contribute to this body of research by investigating the physical mechanisms linked to intensification using a coupled high-resolution mesoscale model and land surface model.